

J

Earth Resources Laboratory
Department of Earth, Atmospheric, and Planetary Sciences
Massachusetts Institute of Technology
Cambridge, MA 02139

GOODMAN GRANT

11-46

C.R.

99096

133P.

**SEMI-ANNUAL REPORT TO: National Aeronautics and Space Administration
(Crustal Dynamics)**

**TITLE: The Interpretation of Crustal Dynamics Data in Terms of Plate
Interactions and Active Tectonics of the "Anatolian Plate" and
Surrounding Regions in the Middle East**

NASA GRANT: NAG5-753

PRINCIPAL INVESTIGATOR: M. Nafi Toksoz

PERIOD: 15 March 1987-14 September 1987

DATE: 7 October 1987

(NASA-CR-181315) THE INTERPRETATION OF
CRUSTAL DYNAMICS DATA IN TERMS OF PLATE
INTERACTIONS AND ACTIVE TECTONICS OF THE
ANATOLIAN PLATE AND SUBCENDING REGIONS IN
THE MIDDLE (Massachusetts Inst. of Tech.)

N87-29053

63/46

Unclas
0099096

THE INTERPRETATION OF CRUSTAL DYNAMICS DATA IN TERMS OF PLATE INTERACTIONS AND ACTIVE TECTONICS OF THE "ANATOLIAN PLATE" AND SURROUNDING REGIONS IN THE MIDDLE EAST

INTRODUCTION

The long term objective of this project is to interpret NASA's Crustal Dynamics measurements (SLR) in the Eastern Mediterranean region in terms of relative plate motions and intraplate deformation. Our approach is to combine realistic modeling studies with analysis of available geophysical and geological observations to provide a framework for interpreting NASA's measurements. This semi-annual report concentrates on our recent results regarding the tectonics of Anatolia and surrounding regions from ground based observations. We also briefly report on our progress to use GPS measurements to densify SLR observations in the Eastern Mediterranean. Refer to the previous annual report for a discussion of our modeling results.

I. STRIKE-SLIP FAULT GEOMETRY IN TURKEY AND ITS INFLUENCE ON EARTHQUAKE ACTIVITY (see Appendix I)

Analysis of Turkish strike-slip faults indicates that detailed fault geometry plays an important role in controlling earthquake rupture. Empirical relationships are used to estimate possible locations and sizes of future strike-slip events. These results have implications for earthquake activity on other strike-slip faults such as the San Andreas in California.

II. THE SEGMENTATION, SEISMICITY AND EARTHQUAKE POTENTIAL OF THE EASTERN PART OF THE NORTH ANATOLIAN FAULT ZONE (see Appendix II)

Historical and instrumental earthquakes of the North Anatolian fault zone in the vicinity of the Erzincan basin show a close relation to fault geometry. Results of this detailed study suggest that each segment may have its own characteristic earthquake. Furthermore, we have identified a 100 km long seismic gap along the North Anatolian fault east of Erzincan. This segment last ruptured in 1784, and is the only segment of the 900 km long main section of the NAF that did not experience a large earthquake during the well known 1939-1967 sequence. Future monitoring of this area with GPS could provide important information on possible earthquake precursors (see section IV below).

III. TECTONIC ESCAPE ORIGIN AND COMPLEX EVOLUTION OF THE ERZINCAN PULL-APART BASIN, EASTERN TURKEY (see Appendix III)

A new tectonic model is presented for the pull-apart opening of the Erzincan basin in an effort to explain the relationship between continental block kinematics and basin formation. We propose a two stage pull-apart mechanism associated with the continental collision of the Arabian and Eurasian plates along the Bitlis Suture Zone in eastern Turkey. The first stage of westward pull-apart opening occurs between two divergent segments of the North Anatolian Fault Zone, accommodating westward tectonic escape of the Anatolian block. The second stage involves translational-rotational opening by the formation of the obliquely oriented, left-lateral Ovacik fault. This interpretation has implications for the detailed nature of plate interactions in this region.

IV. GLOBAL POSITIONING SYSTEM (GPS) MEASUREMENTS OF FAULTING AND REGIONAL DEFORMATION IN THE EASTERN MEDITERRANEAN (see Appendix IV)

We are currently involved in a collaborative effort to use GPS technology to investigate relative plate motions and intraplate deformation in the Eastern Mediterranean region. At this point, the project involves MIT, Lamont-Doherty Geological Observatory, University of Colorado, WEGENER, and local participants from Greece and Turkey. Our major effort has been devoted to coordinating planned activities with the various participants and establishing a detailed field program for measurements in Turkey. Our primary objectives include:

- (1) To monitor strain accumulation and release along the major fault systems in Turkey with special emphasis on the North Anatolian fault (NAF) and East Anatolian fault (EAF).
- (2) To measure directly internal deformations of the Anatolian plate wedged between the Arabian, African, and Eurasian plates. These measurements include: a) Westward "escape" of the Anatolian plate; b) Eastward "escape" of the Northeast Anatolian block; c) North-south compression in Eastern Anatolia; and d) North-south extension in Western Anatolia.
- (3) To determine present-day relative movements of the African, Arabian, Anatolian, and Eurasian plates. This objective is an extension of the NASA/WEGENER Geodynamics Project to measure relative plate movements in the Eastern Mediterranean with Satellite Laser Ranging (SLR) observations.

While our participation in this project is being supported primarily by NSF, we report on it here because: a) it is directly relevant to interpretation of the SLR measurements in the eastern Mediterranean, b) NASA (Ted Flinn) has played a major role in coordinating the various groups involved, and c) NASA will likely provide logistical and data support for this field effort.

PUBLICATIONS

- Barka, A., and L. Gulen, Tectonic escape origin and complex evolution of the Erzincan pull-apart basin, eastern Turkey, *Geological Society of America Bulletin*, submitted, 1987.
- Barka, A., and K. Kadinsky-Cade, Strike-slip fault geometry in Turkey and its influence on earthquake activity, *Tectonics*, submitted, 1987.
- Barka, A., M.N. Toksoz, K. Kadinsky-Cade, and L. Gulen, The segmentation, seismicity and earthquake potential of the eastern part of the North Anatolian fault zone, *Tectonophysics*, in preparation, 1987.
- Barka, A., and K. Kadinsky-Cade, Strike-slip fault geometry and earthquake activity in Turkey, *EOS, Trans. Am. Geophys. Union*, 68, 362, 1987.
- Barka, A., K. Kadinsky-Cade, and M.N. Toksoz, North Anatolian fault geometry and earthquake activity, *Seismol. Res. Lett.*, 58, 31-32, 1987.

APPENDIX I

**STRIKE-SLIP FAULT GEOMETRY IN TURKEY AND ITS INFLUENCE
ON EARTHQUAKE ACTIVITY**

by

A. Barka and K. Kadinsky-Cade

Earth Resources Laboratory

Department of Earth, Atmospheric and Planetary Sciences

Massachusetts Institute of Technology

Cambridge, MA 02142

September, 1987

ABSTRACT

The geometry of Turkish strike-slip faults has been reviewed and described. From this data set it appears that fault geometry (the distribution of discontinuities such as bends and stepovers along the main fault trace) plays an important role in the segmentation of the Turkish fault zones into large earthquake rupture zones. Large earthquake ruptures generally do not propagate past individual stepovers that are wider than 5-10 km, or bends that have angles greater than 30° - 35° . Most important, however, is the effect on segmentation of the total "geometric pattern", i.e., the distribution of adjacent bends and stepovers based not only on distance from one another but also on relative discontinuity size. Certain geometric patterns are particularly common, and can be viewed as responsible for strain accumulation along portions of the fault zone. Fault geometry not only plays a role in segmentation, but also in characteristics of earthquake behavior. For example, large earthquake epicenters often occur near restraining bends or double bends. However, the epicenters are generally not observed within the actual restraining areas (i.e., along subsegments or within stepovers along the fault zone that are subject to a relatively high amount of compressive stress). Furthermore, aftershocks and swarm activity can often be associated with releasing areas (areas subject to a relatively large component of extension). The direction of block motion relative to the geometric pattern also plays an important role in earthquake occurrence and rupture behavior. The direction of block motion was constrained in this study using focal mechanisms and fault zone morphology.

INTRODUCTION

There has been a lot of recent interest in relationships between fault geometry, fault segmentation and seismic activity (e.g., Allen, 1988; Bakun *et al.*, 1980; Barka and Hancock, 1982; Koide, 1983; King and Nabelek, 1985; Bilham and Hurst, 1986; Slemmons and Depolo, 1986; Schwartz and Coppersmith, 1986; Sibson, 1986; King, 1986). The terms fault "geometry" and "segmentation" are taken here to mean respectively, (1) the distribution of bends and offsets along the main fault trace and (2) the rupture zone of a single large or great earthquake that has occurred recently or could be expected to occur in the future. Strike-slip faults lend themselves particularly well to the study of these relationships because variations in strike-slip fault geometry are easy to observe at the surface. Furthermore, because depths of shallow earthquakes are usually not as well constrained as their epicentral locations (except when the events are directly overlain by a seismic network), it is usually difficult to associate earthquake locations with geometric features at specified depths as would be required by the study of dip-slip fault geometry. In this study we examine the relationships between fault geometry, fault segmentation and seismic activity in detail, focusing on strike-slip fault geometry and earthquakes in Turkey. There is a wealth of data available for Turkish faults that has not been examined in a comprehensive way from this perspective. This region will be used as a case study. Results will be applicable to strike-slip faults in other parts of the world.

Fault Segmentation

The concept of fault segmentation is based on the observations that large earthquakes in major fault zones tend to have abutting rupture zones with very little overlap and that large earthquakes have been known to occur repeatedly along identical sections of a fault zone (e.g., Kelleher *et al.*, 1973; Ando, 1975; Nishenko and McCann, 1981; Sieh, 1981; Sykes and Nishenko, 1984). Based on an

examination of seismic and structural geology data in Turkey, we have settled on the following scheme for defining fault segments. We have used two independent data sources to determine segmentation: (a) the extent of surface rupture zones produced by large earthquakes when known, and (b) the location of "moderate" or "large" geometric discontinuities (see definitions below), as well as characteristics of seismicity along the fault zone.

Geometric discontinuities include stepovers (offsets in the fault trace) and bends (see Figure 1). From mapping active fault traces and surface ruptures produced by large earthquakes, it is clear that the main fault trace is discontinuous at many scales. For example, extensional features such as sag ponds or extension cracks (formed by releasing stepovers), and compressional features such as pressure ridges (formed by restraining stepovers) can occur at scales ranging from a few centimeters to several tens of meters. We have chosen to divide geometric discontinuities into three categories in this study: small, moderate and large. Each category has characteristic ranges of stepover width d and bend angle α : for small discontinuities $d < 1$ Km and $\alpha < 5^\circ$; for moderate discontinuities $d = 1-5$ Km and $\alpha = 5^\circ - 30^\circ$; and for large discontinuities $d > 5$ Km and $\alpha > 30^\circ$. These values are listed in Table 1. From observations made during the course of this study, we have determined that the small discontinuities are very common, and that they do not play an important role in earthquake rupture behavior, unless many of them occur in close proximity to one another and can effectively be added together to form a larger discontinuity.

During the procedure of defining fault segmentation we give first priority to the extent of surface rupture from large earthquakes. When the surface rupture crosses several moderate discontinuities, we divide the fault segments into subsegments. When there has not been a recent large earthquake along the fault zone, segmentation is defined by comparing fault geometry characteristics

with those of other fault segments that have experienced a recent large earthquake.

Distribution of geometric discontinuities with depth.

One difficulty in this analysis is that we cannot constrain how far the surface discontinuities extend through the crustal thickness. For example, two types of stepover are assumed to exist in cross-section. The first type involves a "flower-like structure" (Bakun *et al.*, 1980; Segall and Pollard, 1980; Harding, 1985; Naylor *et al.*, 1986). In this case the stepover does not extend through the whole crust. The segments separated by the stepover are connected at depth (Figure 1-Ca and Cb). Many sag ponds and pressure ridges may overlie these flower structures. The maximum width of this type of stepover can reach 10 km. This maximum width may be controlled by the thickness and rheology of the brittle-ductile zone at the top of the upper crust (see King, 1986). A single earthquake rupture may propagate through this type of stepover. The second type of stepover extends through the whole crust, thus really separating two different fault segments (Figure 1-Cc). This type may be characteristic of a more brittle upper crust. It can be as narrow as 1 km. The character of the earthquakes may be variable, both from one segment to the next across a stepover, and in the stepover region itself (characteristic size, focal mechanism, etc.) This second type of stepover is more likely to control fault segmentation than the first type. From surface observations alone we cannot distinguish between the two stepover types.

Tectonic Overview of Turkey

Major tectonic elements of Turkey and adjacent areas are illustrated in Figure 2. Northward motion of the Arabian plate relative to Eurasia causes lateral escape of the Anatolian block to the west (e.g., Ketin, 1948; McKenzie, 1972; Sengör, 1979) and the Northeast Anatolian block to the east. The North

Anatolian fault and the East Anatolian fault constitute the northern and southern boundaries, respectively, of the westward-moving Anatolian block. The motion of the Northeast Anatolian block is complicated by an extensive internal deformation of the block along conjugate faults.

In this study fault segmentation within four regions will be reviewed in detail. The location of these regions is shown in Figure 2. The regions include: (1) the main part of the North Anatolian fault (NAF) zone, (2) the western part of the NAF in the vicinity of the Sea of Marmara and Istanbul, (3) the East Anatolian Fault (EAF) zone, and (4) the complex conjugate fault system of the Northeast Anatolian block. After reviewing fault segmentation in these four regions, we shall discuss the factors that appear to control segmentation, and the distribution of large earthquake epicenters, foreshocks and aftershocks, relative to the fault segments.

SEGMENTATION OF MAJOR STRIKE-SLIP FAULT ZONES IN TURKEY

1) THE NORTH ANATOLIAN FAULT ZONE

The North Anatolian fault zone is a 1500 km long seismically active right-lateral strike-slip fault that takes up the relative motion between the Anatolian Block and Black Sea plate. This fault zone extends from the Karliova triple junction (39.3° N, 41.1° E; "K" in Figure 2) as far as mainland Greece. The main fault trace contains mainly moderate and large stepovers, bends or combinations of these discontinuities (Figure 3). Estimates of the age of the North Anatolian fault zone range from late Miocene to Pliocene (13-5 Ma; see, e.g., Ketin, 1969; Barka and Hancock, 1984; Sengör *et al.*, 1985). Estimates of the total relative displacement along the fault range from 25 to 120 km (e.g., Bergougnan, 1976; Seymen, 1975; Sengör, 1979; Barka, 1981; Barka and Hancock, 1984; Sengör *et al.*, 1985). Based on field observations by the first

author, we believe that the age of the NAF is uppermost Miocene to Pliocene, and that the total relative displacement varies from 40 km near Erzincan (Figure 3B) to approximately 15 km near the Marmara sea (decreasing to the west; Barka and Gülen, in press).

Between 1939 and 1967, most of the North-Anatolian fault ruptured in a westward-migrating series of 6 large earthquakes (magnitude 7-8), producing continuous surface breaks from Erzincan to the west end of the Mudurnu Valley (39.5°E - 31° E; see Ketin, 1948, 1969; Ambraseys, 1970, 1975). There is evidence for at least two other similar large earthquake sequences in the last 1000 years along the NAF zone: in 994-1045 and in 1667-1668 (Ambraseys, 1970, 1975; Ambraseys and Finkel, 1987). Focal mechanisms for moderate and large earthquakes along this portion of the fault zone are mostly pure right-lateral strike-slip solutions (Canitez and Ucer, 1967; McKenzie, 1972). Rates of slip along the North Anatolian fault zone are estimated at 0.5 - 0.8 cm/year from geological data (Tokay, 1973; Seymen, 1975; Barka and Hancock, 1984), and 1-11 cm/yr from seismological results (Brune, 1968; McKenzie, 1972; Canitez, 1973; Toksöz *et al.*, 1979). Segmentation of the North Anatolian fault will be described below by reference to segment numbers shown in Figure 3. The same procedure will be followed for other parts of Turkey, by reference to the appropriate figure in each case.

(1) This segment is roughly 50 km long, and extends from the Karliova triple junction to the stepover separating segments (1) and (2) (see Figure 3A). It has a clear physiographic expression (Allen, 1969), and includes a 16° smooth bend near its west end. The 8/17/49 earthquake ($M = 6.7-7$) is associated with this fault segment based on damage reports (Lahn, 1952), on a relocated epicenter (Dewey, 1976) that is only 10 km from the western end of the fault (with epicentral error 10-20 km) and on general agreement between earthquake

magnitude and fault length (based on $\log L = 0.78 M - 3.62$ for the North Anatolian fault system from Toksöz *et al.*, 1979). During the 1949 earthquake surface rupture over a length of at least 25 km occurred along this segment (Ambraseys, 1987 pers. comm.). The 1948 and 1968 earthquakes shown in Figure 3A occurred to the east of the intersection of the North and East Anatolian faults, based on surface breaks (Tasman, 1948; Wallace, 1968; Ketin, 1969; see also Barka *et al.*, 1987). Some of the large aftershocks of the 1968 Varto earthquake also created surface ruptures on the 1949 segment (segment 1; Ketin, 1969).

(2) This segment is 100 km long, and extends from the restraining stepover that separates it from segment (1) to the Erzincan releasing stepover (segment (3); see Figure 3B). According to Ambraseys (1975) the last large earthquake on this fault segment occurred in 1784. The surface rupture during that earthquake was 90 km long. An $M_s = 6$ earthquake occurred near the middle of segment (2) in 1967 (Dewey, 1976). It was characterized by pure strike-slip faulting (McKenzie, 1972), and produced a surface break approximately 4 km long with a horizontal slip of 20 cm (Ambraseys, 1975). This is the only segment along the North Anatolian fault zone between Varto (east of segment 1, Figure 3A) and the western end of the Mudurnu valley (western end of segment 8, Figure 4A) that has not experienced a large earthquake during this century. Segment (2) thus appears to be a seismic gap (for further discussion see Barka *et al.*, 1987).

3) This segment is defined by the extent of surface rupture produced by the 12/26/1939 Great Erzincan earthquake ($M_s = 8$). Segment (3) is divided into 4 subsegments. Subsegment 3a is 60 km long, and has a strong physiographic expression in its western half. It is separated from segment (2) by a 4-5 km wide releasing stepover which forms the Erzincan basin. This basin is characterized by short en-echelon strike-slip faults and contemporaneous volcanics.

Subsegment 3a is separated from 3b by a 20° restraining bend (Tatar, 1978; Barka, 1981). Subsegment 3b is about 100 km long, and extends from this bend, situated about 10 km NW of the Erzincan basin, to Susehri - the location of another pull-apart basin (Hempton and Dunn, 1984). The Susehri stepover is located between boxes b and c in the inset map of Figure 3. Subsegment 3c extends from Susehri to the Niksar basin, through the Kelkit valley. It is 110 km long and relatively straight. Southwest of the Niksar basin a 15° restraining bend separates subsegment 3c from 3d. Subsegment 3d is 90 km long and ends south of Amasya where the 1939 earthquake rupture stopped.

The epicenter of the 1939 Great Erzincan earthquake was located near the 20° restraining bend separating subsegments 3a and 3b. Many of the 1939 earthquake aftershocks caused damage in the Erzincan and Niksar pull-apart basins (Ergin *et al.*, 1987; Tabban, 1980; see also Riad and Meyer, 1983). A fault plane solution for a moderate size earthquake ($m_b = 4.8$, 11/18/1983) near the city of Erzincan is characterized by ENE-WSW extension (International Seismological Centre Bulletin solution) in agreement with our interpreted pull-apart character of the Erzincan basin.

(4) This segment is 50 km long, and defined by the $M_s = 7$ earthquake of 11/20/1942. Segment (4) extends from Niksar to the Erbaa basin. It contains a 14° sharp restraining bend north of Erbaa. Pull-apart basins separate segments (3c) from (4) and (4) from (5) (south of Niksar and between Erbaa and Tasova; see Figure 3c). Dewey's relocated epicenter for the 1942 earthquake is not well constrained. Isoseismals for this event (Blumenthal, 1943; 1945a,b; Pamir and Akyol, 1943) outline a zone of maximum intensity ($I=IX$) along the fault segment that is about 5 km long and centered on the 14° sharp bend north of Erbaa. The rupture zone for this event extended along the full length of segment (4) (Dewey, 1976; Gündođdu, 1984).

(5) This segment is 250 km long, and extends from east of Tasova (Figure 3c) to northwest of Kursunlu (Figure 3d). It is defined by the rupture zone of the 11/20/1943 $M_s = 7.3$ earthquake. Segment (5) has two bends: a smooth bend (about 25°) in the eastern part between Tasova and Kargi, and a sharp bend at 34° E, north of Tosya (about 15°). Subsegment 5a corresponds to the smooth bend area, and contains three releasing stepovers. From west to east these are located at Kargi (41.1° N, 34.4° E), with fault separation 1 km; at 41.1° N, 35.2° E, with fault separation 1.5 km, and at 40.9° N, 36.0° E, with separation 1 km. Only the second stepover exhibits a clear pull-apart morphology (Ladik Lake). Subsegment 5b comprises the fault zone west of the sharp bend, and contains several small releasing stepovers in the area just north of Kursunlu-Ilgaz. The westernmost stepover is about 1.5 km wide, and defines the termination of segment 5. The relocated epicenter of the 1943 earthquake ($M = 7.3$) is not well constrained (± 20 -30 km; Dewey, 1976), but was definitely located near the western end of segment (5) (near Tosya; see also relocations by Alsan *et al.*, 1975, and Canitez and Büyükasikoglu, 1984). The area of maximum damage during this event was also Tosya near the 15° restraining sharp bend (Figure 3D). The 1943 earthquake caused surface breaks along the full length of segment (5) (Ketin, 1948, 1969; Ambraseys, 1970). Aftershocks of the 1943 earthquake (Karnik, 1969; magnitudes 4.5-5.) appear to have occurred near the western end of the fault, although these events have not been relocated.

(6) This segment is about 180 km long, and extends from the area northwest of Kursunlu (Bayramoren) to Abant Lake (Figures 3D, 4A). the surface rupture of the 1944 earthquake ($M = 7.3$) covered this whole segment (Ketin, 1948, 1969; Ambraseys, 1970). The relocated epicenter of the 1944 event (Dewey, 1976) occurred at the east end of segment (6), north of Cerkes. Aftershocks of the 1944 earthquake with magnitude $M > 5$ were mostly concentrated near the ends

of segment (6) (Ambraseys and Zatopek, 1969; Dewey, 1976) and caused additional damage at Düzce and Gerede, and in the Mudurnu Valley (Ambraseys and Zatopek, 1969; Dewey, 1976; Riad and Meyers, 1985). The area of the 1.5 km releasing stepover that separates segments (5) and (6) just northwest of Kursunlu has been the site of continuous earthquake activity (small and moderate-sized events), both before and after the 1943 earthquake sequence. A survey conducted by one of the authors of this paper (A. Barka) in the towns of Cerkes, Kursunlu, Ilgaz and Tosya (Figure 3D) indicates that the 1943 earthquake only damaged the region east of Kursunlu, whereas damage from the 1944 earthquake was restricted to areas west of Kursunlu. The town of Kursunlu and surrounding villages were most affected not by the 1943 and 1944 events, but by an $M_5=6.8$ earthquake that occurred in 1951 along a strike-slip fault parallel to the main trace (Pinar, 1953). This earthquake also caused reactivation of the eastern part of the 1944 rupture zone (Pinar, 1953). Segment 6 is relatively straight, except for a 15° restraining double bend that is located 10 km east of Ismetpasa ($40.^\circ$ N, 32.6° E; Tokay, 1973). Fault creep at Ismetpasa, first recognized by Ambraseys (1970), is about 1 cm/year (Aytun, 1982). Segment 6 has been subdivided (6a, b, c) to reflect different characteristics of recent seismicity along the segment. Subsegment 6a, along with 5b, has been subject to continuous background activity (e.g., Dewey, 1976). Subsegment 6b is the restraining double bend area. Subsegment 6c is much straighter than the others, and has been undergoing aseismic creep at least at its eastern end.

II) THE MARMARA SEA REGION

A) Onshore areas

In these areas segmentation is defined both by the location of geometric discontinuities and by surface ruptures corresponding to known earthquakes.

Several segments correspond to portions of the fault that have not ruptured recently, but that have the potential to rupture by analogy with nearby ruptured segments. To the west of segments (7), (8) and (9) (see Figure 4A) the NAF can be divided into three strands (Southern, Middle, and Northern strands). This division is based on field observations, offshore bathymetry and some surface breaks for large earthquakes. After a review of segments (7) - (9), the three strands will be described separately.

(7), (8) and (9) Segments 7 and 8 are 45 and 79 km long respectively, and are separated by a restraining double bend. The 1957 $M_s = 7.0$ earthquake caused surface breaks to occur along most of segment 7. During the 1967 $M_s = 6.8$ earthquake the westernmost 20 km of segment 7 reruptured in addition to segment 8. Surface displacement on the reruptured fault segment was smaller, however, than that on segment 8 (Ambraseys and Zatopek, 1969). The relocated epicenters for the 1957 and 1967 earthquakes are both very near the zone of overlap between segments 7 and 8 (Dewey, 1976). The epicentral locations and surface breaks for these events (although the surface breaks are much better documented for the 1967 shock than for the 1957 case; see Ambraseys and Zatopek, 1969; Ambraseys, 1970) suggest that both earthquakes ruptured away from the zone of overlap: 1967 to the west and 1957 to the east. The eastern end of segment 7 corresponds to a directional change in the fault which is 11° between segments 6 and 7. Observations of slip produced by the 1967 earthquake (Ambraseys and Zatopek, 1969; Ambraseys, 1970) show that in general the ratio of strike-slip to dip-slip motion along the main fault trace decreases towards the west and northwest as the strike of the fault changes. The largest aftershock (1967/7/30; $M=5.6$) of the 1967 earthquake occurred at the west end of segment 8, south of Adapazari. It had a normal faulting focal mechanism, with extension in a NE-SW direction (McKenzie, 1972). This type of

mechanism and the reduced strike-slip to dip-slip ratio at the west end of the fault appear to be caused by the change in trend of the fault segment from NE-SW to WNW-ESE. The appearance of normal faulting west of 30.5° E has been noted by McKenzie (1972, 1978), Evans *et al.* (1984) and Jackson and McKenzie (1984) as well. The exact location of the 1943/8/20 earthquake ($M = 6.5$, Figure 4A) is not well known. It caused most damage in the towns of Adapazari and Hendek, and its relocated epicenter (Dewey, 1976) lies between those towns as well. It could be related to segment 9, which is active based on field observations by one of the authors (A. Barka), or to the western half of segment 8.

Southern Strand

From a review of available literature concerning historical earthquakes that have occurred near the Marmara Sea during the past 2000 years it appears that there is no evidence for significant seismic activity along the southern strand before the Nineteenth Century (except for an earthquake in 170 AD, which caused intensity IX-X effects in Manyas (Figure 4c; see Sipahioglu, 1983). However, since 1855 at least four large earthquakes have occurred along the Southern strand. A combination of rupture zones caused by these events and of geometric discontinuities along the Southern strand has been used to divide the strand into segments.

(10) - (13) The two NE-SW trending strike-slip faults forming segment 10 (Figure 4B) bound the Yenisehir Basin, which is considered here to be a pull-apart basin from examination of aerial photographs. Segment 11 (Figure 4C) trends E-W and is dominated by normal faulting, and 12 is a NE-SW trending segment dominated by right-lateral strike-slip motion. The last large earthquakes to occur on these segments were two intensity IX events in 1855 (Sandison, 1855; Sieberg, 1932; Ergin *et al.*, 1967; Karnik, 1971; Soysal *et al.*, 1981). The first event (Feb. 28, 1855) caused damage near segment 12, whereas the second event (April 11,

1855) produced extensive damage mostly to the north of Bursa, near segment 11 (Sandison, 1855). In segments 10, 11, and 12 NE-SW trending faults are associated with predominantly strike-slip motion, whereas E-W trending faults exhibit a predominantly normal slip motion that is clearly identifiable in the surface morphology of the region. The extensive damage to the north of Bursa during the April 11, 1855 event is compatible with the north-dipping geometry of the E-W trending segment 11, which is clearly reflected by the fault morphology. Segment 13 is composed of poorly-defined NW-SE trending surface breaks characterized by NE-SW extension. The 1964 $M=6.8$ earthquake had a NW-SE trending pure dip-slip mechanism with NE-SW extension (McKenzie, 1972, 1978). Surface ruptures for this earthquake, as mapped by Erentöz and Kurtman (1984) and by Ketin (1966), confirm the extensional nature of this segment. Dewey's (1976) relocated epicenter for the 1964 event is well constrained and lies only about 15 km north of the mapped surface breaks.

(14) - (15) The Yenice-Gönen segment (14) experienced a magnitude 7.2 right-lateral strike-slip earthquake in 1953 (McKenzie, 1972; Dewey, 1976). The mapped surface break for this event was 50 km long (Ketin and Roesli, 1953). No previous historical activity has been recorded for this segment. Segment (14) includes a restraining double bend with a bend angle of 17° . Segment (15) is separated from (14) by a ~ 15 km wide restraining stepover that extends from Pazarköy to Edremit (Bingöl *et al.*, 1973). We have found no information about historical activity on segment (15) which continues to the southwest as far as the Aegean Sea.

In summary, the Southern strand between Yenisehir and Edremit contains two segments for which there is no evidence for recent rupture: segments (10) and (15).

Middle Strand

According to reliable records, the middle strand is not known to have experienced any large earthquakes for at least 200 years. From an examination of historical records, the last known large earthquake in this area occurred in 1064 A.D. Fault segmentation is thus defined by the distribution of geometric discontinuities and by analogy with already ruptured segments along the northern and southern strands.

(16) Although this segment has not experienced any large earthquakes during this century, it is very distinct morphologically. The NE end of segment 16 splays off clearly from segment 8. About 10 km west of the splay area the fault zone widens and turns into many short subparallel segments as it changes direction towards the SW by 17°. In contrast, the main part of segment 16 to the SW of this directional change, is narrower and more distinct. Segment 16 terminates at a releasing stepover near Geyve which is characterized by a pull-apart morphology.

(17) The NW side of the Geyve pull-apart is the NE end of segment 17. This segment passes south of Iznik (Figure 4B), and skirts the southern shore of Lake Iznik. It changes direction at Sölöz and then terminates abruptly as shown in Figure 4B. The region near segment 17 has not experienced a known large earthquake since 1064 (Sieberg, 1932; Sipahioglu, 1983).

(18) Segment 18 consists of three subsegments. The two western ones trend ENE-WSW (Figure 4B; subsegments 18b, 18c). They are parallel to each other, separated by 4-7 km, and have lengths 20 and 35 km respectively. The eastern subsegment trends E-W, extends from Soloz to Gemlik, and is approximately 25 km long (Figure 4B, subsegment 18a). The onshore portion of subsegments 18b and 18c is clearly visible at the surface. The offshore portions of these

subsegments are inferred from unpublished seismic reflection data and bathymetry (personal communication; M.T.A., 1984) and by comparison with a similar geometric fault pattern near Izmit (segments 24a, b in Figure 4B; to be discussed later).

(19) This segment is composed of two strands. The first strand has an onshore portion that is morphologically distinct. The offshore portion of both strands is inferred from the shape of Bandirma Bay from bathymetric observations and by comparison with the interpreted geometry of segments 18 and 24 (Figure 4B). Segment 19 has not experienced an earthquake with intensity larger than VII in the last 1400 years; the area was last seriously damaged by an earthquake in 543 (Sieberg, 1932; Soysal *et al.*, 1981).

The offshore fault pattern in the Southern Marmara Sea between segments 18 and 19 (Figures 4B-4C) is not clear. This area could be similar to the segment 13 area (a normal fault segment separating two strike-slip faults) or alternatively it could be made up of a series of releasing en-echelon strike slip faults. Two historical earthquakes which may have some relation to this part of the fault zone occurred in 985 and 1084. These events were felt strongly between Bandirma and Gemlik (Sipahioglu, 1983).

(20) This segment has not experienced any known earthquakes historically, but that may be due to the sparse population in the area. Segment 20 is very clear in aerial photographs. It can also be seen on LANDSAT images (McKenzie, 1978). Its morphological expression is much clearer than that of segment 14. Segment 20 has a sharp restraining bend in its central part (17-18°) and a classic pull-apart basin (containing the village Asagiinova, which means "descending into a plain") at location x in Figure 4C.

(21) This segment extends from Can to Bayramic. It has a 15°-20° sharp bend

near its southwest end, north of Bayramic (Bingöl *et al.*, 1973). No earthquakes have been reported historically along this segment.

(22) The southwest continuation of the fault zone beyond segment 21 has not been studied so far. However, this branch of the fault zone (loosely labelled segment 22) appears to continue towards the southwest as far as Ezine (Bingöl *et al.*, 1973). Subsequently it may continue into the Aegean Sea.

Northern Strand

Most of this strand lies offshore, beneath the northern half of the Marmara Sea. In this section we shall review the onshore segments that can be identified and described based on field surveys. In the next section we shall present our interpretation of the offshore structures and segmentation.

(23)-(24) Segment 23 extends from Sapanca Lake through Gölcük, where it changes direction and continues to the SW (see Figure 4B). This directional change is 20°. Segment 24a is separated from segment 23 by a releasing stepover that is about 4-5 km wide (Izmit Bay). Segment 24b is separated from segment 24a by another releasing stepover, also about 7 km wide. In these three segments (24a, 24b, and the western part of 23) the NE-SW trending fault branches are dominated by right-lateral strike-slip motion, whereas the eastern half of segment 23, which trends E-W, has a combination of normal slip and strike-slip motion. This difference is clearly reflected in the morphology of the area. Although historical earthquakes have damaged Izmit and Karamürsel frequently (Sipahioglu, 1983), this region has not experienced a large earthquake during the 20th century. Toksöz *et al.*, (1979) consider this area to be a seismic gap. The most recent notable earthquakes to have affected the segment 23-24 area occurred in 1878 (Izmit-Sapanca Lake region; estimated maximum magnitude 6.7 according to Karnik, 1971) and in 1894 (intensity IX,

damaging the area between Izmit and Istanbul; see Eginitis, 1894, 1895). Until now the area extending from Sapanca lake through the Gulf of Izmit has been considered to be a single through-going graben characterized by N-S extension (Crampin and Evans, 1986). The interpretation described here, which includes segments 23, 24a and 24b, is derived by extending aerial photograph observations and detailed field work by one of the authors (A.B.) offshore along bathymetric trends.

(25) This segment is located at the west end of the Marmara Sea. It has a 14° restraining bend in the central part and a 5 km restraining stepover at its eastern end which creates the Ganos mountains ("GM" in Figure 4D). The 1912 $M_s = 7.3$ earthquake produced surface rupture along most of segment 25 (Macovei, 1912; Karnik, 1971; Tabban and Ates, 1976; Ambraseys and Finkel, 1987). The eastern and western ends of the segment run into the western Marmara basin and Saros basin respectively (Lyberis, 1984; Le Pichon *et al.*, 1984) both of which are interpreted here as pull-apart basins.

B) Offshore areas

The Marmara Sea is composed of a series of basins and ridges that are discontinuous in nature. Our interpretation of the distribution of active fault segments beneath the Marmara Sea is shown in Figure 5. This interpretation is much less well constrained than that in the onshore areas. It is put forward here in an attempt to provide a comprehensive model of active fault trends in northwestern Turkey. The deepest part of the sea is the northern half. Basins A, B and C are approximately 1152, 1265 and 1276 meters deep respectively. The depths of intervening ridges are 648 m between A and B, and 450 m between B and C (Pfannenstiel, 1944; Turkish Navy bathymetry map, 1984). The northern half of the Marmara Sea is interpreted as a large pull-apart basin between

segments 24 and 25 (Figure 4). This basin is subdivided into smaller basins (A, B, C) separated by strike-slip fault segments trending NE-SW. The southern half of the Marmara Sea is shallower than 100 m, but can also be divided into ridges and basins which are visible on reflection profiles (Marathon, 1974). A reexamination of these profiles suggests that the size of these structures and the amount of vertical offset along bounding faults are smaller in the southern half of the Marmara Sea than in the northern half. The interpretation shown in Figure 5 results from an extrapolation of onshore fault geometry, from bathymetry and from examination of seismic reflection profiles. The normal faults bounding the basins are unmistakable features on the reflection profiles. In contrast the strike-slip faults are zones of disturbed and discontinuous reflectors, more difficult to interpret, that can be traced from one profile to the next, often crossing several profiles. The strike-slip faults are less well imaged by the seismic reflection technique due to their near-vertical dip.

The interpretation presented in Figure 5 is different from previous ones in the area. It is based on the onshore results described above. In Figure 6 four other interpretations are shown. In Figure 6B, Pinar (1943) correctly identifies faults south of the Marmara sea (including segment 14, that would later rupture in 1953), but simply draws a line through the Marmara Sea basins, interpreting their origin as tectonic. In Figure 6C, Pfannenstiel (1944) describes the northern ridges and basins as normal fault-bounded horsts and grabens, and suggests that the basins are connected by NE-SW trending faults. In Figure 6D, Sengör (1986) includes basins C and A (as labeled in Figure 5), and connects them with a suspected fault. In Figure 6E, Crampin and Evans (1986) consider the Marmara Sea to be one long E-W trending graben. Figure 6A is our interpretation for comparison. It is characterized by long NE-SW trending strike-slip faults separated by pull-apart areas. This model is by no means finalized, however. Future work needs to be done in the offshore areas.

Historical earthquake activity in the Marmara Sea region indicates that the fault system in the northern half of the sea is more active than in the southern half. Istanbul, on the North Shore, has been repeatedly affected by damaging (I>VIII) earthquakes throughout historical record (about 2000 years; see, e.g., Ambraseys, 1971; Soysal *et al.*, 1981), whereas Bandirma, Bursa, and Iznik, along the south shore, have been damaged much less frequently (Sipahioglu, 1983). The area of maximum damage caused by the 1894 Istanbul earthquake (I=IX; see Eginitis, 1894, 1895), may coincide with two major strike-slip fault segments, 24a and 24b. The size of the earthquake and the combined length of the fault segments are quite comparable. The only focal mechanism available from the northern half of the Marmara Sea is that of the 1963 earthquake located near basin C (see Figure 5), which is characterized by NNE-SSW extension (McKenzie, 1972).

Microseismicity in the Marmara Sea region (both onshore and offshore), recorded during the past 10 years, exhibits a swarm-like character (Ucer *et al.*, 1985) with swarms concentrated mostly near our inferred pull-apart basins, and also near normal faults that have a strike-slip component (e.g., segments 11 and 23).

In conclusion, we feel that the offshore structures in the Marmara Sea are consistent with a simple offshore extrapolation of onshore structures around the Marmara Sea. Thus the area could be described as a series of long strike slip-faults separated by pull-apart basins. The latter would be associated with bathymetric lows, concentrations of microseismicity, and extensional focal mechanisms such as that of the 1963 earthquake. Further data are needed to verify this model.

III) THE EAST ANATOLIAN FAULT ZONE

Relative motion between the Anatolian Block and the Arabian plate is taken up by the left-lateral East Anatolian fault zone. This fault zone extends from the Karliova triple junction (39.3° N, 41.1° E) to the Mediterranean (see Figures 1 and 7). The East Anatolian fault zone is similar in many ways to the North Anatolian fault zone. It is characterized by a series of major discontinuities (bends and stepovers). The age of the fault zone is Pliocene (Arpat and Saroglu, 1972, 1975) and the total displacement along the fault has been 22-27 km (Arpat and Saroglu, 1972, 1975; Yalcin, 1978). This implies a geological slip rate of about 0.5 cm/yr, which is comparable to that along the NAF zone (see also Dewey *et al.*, 1986). Only a few $M > 6.5$ earthquakes have occurred during this century along the East Anatolian fault (EAF) zone: in 1905, 1908 and 1971. The 1971 $M=6.7$ Bingöl earthquake, which occurred near the northeast end of the fault zone, had a pure left-lateral strike-slip mechanism (McKenzie, 1972). However, the fault zone is known to have experienced several intensity \geq VIII earthquakes historically. Most of these events occurred within the first 1000 years A.D. (Ambraseys, 1970). In addition, some earthquakes caused damage in towns along the fault zone after 1000 A.D. (Soysal *et al.*, 1981). These were mostly concentrated near the NE and SW ends of the fault zone, but cannot be tied to specific segments.

(1) This segment extends from the Karliova triple junction to Bingöl (Figure 7). It is about 60 km long and is composed of many closely-spaced parallel strike-slip fault strands. A detailed map of these fault traces is provided by Arpat and Saroglu (1972). The 1971 Bingöl earthquake ($M = 6.7$) produced surface breaks mostly along the southwestern half of segment 1 (Seymen and Aydin, 1972; Arpat and Saroglu, 1972). The relocated epicenter for the 1971 earthquake is at the southwestern end of the surface breaks (Dewey, 1976). Two historical

earthquakes of a similar size have been documented for the general area surrounding this segment (1789 and 1875; exact locations not known; see Soysal *et al.*, 1981).

(2) This segment can best be described as a restraining double bend. It extends from Hazar Lake to Genc (see Figure 7a). It can be divided into 3 subsegments: a straight section between Hazar Lake and Palu (2a), a restraining area near Gokdere (2b), and a continuation section near Genc (2c). The restraining bend angle at Palu is about 30° . The restraining area is characterized by thrusting and folding structures (Arpat and Saroglu, 1972; Sengör *et al.*, 1985). The largest known and most recent seriously destructive earthquake along the EAF zone occurred in 995 A.D. (Ambraseys, 1970) along segment 2. This earthquake damaged towns all along segment 2, and had a particularly destructive effect on the area between Palu and Gökdere (double bend area), where streams were diverted (Ambraseys, 1970). Within this century a number of moderate-sized earthquakes have affected segment 2, particularly since about 1948 (e.g., Tabban, 1980).

The Palu-Hazar trend of subsegment 2a continues to the southwest as far as Hazar lake (Figure 7d), over a distance of about 125 km. The directional change between this trend and that of segment 1 (Bingöl-Karliova segment) is 19° . The extended trend of segment 2a may be related to the proximity of the Bitlis thrust system, which is located just southeast of and adjacent to the fault zone in that area. The strike of the thrust system is approximately parallel to the EAF zone. This situation suggests that the fault zone is subject to a relatively high convergent strain in this area (see also Jackson and McKenzie, 1984; Sengör *et al.*, 1985).

(3) This segment is about 50 km long, and is centered north of Pötürge (Figure 7B). The northeast end of the segment, near Keferdiz, is a 17° restraining bend.

The historical site of Claudius (coinciding approximately with Keferdiz) experienced at least four damaging earthquakes in the period 10-1000 A.D. (Ambraseys, 1970), but the exact location of these events relative to segment (3) is unknown. Ambraseys and Finkel (1987) recently suggested that the 1908 M=6.7 earthquake may have been associated with this segment. This event would not have been large enough to rupture all of segment 3.

(4) This segment runs mostly along the Siro valley, between a 2 km wide releasing stepover at its northeast end and a 7.5 km wide restraining stepover near Celikhan. Segment 4 ruptured during the 1905 M = 6.8 Malatya earthquake (Ambraseys and Finkel, 1987).

(5) Segment 5 corresponds to the Celikhan restraining area. It has been deformed by extensive thrusting and folding which is directly connected to the main Bitlis frontal thrust system. A moderate size earthquake (6/14/84, M = 5.9, Jackson and McKenzie, 1984) was relocated by Dewey (1976) within the restraining area. Its focal mechanism was characterized by east-west extension.

(6) This segment is about 70 km long, and extends from the Celikhan restraining bend area to the Gölbaşı releasing area shown in Figure 7d. A pair of moderate-size-earthquakes occurred recently in this area (May 5, 1986; Erdik, 1986). The first event was located northeast of Gölbaşı (Bayraktutan, pers. comm., 1987). Its focal mechanism indicates NE-SW compression, resulting in a combination of thrusting and left-lateral strike-slip faulting on a north-dipping fault (based on Harvard moment tensor solution in U.S. Geological Survey Earthquake Data Report). The second event had a pure strike-slip mechanism (from Harvard moment tensor solution in U.S. Geological Survey Earthquake Data Report) that was consistent with left lateral slip on the East Anatolian fault near the Sürgü splay fault.

(7) We are defining segment 7 to extend from the Gölbası area at least as far as the Türkoglu triple junction (a length of 90 km). This segment has been mapped by Yalcin (1978). The East Anatolian fault continues towards the southwest beyond its intersection with the Dead Sea fault. When it reaches the NE end of the Adana basin, the East Anatolian fault changes direction towards the southwest, where it becomes the Misis-Yumurtalik fault segment (Figure 1; Ketin, 1948; McKenzie, 1976; Sengör *et al.*, 1985; Gülen *et al.*, 1987). Segment (7) contains a small double bend (Figure 7e: (x), (y)). The portion of segment (7) that lies between (x) and (y) makes an angle of 18° with the fault trace on either side, is characterized by P-shear, and acts as a 1.5 km wide restraining area. Several moderate-sized earthquakes have occurred in the segment 7 area during this century, as defined by damage at or near the nearby town of K. Maras (Tabban, 1980; Ercan, 1982). The last seriously damaging earthquakes near Maras-Ceyhan occurred in 1114-1115 (Sieberg, 1932; Salomon-Calvi, 1941; Soysal *et al.*, 1981), but descriptions of damage are not detailed enough to assign these events to a specific fault segment. The Gölbası area which separates segments 6 and 7 is a 13 km wide releasing bend and stepover combination. It has R-shear characteristics. The bend angle between segments 6 and 7a is about 18° . In the Gölbası area the fault zone is divided into two main strands. These are separated from each other by a series of lakes, which are caused by the pull-apart geometry. There are no known damaging earthquakes in this area in the historical record.

A few general speculative comments can be made about the EAF zone as compared with the NAF zone. Although the total displacement along these fault zones are comparable, the characteristic earthquake sizes and recurrence times are likely to be different. This is due to differences in fault geometry between the two zones: (a) Major geometric discontinuities along the fault zone are more

closely spaced in the EAF case than in the NAF case, making the EAF segments shorter than the NAF segments. (b) The two major restraining features (segments 2b and 5) along the EAF zone contribute to a longer recurrence time for larger earthquakes than in the NAF case. There is evidence in the historical record, for example, that the NAF near Erzincan has experienced a great earthquake every 300 years (Barka *et al.*, 1987), whereas the historical record for the EAF zone suggests a longer recurrence interval of, perhaps, 1000 years. Segment 2 is the longest segment along the EAF zone, and is capable of experiencing very large earthquakes due to its large restraining double bend geometry. Almost 1000 years have elapsed since the last earthquake occurred in this area. Ignoring possible creep effects, or other inelastic deformation, as much as 5 m of left-lateral strain may have accumulated along this segment (0.5 cm/yr, 1000 years).

IV) NORTHEASTERN TURKEY BLOCK

The Eastern Turkey block, a wedge-shaped region located to the east of 39° E, is bounded by the Northeast Anatolian fault to the north and by the North Anatolian fault zone and its eastward extension to the south (see Figure 1). East of 41.5° E this southern boundary disappears: it is no longer defined by surface morphology or seismological observations (Tchalenko, 1977). The Eastern Turkey block differs from the Anatolian block to the west in that strain is released by internal fault zones (mozaic structure) in the former, whereas in the latter most of the strain is released along major boundary faults. Internal deformation in the Eastern Turkey block occurs along the following structures; (a) NNE-SSW and/or NE-SW trending left-lateral strike-slip faults, (b) NW-SE trending right-lateral strike-slip faults, (c) E-W trending thrusts and folds, and (d) N-S trending extension cracks (Arpat *et al.*, 1977; Sengör, 1980; Saroglu and Guner, 1981; Saroglu and Yilmaz, 1985; Saroglu, 1985).

This phase of deformation in the Eastern Turkey block began in Late Miocene time (Sengör *et al.*, 1985). Large earthquakes within the last century in this region have occurred mostly along the strike-slip faults (e.g., Toksöz *et al.*, 1977; Toksöz *et al.*, 1983; Eyidogan *et al.*, 1986).

We shall restrict our attention in this area to strike-slip faults, although not all of these strike-slip fault segments have experienced large earthquakes during this century.

Horasan -Narman fault zone (Figure 8A)

This strike-slip fault zone is about 50 km long, and is characterized by left-lateral strike-slip motion. At the surface the fault zone is divided into many short parallel segments, forming a shear zone that is about 5 km wide. An abrupt change in strike (about 15°-16°) occurs NNW of Horasan. On 10/30/83 a magnitude 6.9 earthquake occurred along this fault zone, north of the bend. Surface breaks and the highest intensities produced by this event were both located within 20 km and northeast of the bend (Barka *et al.*, 1983). More than 3000 aftershocks were recorded during a portable network survey in the epicentral area (Toksöz *et al.*, 1983; Eyidogan *et al.*, 1986). The aftershocks were clustered near the zone of highest intensity during the first month, and then migrated away from the bend. Most of the aftershock migration was to the northeast along the fault zone, although some aftershocks were recorded southwest of the bend and on either side of the main fault zone. Although the 1983 earthquake had a focal mechanism that was predominantly left-lateral strike-slip with a small thrust component (Eyidogan *et al.*, 1986), the continuation of the fault zone southwest of the bend could be expected to rupture (in the future) with a higher component of thrusting.

Caldiran fault (Figure 8B)

This fault is approximately 50 km long, and contains a 17°-19° bend near Caldiran (Arpat *et al.*, 1977; Toksöz *et al.*, 1977). According to seismic waveform modeling, the 1976 Caldiran earthquake (M=7.3) ruptured the fault bilaterally starting from the bend (surface and body wave modeling; see King and Nabelek, 1985).

Baliköglü fault (Figure 8C)

This fault zone is about 80 m long in Turkey, and extends into Iran where it is called the Northwest Fault System (Tchalenko, 1977). The Turkish section has been mapped in detail by Arpat *et al.* (1977). It consists of many small subparallel segments, some of which may combine at depth. The northwestern section is divided into 2 branches with an angular separation of about 35°. This geometry creates a releasing area, a "negative flower structure" (Harding, 1985), characterized by an abundance of N-S trending normal faults and the presence of a lake. Southeast of that area the two branches converge, and the motion on the fault has a larger strike-slip component. A short segment near Dogubeyazit is separated from the main fault strand. It is bounded by a releasing stepover at one end and a restraining stepover at the other end. According to Ambraseys and Melville (1982) an earthquake of intensity IX (known as the "Ararat earthquake") occurred on the Turkish part of the Baliköglü fault in 1840.

Tutak and Karayazi faults (Figure 8D)

The Tutak fault is about 95 km long and has been mapped by Saroglu and Güner (1979). It includes a 19° bend near Mizrak. Northwest of that bend the fault segment is parallel to the Karayazi fault (mapped by Kocyigit, 1985) and the area between the parallel segments is a 16 km wide restraining stepover. Southeast of the bend the Tutak fault is not represented by a continuous surface

trace. In the middle of that southeast segment in particular, the fault is broken up into short discontinuous pieces. Saroglu and Güner (1979) assume that the Tutak fault is active, based on a fault morphology which is very similar to that of the Caldiran fault and on the existence of many relics of destroyed sites. However, details of these historical events are not well known. Both the Tutak and Karayazi faults are clearly visible in aerial photographs.

Erzurum fault zone (Figure 8E)

This is a 5-10 km wide left-lateral shear zone. Its southern end truncates a series of ENE-WSW trending thrust faults. Near its northern end the Erzurum fault zone changes direction abruptly (a 30° restraining bend). Immediately northeast of that bend the fault zone still has a predominantly strike-slip character, distinctly different from the southwest trending thrust faults south of Erzurum. The town of Erzurum has experienced several earthquakes historically. Records of activity go back as far as 1200 A.D. with notable events occurring in 1482 (30,000 people killed) and 1859 (heavy damage in the vicinity of Erzurum, in particular along the southern thrust system; see Karnik, 1969), and many moderate size earthquakes listed for the 18th and 19th centuries (Sipahioglu, 1983). Both the left-lateral strike-slip fault zone and southern thrust fault appear to be active, as evidenced by displaced streams and other morphological features (Barka *et al.*, 1983; Saroglu, 1985; Barka and Bayraktutan, 1985; Kocyigit *et al.*, 1985).

DISCUSSION

From the Turkish data it can be seen that a finite number of geometric patterns recur in the segmentation, with some being more common than others. This point is illustrated by the classification of geometric patterns shown in Figure 9. All of the earthquakes with known surface rupture discussed earlier in this study have been fit in the categories of Figure 9. Unruptured segments are shown on the right. They have been recognized as possible future ruptured segments based on (poorly known) rupture in the historical record and/or comparison of fault geometry with that of ruptured segments in the central column of Figure 9. Geometric patterns such as those in Figure 9 can be associated with strike-slip earthquakes in other parts of the world as well. A compilation of these data is currently under way (Barka and Kadinsky-Cade, in prep.).

Segmentation appears from these data to be caused by two main factors: (1) the distribution of moderate to large geometric discontinuities (as defined in Table 1) along the fault zone, and (2) the direction of block motion relative to the main trend of the fault zone (as evidenced, for example, by earthquake slip vectors). These effects will be discussed in the cases of restraining and releasing discontinuities.

Restraining discontinuities

From Figure 9 the restraining bends associated with ruptured segments mostly fall into the "moderate" category of Table 1 (5° - 30°). Smaller bends seem to neither impede nor concentrate earthquake rupture. Larger bends are not present in our data set, although one situation where larger bends may have actually prevented the propagation of earthquake rupture is at the 40° Manyas-Gönen restraining bend separating the 1953 and 1964 earthquakes (NAF segments 13-14). Moderate size restraining bends tend to occur within the

rupture zone rather than at either end of it, and are very common. We feel that the change in fault direction may cause strain to accumulate along the fault strand located on one side of the bend, the restraining side (that which offers most resistance to fault slip due to its orientation relative to the direction of block motion), so that fault bends may actually contribute to the occurrence of large earthquakes. Thus the angle of the restraining bend and length of the restraining segment could both be expected to influence the amount of strain accumulation and resulting earthquake size. We do not have enough data in Turkey alone to verify this hypothesis, but examination of strike slip earthquakes in other parts of the world suggests that this is true (Barka and Kadinsky-Cade, in prep.).

Restraining stepovers associated with ruptured segments are not as common in the Turkish data set. Rupture propagation is prevented by restraining stepovers in the cases of the 1949 NAF segment 1 earthquake ($d=5$ km) and the 1971 EAF segment 1 earthquake ($d=10$ km). Smaller stepovers occurring in our data set do not usually impede rupture propagation.

An important point is that the discontinuities do not act in isolation from one another. If two discontinuities occur along a given segment, controlling factors are their relative sizes and their separation from each other. This can be seen in two examples. First, the 1939 segment of the NAF (segment 3): In this situation the 20° bend separating 3a from 3b, north of Erzincan, dominates the 15° bend on segment 3d south of Niksar, even though the two bends are separated by more than 200 km and by the Susehri releasing stepover (2 km wide; located at the subsegment 3b-3c intersection). When we say "dominates", we mean that the earthquake rupture is controlled more by the 20° bend. In this case the 1939 earthquake initiated near the 20° bend and ruptured away from it bilaterally, as will be seen later. Note that the 15° bend was located adjacent to the 10 km wide releasing stepover separating NAF segments 3 and 4.

The second example of relationships between discontinuities within a segment is NAF segment 8 (1967 earthquake, Mudurnu valley). Here we have two restraining double bends along the same segment. The eastern one, which is mentioned in Figure 9, dominates. The epicenters of the 1957 and 1967 earthquakes were located at this double bend. Rupture occurred mostly away from this area in both cases. The other smaller double bend plays no role in the rupture. The 1967 event ruptures right through it. The conclusion to be drawn from these two examples is that the complete geometric pattern needs to be examined in each case, not just one discontinuity at a time.

Epicenters of large earthquakes often seem to occur near restraining bends within a segment (see also Barka and Hancock, 1982; King and Nabelek, 1985; Barka and Kadinsky-Cade, in prep.). There are two examples of well-constrained epicenters that fall into this category. The 1976 Caldiran (Eastern Turkey, Figure 8b) earthquake epicenter was located very close to the 17°-19° restraining bend, and the earthquake ruptured bilaterally based on an inversion of teleseismic body waves (King and Nabelek, 1985). Examples of this and other epicenters near restraining bends are shown in Figure 10. The 1939 Erzincan earthquake had an epicenter near the bend (the accuracy of the location is not ideal, but adequate here because the fault was very long; see Figure 3 and 10), and ruptured bilaterally. Other Turkish earthquakes (1942, 1943, and 1967 along the NAF) had epicenters close to restraining bends, but the resolution of these locations relative to the length of the surface fault trace is not sufficient for a detailed comparison of epicenter with fault geometry. In both of the better constrained cases the epicenter was located near the bend, and rupture took place away from the bend. In general we saw no evidence for epicenters within restraining areas - i.e., on the section of the fault segment that is located on one side of the restraining bend and is subject to a higher amount of compressive strain than the other side or, alternatively, within a restraining stepover area.

A critical factor influencing the occurrence of large earthquakes, other than the fault geometry, is the direction of block motion relative to the geometric pattern. An example of this can be seen by looking at the single restraining bend examples at the top of Figure 9. The 1976 Cildiran earthquake ruptured bilaterally from the bend area. The 1855 earthquakes occurred separately, one on either side of the bend. The 1983 Horasan-Narman earthquake only ruptured one side of the segment, between the bend and one end of the fault. From an examination of fault morphology, the 1976 case caused pure strike-slip faulting on one side of the bend. However the 1855 earthquakes were characterized by pure strike-slip motion on one side of the bend and a strong component of normal faulting on the other side. The 1983 earthquake had pure strike-slip motion, but the morphology of the fault on the unruptured side of the bend shows a strong component of compression. These 3 examples illustrate the influence of the direction of block motion. This direction can be defined using geodetic measurements (generally not available in Turkey), fault plane solutions if available, or fault morphology, the latter including primarily observations of physiographic fault expressions at the surface.

Releasing discontinuities

Releasing stepovers and bends can be recognized by morphological depressions (basins) and/or extensional structures. Releasing discontinuities control segmentation, although compared with restraining stepovers we have fewer examples in Turkey that can be used to constrain the sizes of discontinuities responsible for segmentation. The 1840 Balıkgölü (Figure 8c) releasing bend (40°) seems to have been too large to allow the propagation of rupture through the bend. The 5 km wide stepover separating NAF segments 2 and 3 (near Erzincan) and the 10 km wide stepover separating NAF segments 3 and 4 (near Niksar) both acted as barriers to rupture propagation. The 1 km

wide stepover separating NAF segments 4 and 5 also prevented rupture propagation. However the 1 km stepover west of the restraining bend in NAF segment 8 did not stop the 1944 earthquake rupture. The difference between these last two cases may have been the added contribution of a restraining bend adjacent to the stepover in the first case. In general the size and distance of discontinuities relative to restraining discontinuities is important. NAF segment 5 has several small to moderate releasing stepovers to the west of the 15° restraining bend, but the segment only terminates at one of them, a 1.5 km wide stepover. Three other moderate releasing stepovers are located east of the bend, but none of them cause segmentation. The 1.5 km wide Susehri releasing stepover that separates subsegments 3b and 3c did not cause segmentation in 1939. In conclusion, from available observations, it seems that the large releasing discontinuities (Table 1) cause segmentation (i.e., bound the fault segments), but the small to moderate ones often do not. Influencing factors in the moderate discontinuity cases are their location and size relative to one another and to the restraining discontinuities along the segment.

Aftershocks of large earthquakes and earthquake swarm activity both tend to occur in releasing bend and releasing stepover areas. Although epicentral locations of small and moderate earthquakes are often not well determined in Turkey, there is still some evidence for this phenomenon. The first example of this is the 1939 Erzincan earthquake (NAF segment 3), where large felt aftershocks occurred in the segment 2-3 releasing bend/releasing stepover area and in the segment 3-4 stepover area. Another example is the 1967 Mudurnu valley earthquake (NAF segment 8), where aftershocks were concentrated along the releasing segment (with a higher normal faulting component) west of the smooth releasing bend. The third example is the Marmara Sea region. In this last case, earthquake swarms (Ucer *et al.*, 1985) coincide with pull-apart basins. This observation confirms previous results in California (e.g., Eaton *et al.*, 1970; Hill,

1977; Weaver and Hill, 1979; Segall and Pollard, 1980). In the case of aftershocks it has been explained by fluid pore pressure arguments (Sibson, 1986).

Most of the earthquakes in this study do not have well-located foreshocks, either because they did not occur or because they were difficult to locate due to their small magnitude. In the case of the 1939 great Erzincan earthquake, however, local residents reported that several small earthquakes were felt in the Erzincan basin about one week preceding the 1939 event (Pamir and Ketin, 1941; Parejas *et al.*, 1942). This basin is a large releasing stepover/bend combination located relatively close to the main 20° restraining stepover of NAF segment 3. A secondary releasing feature within or near a restraining area provides a weak point that may rupture first. This appears to have been the case also for the 1975 Haicheng, China earthquake (Jones *et al.*, 1982), and for the 1930 Salmas, Iran earthquake (Tchalenko and Berberian, 1974). The damaging foreshock that occurred in the Iran case has not been accurately located, but the distribution of damaged villages during the foreshock is not inconsistent with a location in the releasing stepover area adjacent to a restraining stepover.

Geological factors associated with fault discontinuities

Although it is beyond the scope of this paper to document all of the geological effects that are responsible for the observed fault discontinuities, some of the more important effects will be reviewed here. First it should be noted that complex fracture patterns are characteristic of simple shear laboratory experiments (e.g., Tchalenko, 1970; Wilcox *et al.*, 1973; Barlett *et al.*, 1981; Naylor *et al.*, 1986). These patterns can be due, for example, to rotation of the material within the fault zone.

En echelon fault patterns can often be explained by the rheology of the top part of the upper crust. First, the occurrence of ductile material such as a thick pile of sediments (Harding, 1985) or clay-rich rocks can cause discontinuities.

For example Saroglu and Barka (1983) documented some cases in Turkey (e.g., 1983 Horasan-Narman earthquake; see also Barka *et al.*, 1983) in which the effect of serpentinite-rich ophiolitic melange on fault zones was to widen the zones and break them up into many smaller faults with unclear surface expression (compared to the single break areas). Second, a decrease in confining pressure near the earth's surface may in some cases cause a widening of the zone of deformation.

The occurrence of bends can be explained by a number of factors. First, pre-existing zones of weakness can be an important factor at any scale. For example, on a large scale, the eastern half of the North Anatolian fault zone follows the Antolid/Taurid/Pontid suture zone, and the western half follows the Intra Pontid suture zone (both Eocene-Miocene features). Second, changes in stress orientation or magnitude can cause bends. A third factor includes heterogeneities in rock type. The discontinuities may also form progressively as a rupture either follows a boundary (Rogers, 1973) or encounters (at a higher angle) a boundary between dissimilar rock types (Jackson and McKenzie, 1984). In the second case, the rupture could initially change direction due to a refraction effect; subsequently the bend angle could increase due to differential deformation across the boundary.

Geometric fault discontinuities are often associated with clear morphological features. Near restraining segments mountains are often observed. An example of this is the Ilgaz Mountains on segment 5 of the North Anatolian fault (near Tosya). These mountains are comparable to the San Gabriel Mountain range (1875 earthquake), Black Mountain (1906 earthquake) or Middle Mountain (1966 Parkfield earthquake) along the San Andreas fault. Releasing features are often associated with low areas as has been seen several times in the detailed Turkish fault descriptions.

Finally, restraining bends are sometimes associated with kink structures or folds with an orientation that is oblique to the fault zone, indicating variations in rheology within the moving blocks or plates. Examples of this are the Palmyra kink (Lebanon-Syria) or the Kirikhan-Gaziantep kink (southern Turkey), both adjacent to the Dead Sea fault.

Geometric discontinuities along strike-slip faults are stable in the short term, but they can be subject to progressive deformation over a longer time period. For example progressive deformation of single or double bends can cause an increase in α which eventually blocks movement on the fault. The fault is then replaced by newer faults. Examples of this can be observed in New Zealand and California. A progressive increase of α to 40° at a restraining double bend along the Alpine fault in New Zealand has caused motion along subparallel faults (Awatara, Clarence, Hope faults; see Rynn and Scholz, 1978). Similarly, near the Black Mountain - San Juan Bautista double bend (California) motion is taken up by the Calaveras and Hayward faults (Sykes and Nishenko, 1984). In southern California many subparallel faults take up motion near bends in the San Andreas fault (e.g., Scholz 1977; Ziong and Yerkes, 1985). One possible interpretation for these subparallel faults is that slip has become difficult along the main fault strand.

CONCLUSIONS

By reviewing the geometry of Turkish strike-slip faults we have reached the conclusions that fault geometry plays an important role in the segmentation of strike-slip faults and in earthquake rupture processes. By increasing our data base to include other strike-slip faults in the world (particularly the well-studied California cases) we feel confident that a careful examination of fault geometry can help define or estimate rupture lengths of large earthquakes, and possibly mainshock epicenter, foreshock and aftershock locations in some cases. From

the Turkish data we can say specifically that:

a) The geometric discontinuities tend to occur in characteristic patterns, each associated with a characteristic earthquake mechanism.

b) The size of the discontinuities is important. Small discontinuities (see Table 1) generally do not cause segmentation. Large discontinuities usually do cause segmentation. Moderate discontinuities have to be examined carefully in relation to one another and to the direction of block motion in order to determine their role.

c) The distribution and size of moderate discontinuities relative to one another along a segment are very important in determining the nature of the earthquake mechanism along the segment. It is therefore advisable to be very cautious about analyzing fault geometry statistically.

d) Seismological background information and additional information such as geodetic measurements or fault morphology need to be included in the interpretation of segmentation based on fault geometry.

e) Epicenters of large earthquakes seem to be associated with restraining bends in fault segments, but not actually occur within restraining subsegments (on one side of the bend) or within restraining stepovers.

f) Aftershocks and swarm activity can sometimes be related to releasing discontinuities. Foreshocks may be related to releasing

features located close to areas of major strain accumulation.

ACKNOWLEDGMENTS

The field work on which a large part of this study was based would not have been possible without the M.T.A. Institute's (Ankara, Turkey) support of one of the authors. We would like to thank M. Nafi Toksöz for many helpful discussions. This work was supported by U.S. Geological contract number 14-08-0001-G1151, and by NASA grant # NAG5-753.

REFERENCES

- Allen, C.R., The tectonic environments of seismically active and inactive areas along the San Andreas fault system, in Proceedings of the Conference on Geologic Problems of the San Andreas Fault System, edited by W.R. Dickinson and A. Grantz, *Stanford Univ. Publ. Geol. Sci.*, 11, 70-82, 1968.
- Allen, C.R., Active faulting in northern Turkey: Contr. No. 1577. Div. Geol. Sci., Calif. Inst. Tech., 32 p., 1969.
- Allen, C.R., Geological criteria for evaluating seismicity, *Bull. Geol. Soc. Am.*, 86, 1041-1057, 1975.
- Alsan, E., Tezuan, L. & Bath, M., An earthquake catalogue for Turkey for the interval 1913-1970, Kandilli Observatory, Istanbul, 1975.
- Ambraseys, N.N., Some characteristic features of the North Anatolian fault zone. *Tectonophysics* 9, pp. 143-165, 1970.
- Ambraseys, N.N., Value of historical records of earthquakes, *Nature*, Lond. 232, 379-97, 1971.
- Ambraseys, N.N., Studies in historical seismicity and tectonics. In: *Geodynamics of Today*, The Royal Soc., London, 9-16, 1975.
- Ambraseys, N.N. and Zatopek, A., The Mudurnu valley, West Anatolia, Turkey, earthquake of 22 July 1967. *Bull. Seis. Soc. Amer.*, 59, 521-589, 1969.
- Ambraseys, N.N. and Melville, C.P., *A history of Persian earthquakes*, *Cambr. Earth Sci. Ser.*, Cambridge Univ. Press. 219 pp., 1982.
- Ambraseys, N.N. and Finkel, C.F., The Saros-Marmara earthquake of 9 August 1912. *Jour. Earthq. Eng. Struct. Dyn.*, 15/2, 189-211, 1987a.
- Ambraseys, N.N. and Finkel, C.F., The Seismicity of the Northeast Mediterranean Region during the Early Twentieth Century, *Annales Geophysicae*, 1987b, in press.
- Ando, M., Source mechanism and tectonic significance of historical earthquakes along the Nankai Through, Japan, *Tectonophysics*, 27, 119-140, 1975.
- Arpat, E., Saroglu, F. and Iz, H.B., The 1976 Caldiran earthquake: *Yer Yuvarı ve İnsan*, 2, 29-41, 1977.
- Arpat, E. and Saroglu, F., The East Anatolian Fault System: thoughts on its development. *Bull. Mineral Res. Explor. Inst.*, Ankara, 78, 33-39, 1972.

- Arpat E. and Saroglu, F., Some recent tectonic events in Turkey. In Turkish. *Bull. Geol. Soc. Turkey*, 18, pp. 91-101, 1975.
- Ates, R. and Tabban, A., Preliminary report for the Murefte-Sarkay earthquake of 9th August 1912. *Publ. Earthquake. Res. Institute*, Ankara, Turkey (in Turkish), 1976.
- Aytun, A., Creep measurements in the Ismetpasa region of the North Anatolian fault zone, In *Multidisciplinary approach to earthquake prediction*, edited by A. M. Isikara and A. Vogel., Friedr. Vieweg & Sohn, 279-295, 1982.
- Bakun, W.H., Stewart, R.M., Bufe, C.G. and Marks, S.M., Implication of seismicity for failure of a section of San Andreas Fault. *Bull. Seism. Soc. Am.* 70, 185-202, 1980.
- Barka, A.A. and Hancock, P.L., Relationship between fault geometry and some earthquake epicenters within the North Anatolian fault zone. In *Progress in earthquake prediction*, edited by A.M. Isikara and A. Vogel, Friedr. Vieweg and John, F.R.G. Vol. 2, pp. 137-142, 1982.
- Barka, A.A., Saroglu, F. and Güner, Y., Horasan-Narman earthquake and its relation to the neotectonics of Eastern Turkey. *Yeruvari ve Insan*, 8, 16-21, 1983.
- Barka, A.A. and Hancock, P.L., Neotectonic deformation patterns in the convex-northwards arc of the North Anatolian fault, in *The Geological Evolution of the Eastern Mediterranean*, edited by J.G. Dixon and A.H.F. Robertson. Special publication, Geol. Soc. London, 763-773, 1984.
- Barka, A.A. and Bayraktutan, S., Active fault patterns in the vicinity of the Erzurum basin. Abstract. 39th Ann. Geol. Cong. Geol. Soc. Turkey. p. 11, 1985.
- Barka, A.A., Toksöz, M.N. and Gülen, L., The structure, seismicity and earthquake potential of the eastern part of the North Anatolian fault zone, 1987, in prep.
- Barka, A.A., Seismo-tectonic aspects of the North Anatolian fault zone, Ph.D. thesis, University of Bristol, England, 335 pp, 1981.
- Barka, A. and Kadinsky-Cade, K. Strike-slip fault geometry and earthquake activity. (in prep.)
- Barlett, W.L., Friedman, M., and Logan, J.M., Experimental folding and faulting of rocks under confining pressure: Part IX: wrench faults in limestone layers., *Tectonophysics*, 79, 155-277, 1981.
- Bergougnan, H., Structure de la Chaine pontique dans le Haut-Kelkit (Nord-Est de l'Anatolie). *Bull. Soc. Géol. Fr.*, 18, 675-686, 1976.

- Bilham, R. and Hurst, K., Relationships between fault zone deformation and segment obliquity on the San Andreas fault, California. *The China-U.S. Symposium on Crustal Deformation and Earthquakes*. Wuhan, 1985.
- Bingöl, E., Akyürek, B. and Korkmazer, Biga xarim-adasinin jeolojisi ve karakaya formasyonunun basi özellikleri. *Geol. Conj. 50 Aniver. Spec. Publ. M.T.A. Ankara, Turkey*, 70-76, 1973.
- Blumenthal, M.M., Ladik earthquake zone. *Bull. Min. Res. Expl. Inst. Turkey* 1/33, 153-174, 1945a
- Blumenthal, M. M., Die Kelkit-Dislokation und ihre tektonische Rolle. *MTA Mecmuasi*, 2/34, 372-386, 1945b.
- Blumenthal, M., Zur Geologie der Landstrecken der Erdbeben von Ende 1942 in Nord Anatolien und dort ausgeführte Macro Seismische Beobachtungen (Osmancik-Erbaa) Unter Mitwirkung von H.N. Pamir und C.H. Akyol. *M.T.A. Bull.* 1/29, 46 pp., 1943.
- Brune, J.N.M., Seismic moment, seismicity and rate of slip along major fault zones. *J. Geophys. Res.*, 73, 777-784, 1968.
- Canitez, N. and Ucer, B., Computer determinations for the fault plane solutions in and near Anatolia. *Tectonophysics*, 4, 235-244, 1967.
- Canitez, N., Studies on recent crustal movements and the North anatolian fault problem, in: *Symposium on the North Anatolian fault zone*, Spec. Publ. of Min. Res. Expl. Inst. Turkey, 35-58, 1973.
- Canitez, N. and Büyükasikoglu, S., Seismicity of the Sinop Nuclear Power Plant, Final report, Unpubl. Report. Tech. Univ. Istanbul, Turkey, 230 pp., 1984.
- Crampin, S. and Evans, R., Neotectonics of the Marmara Sea region of Turkey. *Jour. Geol. Soc. London*, 143, 343-348, 1986.
- Dewey, J.W., Seismicity of Northern Anatolia, *Bull. Seism. Soc. Am.*, 66, 843-868, 1976.
- Dewey, J.F., Hempton, M.R., Kidd, W.S.F., Saroglu, F. and Sengör, A.M.C., Shortening of continental lithosphere: the neotectonics of eastern Anatolia - a young collision zone. In: *Collision Tectonics*, edited by Coward, M.P. and Ries, A.C., Geol. Soc. Sec. Publ., 19, London, 1-36, 1986.
- Eaton, J.P., O'Neill, M.E. and Murdock, J.N., Aftershocks of the 1966 Parkfield-Cholame, California earthquake: A detailed study. *Bull. Seism. Soc. Am.*, 60, 1151-1197, 1970.
- Eginitis, M.D., Sur le tremblement de terre de Constantinople, du 10 Juillet

1894. *Comp. Rendus*. 52, 480-484, 1894.
- Eginitis, M.D., Le tremblement de terre de Constantinople du 10 Juillet 1894, *Annales de Geographie*, 4, 151-165, 1895.
- Ercan, A., A statistical analysis of the major and micro earthquakes along the East Anatolian fault. In: *Multidisciplinary approach to Earthquake prediction*, edited by A.M. Isikara and A. Vogel, Fried. Vieweg & Sohn, 239-261, 1982.
- Erdik, M., Damage at the Sürgü Dam during May 5, 1986 Malatya earthquake, Turkey. Unpublished report. Middle East Tech. Uni. Turkey, 15, 1986.
- Erentoz, C. and Kurtman, F., Report on 1964 Manyas earthquake, *Bull. Min. Res. Expl. Inst. Turkey*, 63, 1-5, 1964.
- Ergin, K., Guglu, U. & Uz, Z., A catalogue of earthquakes of Turkey and surrounding area (11 AD to 1964 AD) *Publ. Mining Fac. Global Phys. Inst., Istanbul*, 24, 1-28, 1967.
- Evans, R., Asudeh, I., Crampin, S. and Ucer, S.B., Tectonics of the Marmara Sea region of Turkey: new evidence from micro-earthquake fault plane solutions. *Geophys. Jour. R. Astr. Soc.*, 83, 47-80, 1985.
- Eyidogan, H., Toksöz, M.N., Gülen, L., and Nabelek, J., 1986. Aftershock migration following the 1983 Horasan-Narman earthquake, Earth Resources Laboratory unpublished report, 1986.
- Gündoğdu, O., Source characteristics of some major earthquakes in Turkey. Ph.D. Thesis University of Istanbul, 175 pp, 1985.
- Gülen, L., Barka, A.A., and Toksöz, M.N. Continental collision and related complex deformation: Maras Triple Junction and surrounding structures SE Turkey. Spec. Publ. Hacettepe Uni., Ankara (in press).
- Hancock, P.L., Brittle microtectonics; Principles and practice. *Journ. Struct. Geol.*, 7, 437-357, 1985.
- Harding, T.P., Seismic characteristics and identification of negative flower structures and positive flower structures, and positive structural inversion. *AAPG*, 69, 582-600, 1985.
- Hempton, M.R. and Dunne, L.A., Sedimentation in pull-apart basins: Active examples in eastern Turkey, *J. Geol.*, 92, 513-530, 1984.
- Hill, D.P., A model for earthquake swarms, *J. Geophys. Res.*, 82, 1347-1352, 1977.
- Hobbs, B.E., Means, W.D. and Williams, P.E., *An Outline of Structural Geology*, John Wiley and Sons, Inc., 571 pp., 1976.

- Jackson, J. and McKenzie, D., Active tectonics of the Alpine-Himalayan Belt between western Turkey and Pakistan. *Geophys. Journ. R. Ast. Soc.* 77, 1, 185-265, 1984.
- Jones, L.M., Wang, B., Xu, S. and Fitch, T., The foreshock sequence of the February 4, 1975, Haicheng Earthquake (M= 7.3), *J. Geophys. Res.*, 87, 4575-4584, 1982.
- Karnik, V., *Seismicity of the European area*, D. Reidel Pub. Com., Dordrecht, Holland, Part I, 365, 1969.
- Karnik, V., *Seismicity of the European area*. D. Reidel Pub. Com., Dordrecht, Holland, Part II, 218, 1971.
- Kelleher, J., L. Sykes and J. Oliver, 1973. Possible criteria for predicting earthquake locations and their application to major plate boundaries of the Pacific and the Caribbean, *J. Geophys. Res.*, 78, 2547-2585, 1973.
- Ketin, I., Über die tektonisch-mechanischen Folgerungen aus den grossen anatolischen Erdbeben des letzten Dezenniums. *Geol. Rdsch.*, 36, 77-83, 1948.
- Ketin, I., Über die nordanatolische Horizontalverschiebung: *Bull. Mineral Res. Explor. Inst.*, Ankara, v. 72, p. 1-28, 1969.
- Ketin, I. and Roesli, F., Markoseismische Untersuchungen über das nordwestanatolische Beben vom 18 März 1953. *Ecolog. Geol. Helv.*, 46, 187-208, 1953.
- King, G.S.P., Speculations on the geometry of the initiation and termination process of earthquake rupture and its relation to morphology and geological structure. Submitted to *Pageograph*, topical issue on Friction and Faulting, Ed. T. Tullis, 1986.
- King, G. and Nabelek, J., Role of fault bends in the initiation and termination of earthquake rupture. *Science*, 228, 984-987, 1985.
- Kocyigit, A., The Karayazi fault. *Bull. Geol. Soc. Turkey, (in Turkish)*, 28, 67-71, 1985.
- Kocyigit, A., Oztürk, A., Inan, S. and Gürsay, H., Tectonomorphology and mechanistic interpretation of the Kurasu basin (Erzurum) (in Turkish). *Cambr. Uni. Bull. Earth Sciences*, 2, 3-15, 1985.
- Koide, H., Seismotectonic problem of en echelon systems and earthquake source mechanisms (in Japanese). *Journ. Earth Sci.*, 92, 33-52, 1983.
- Lahn, E., Seismic activity in Turkey from 1947 to 1949. *Bull. Seis. Soc. Ame.*, 42, 111-114, 1952.

- Le Pichon, X., Lyberis, N. and Alvarez, F., Subsidence history of the North Aegean Trough. In the geological evolution of eastern Mediterranean. Edited by J.G. Dixon and A.H.F. Robertson. *Spec. Publ. Geol. Soc.*, London, 726-741, 1984.
- Lyberis, N., Tectonic evolution of the north Aegean Trough. In *The Geological Evolution of Eastern Mediterranean*, edited by J.G. Dixon and A.H.F. Robertson. *Spec. Publ. Geol. Soc.* London, 711-725, 1984.
- Marathon Oil Comp., Unpublished report on abandoned Marmara I well. Unpublished, 15, 711-725, 1974.
- McKenzie, D.P., Active tectonics of the Mediterranean Region. *Geophys. J.R. Astr. Soc.*, 30, 109-85, 1972.
- McKenzie, D.P., The East Anatolian Fault: a major structure in eastern Turkey. *Earth Planet. Sci. Lett.*, 29, 189-93, 1978.
- McKenzie, D.P., Active tectonics of the Alpine-Himalayan belt: The Aegean Sea and surrounding regions: *Geophys. Jour. Roy. Astr. Soc.*, 55, 217-254, 1978.
- Mocavei, G., Sur le tremblement de terre de la Mer de Marmara le 9 Aout, 1912. *Bull. Sect. Sci. Acad. Rumania*, 1, 1., 9-18, 1912.
- Naylor, M.A., Mandl, G. and Siypestieyn, C.H.K., Fault geometries in basement-induced wrench faulting under different initial stress states, *J. Struct. Geol.*, 8, 737-752, 1986.
- Nishenko, S. and W. McCann, Seismic potential for the world's major plate boundaries: 1981, in *Earthquake Prediction, An International Review, Maurice Ewing Ser.*, 4, 20-28. AGU Washington, D.C., 1981.
- Pamir, H.N., and Akyol, I.H., Gormur and Erban earthquakes. *Bull. Geograph. Turkey*, 2, 1-7, 1943.
- Pamir, H.N. and Ketin, I., Das anatolische Erdbeben ende 1939. *Geol. Rdsch.*, 32, 279-87, 1941.
- Parejas, E., Akyol, I.H. and Altinli, E., Le tremblement de terre d'Erzincan du 27 Decembre, 1939. *Revue Fac. Sci. Univ. Istanbul*, B-VI, 177-222, 1942.
- Pfannenstiel, V.M., Diluviale Geologie des Mittelmeer Gebietes. *Geol. Rundschau*, 34, 342-424, 1944.
- Pinar, N., Geological and macroseismic investigation of the August 13th 1951 earthquake. 1st Unive. Fen. Fak. Dergisi, Seri A, Cilt XVIII, 131, 1953.
- Riad, S. and Mayers, H., Earthquake catalog for the Middle East Countries 1900-1983. World Data Center A. Report, SE-40. 133, 1985.

- Rogers, T.H., Fault trace geometry within the San Andreas and Calaveras fault zones. A clue to the evolution of some transcurrent fault zones. In: *Proc. Conf. Tect. Prob. of San Andreas fault system*, edited by R.L. Kovach and A. Nur. Publ. Stanford U. 13, 251-258, 1973.
- Rynn, J.M.W., and Scholz, C.H., Seismotectonics of the Arthur's Pass region, South Island, New Zealand, *Geo. Soc. Am. Bull.*, 89, 1373-1388, 1978.
- Salomon-Calvi, W., Anadolu'nun tektonik tarzi tesekkülü hakkında kısa izahat. *Bull. Min. Res. Explo. Inst. Turkey*, 1/18, 35-47, 1940.
- Sandison, D., Notice of the earthquake of Brussa. *Quart. Journ. of the Geol. Soc. of London*, 11, 543-544, 1855.
- Saroglu, F., Geological and tectonic evolution of Eastern Turkey during Neotectonic period. Ph.D. thesis (in Turkish), University of Istanbul. 242 pp., 1985.
- Saroglu, F., and Güner, Y., The Tutak active fault, its characteristics and relation to the Caldiran fault. (In Turkish) *Yer Yuvarı ve İnsan*, 4 11-14, 1979.
- Saroglu and Güner, Y., Dogu anadolu'nun jeomorfolojik gelismine etki eden ögeler, jeomorfoloji, tektoni, volkanizma iliskileri: *Bull. Geo. Soc. Turkey*, 24, 39-50, 1981.
- Saroglu, F. and Barka, A.A., The importance of rock type for seismic parameters (in Turkish). *Yer Yuvarı ve İnsan*, 8.4, 43, 1983.
- Scholz, C.H., Transform fault systems of California and New Zealand: similarities in their tectonic and seismic styles, *J. Geol. Soc. Lond.*, 133, 215-229, 1977.
- Schwartz, D.P. and Coppersmith, K.J., Seismic hazards: New trends in analysis using geologic data. In *Active tectonics*, National Acad. Press. Washington, D.C., 215-230, 1986.
- Segall, P. and Pollard, D.D., Mechanics of discontinuous faults, *J. Geophys. Res.*, 85, 4337-4350, 1980.
- Sengor, A.M.C., The North Anatolian transform fault: its age, offset and tectonic significance. *Il. Geol. Soc. Lond.*, 136, 269-282, 1979.
- Sengor, A.M.C., 1980. Fundamentals of neotectonics of Turkey, *Turk. Jeol. Kur. Konf. Seri. 2*, 40 pp., 1980.
- Sengor, A.M.C., Cross faults and differential stretching of hanging walls in regions of low-angle normal faulting: examples from western Turkey. *Journ. Struc. Geol.*, 8, 1986.

- Sengor, A.M.C., Görür, N. and Saroglu, F., Strike-slip faulting and related basin formation in zones of tectonic escape: Turkey as a case study. In *Strike-slip Faulting and Basin Formation*, edited by Biddle, K.T. and Christie-Blick, N. Society of Econ. Paleont. Min. Spec. Pub., 37, 1985.
- Seymen, I., *Tectonic characteristics of the North Anatolian fault zone in the Kelkit valley*. Ph.D. thesis. Istanbul Tech. Uni., 192, 1975.
- Seymen, I. and Aydin, A., The Bingöl earthquake fault and its relation to the North Anatolian fault zone. *Bull. Mineral Res. Explor. Inst., Ankara*, 79, 1-8, 1972.
- Sharp, R.V. *et al.*, Surface faulting in the Central Imperial valley, *U.S.G.S. Prof. Pap. 1254*, 119-144, 1982.
- Sibson, R.H., Earthquakes and lineament infrastructure, *Phil. Trans. R. Soc. Lond.*, 317, 63-79, 1986.
- Sieberg, A., Untersuchungen über Erdbeben und Bruchscholenbau im östlichen Mittelmeergebiet. *Denk. d. Midz. Natw. Ges. zu Jena, Bd. 18*, Jena, 159-273, 1932.
- Sieh, K., A review of geological evidence for recurrence times of large earthquakes. In "*Earthquake prediction*", Ed. D.W. Simpson and P.G. Richards. *Am. Geophys. Un., M. Ewing Series*, 4, 181-207, 1981.
- Sipahioglu, S., An evaluation of earthquake activity of the Horasan-Narman region before the 30 October 1983 earthquake. *Yeruvari ve Insan*, 8, 12-15, 1983.
- Slemmons, D.B. and Deplo, C.M., Evaluation of active faulting and associated hazards. In: *Active tectonics*, National Acad. Press, Washington, D.C., 45-62, 1986.
- Soysal, H., Sipahioglu, S., Kolcak, D. and Attinok, Y., Historical earthquake catalogue of Turkey and its vicinity. *Turkish Scien. Res. Found. TBAG*, 341, 122 pp., 1981.
- Sykes, L.R. and Nishenko, S.P., Probabilities of occurrence of large plate rupturing earthquakes for the San Andreas, San Jacinto and Imperial faults, California, 1983-2003. *Jour. Geophys. Res.*, 89, 5905-5927, 1984.
- Tabban, A., Geology and earthquakes of cities. *Imar Isk. Bak. Afet Isleri Genel. Mu. Ankara*, 343 pp., 1980.
- Tasman, C.E., Varto ve van depremleri, *Bull. M.T.A., Ankara, Turkey*, 2, 36, 287-291, 1946.
- Tatar, Y., Tectonic investigations on the North Anatolian fault zone between Erzincan and Refahiye. *Yerbilimleri*, 4 Publ. Inst. Earth. Sci.,

- Hacettepe Univ. (In Turkish) 201-136, 1978.
- Tchalenko, J.S., and Berberian, M., The Salmas (Iran) earthquake of May 8, 1930, *Ann. di Geofis.*, 27, 151-212, 1974.
- Tchalenko, J.S., A reconnaissance of the seismicity and tectonics at the northern border of the Arabian Plate (Lake Van region): *Revue de géographie physique et de géologie dynamique*, v. XIX, 189-208, 1977.
- Tokay, M., Geological observation on the North Anatolian fault zone between Gerede and Ilüz. In: *Symposium on the North Anatolian fault zone*, A Spec. Publ. Mon. Res. Expl. Institute of Turkey, 1973.
- Toksöz, M.N., Arpat, E., and Saroglu, F., East Anatolian earthquake of 24 November 1976: *Nature*, 270, 423-425, 1977.
- Toksöz, M.N., A.F. Shakal, and A.J. Michael, Space-time migration of earthquakes along the N. Anatolian fault zone and seismic gaps. *Pure Appl. Geophys.*, 117, 1258-70, 1979.
- Toksöz, M.N., Guenette, M., Gülen, L., Keough, G. Pulli, J.J., Sav, H. and Olguner, A., source mechanism of 1983 Horasan-Narman earthquake, *Yerüvari ve İnsan*, 8, 47-52, 1983.
- Ucer, S.B., Crampin, S., Evans, R., Miller, A. and Kafadar, N., The MARNET radiolinked seismometer network spanning the Marmara Sea and the seismicity of Western Turkey. *Geoph. J. Roy. Astron. Soc.*, 83, 17-30, 1985.
- Weaver, C.S., and Hill, D.P., 1979. Earthquake swarms and local spreading along major strike-slip faults in California, *Pure App. Geophys.*, 117, 51-64, 1979.
- Wilcox, R.E., Harding, T.P., and Seely, D.R., Basic wrench tectonics, *Bull. Am. Assoc. Petrol. Geol.*, 57, 74-96, 1973.
- Yalcin, N., Characteristics of the East Anatolian fault between Turkoglu and Karagac (K. Maras) in relation to settlement problems. *Bull. Chem. Geol. Eng., Turkey*, 6, 49-55, 1978.
- Ziong, J.L. and Yerkes, R.F., Evaluating earthquake and surface faulting potential. In *Evaluating earthquake hazards in the Los Angeles Region - an Earth-Science Perspective*, edited by J.I Ziong, U.S. Geol. Surv. Prof. Paper, 1360. 43-91, 1985.

FIGURE CAPTIONS

- 1) Geometrical pattern definitions for strike-slip faults, as used in the text. In all map views fault movement is assumed to be right-lateral. The direction of block motion is considered to be east-west. A-Stepovers. These can be of releasing or restraining type depending on the direction of the step. Cases Ab, c, d characterize different amounts of horizontal separation between fault segments as shown on the page. B - Bends. Smooth bends refer to a gradual change in fault orientation. Sharp bends refer to an abrupt change. C - cross-sectional views of stepovers. Whether the two fault segments join at depth or remain as two separate planes depends on the brittle-ductile characteristics of the upper crust. Flower-like structures (fault planes joining at depth) can be either negative or positive depending on whether the stepover is of releasing or restraining type.
- 2) Major tectonic elements of Turkey. Compiled from Arpat and Saroglu (1972, 1975), Sengör *et al.* (1985). Boxes indicate areas shown in Figures 3, 4, 7 and 8. The North and East Anatolian faults intersect at the Karliova triple junction (K, at approximately 39°N, 41°E). Kahraman Maras, also referred to in text, is represented by an M near 37°N, 37°E.
- 2) Geometrical pattern definitions for strike-slip faults, as used in the text. In all map views fault movement is assumed to be right-lateral. The direction of block motion is considered to be east-west. A-Stepovers. These can be of releasing or restraining type depending on the direction of the step. Cases Ab, c, d characterize different amounts of horizontal separation between fault segments as shown on the page. B - Bends. Smooth bends refer to a gradual change in fault orientation. Sharp bends refer to an abrupt change. C - cross-sectional views of stepovers. Whether the two fault segments join at depth or remain as two separate planes depends on the brittle-ductile characteristics of the upper crust. Flower-like structures (fault planes joining at depth) can be either negative or positive depending on whether the stepover is of releasing or restraining type.
- 3) Active fault segments in the central and eastern sections of the North Anatolian fault zone. The inset map shows the general location of the main trace. Boxes in the inset map indicate areas which are blown up in the lower part of the figure. Years displayed as smaller numbers refer to large earthquakes that occurred where numbers are shown. Larger numbers (1-6) along fault zone correspond to fault segments. The interpreted length and position of each segment are described in the text. Thicker dashed lines denote ruptured segments. Thinner plain lines are unruptured faults (e.g., segment 2). For references see text.
- 4) Active fault segments in the western section of the North Anatolian fault zone, near the Marmara Sea (South of Istanbul). For explanation see Figure 3.
- 5) Interpreted distribution of active fault segments beneath the Marmara Sea. Thin lines are bathymetric contours from Pfannenstiel (1944). Major

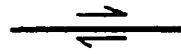
basins are indicated by A, B, and C. Maximum basin depths are derived from the Turkish Navy bathymetry map (1984). The fault plane solution for the 1963 earthquake is taken from McKenzie (1972). Fault segments in the southern half of the Marmara Sea are interpreted from reflection profiles (Marathon, 1974). Note the pull-apart nature of the northern Marmara Sea.

- 6) Comparison of previous figure with published interpretations. A - interpretation of this study. B - from Pinar (1943). C - from Pfannenstiel (1944). D - from Sengör (1986). E - from Crampin and Evans (1986). See text for discussion.
- 7) Active fault segments, East Anatolian fault. Only one large earthquake (1971, segment 1) has occurred here during this century. For explanation see Figure 3.
- 8) Major block boundaries and internal active faults, Eastern Turkey. Note conjugate character of most of these faults. Compiled from Toksöz *et al.* (1977), Arpat (1977), Saroglu and Guner (1979), Barka *et al.* (1983) and Barka and Bayraktutan (1984).
- 9) Schematized geometric fault patterns, and ruptured and unruptured segments that can be associated with the patterns. Details (small discontinuities) are not shown for each case in the schematics. For comparison purposes only (insufficient information for earthquake prediction). Left-lateral faults are inverted to give equivalent right-lateral fault geometry.
- 10) Relationships between single bends, ruptured fault segments and location of epicenters. Solid stars are interpreted epicentral locations. Dashed arrows show distance from interpreted epicenters to the ends of the earthquake surface breaks. A - 1939/12/26 Erzincan earthquake. Dewey's (1976) relocated epicenter is shown as an open star. It is constrained to within about 20 km. Given the rupture length of the event, an epicentral location at the bend is a reasonable assumption. B - 1942/12/20 Erbaa-Niksar earthquake. A well-constrained instrumental epicenter is not available for this event. Maximum intensities were concentrated in the bend area, between Tepekisla and Zilhor (Pamir and Akyol, 1943) C - 1943/11/26 Tosya earthquake. A well-constrained instrumental epicenter is not available for this event either. Maximum intensities were concentrated between Tosya and Ilgaz (see Figure 3; Barka, 1981). D - 1976/11/24 Caldiran earthquake. The International Seismological Centre bulletin epicenter is indicated by the open star. The inversion of seismic waves generated by this event (King and Nabelek, 1986) confirms that rupture took place bilaterally, away from the bend area.

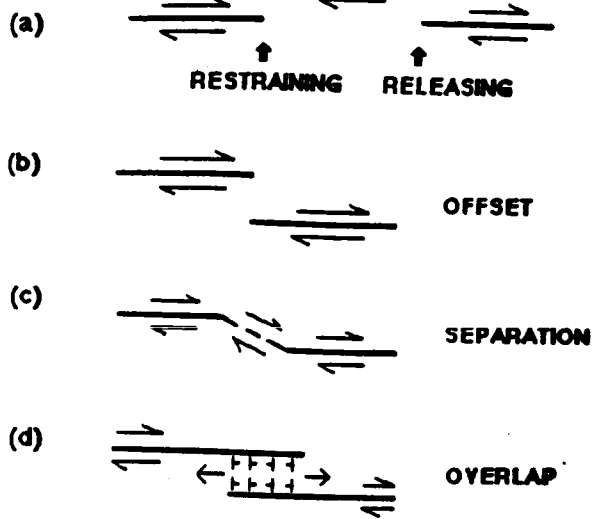
Table 1: Classification of geometric discontinuities

Type of Geometric Discontinuity	small	moderate	large
Stepover Width (d)	$d < 1km$	$1 < d < 5km$	$d > 5km$
Bend Angle (α)	$\alpha < 5^\circ$	$5^\circ < \alpha < 30^\circ$	$\alpha > 30^\circ$

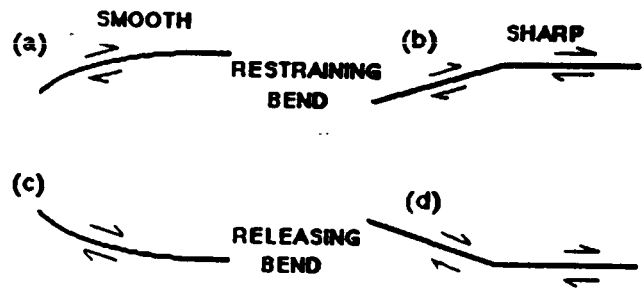
STRAIGHT:



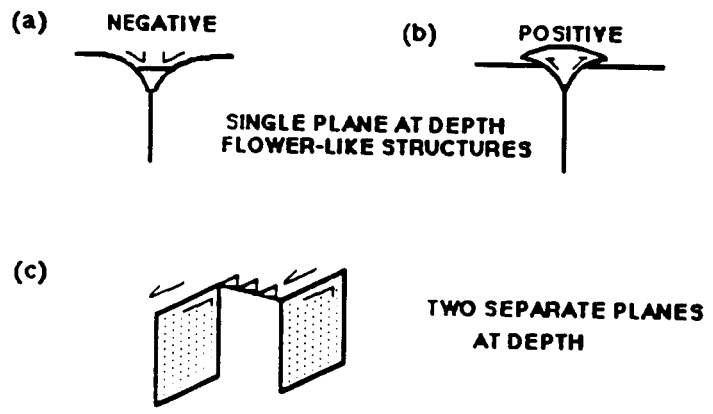
A-STEPOVERS:



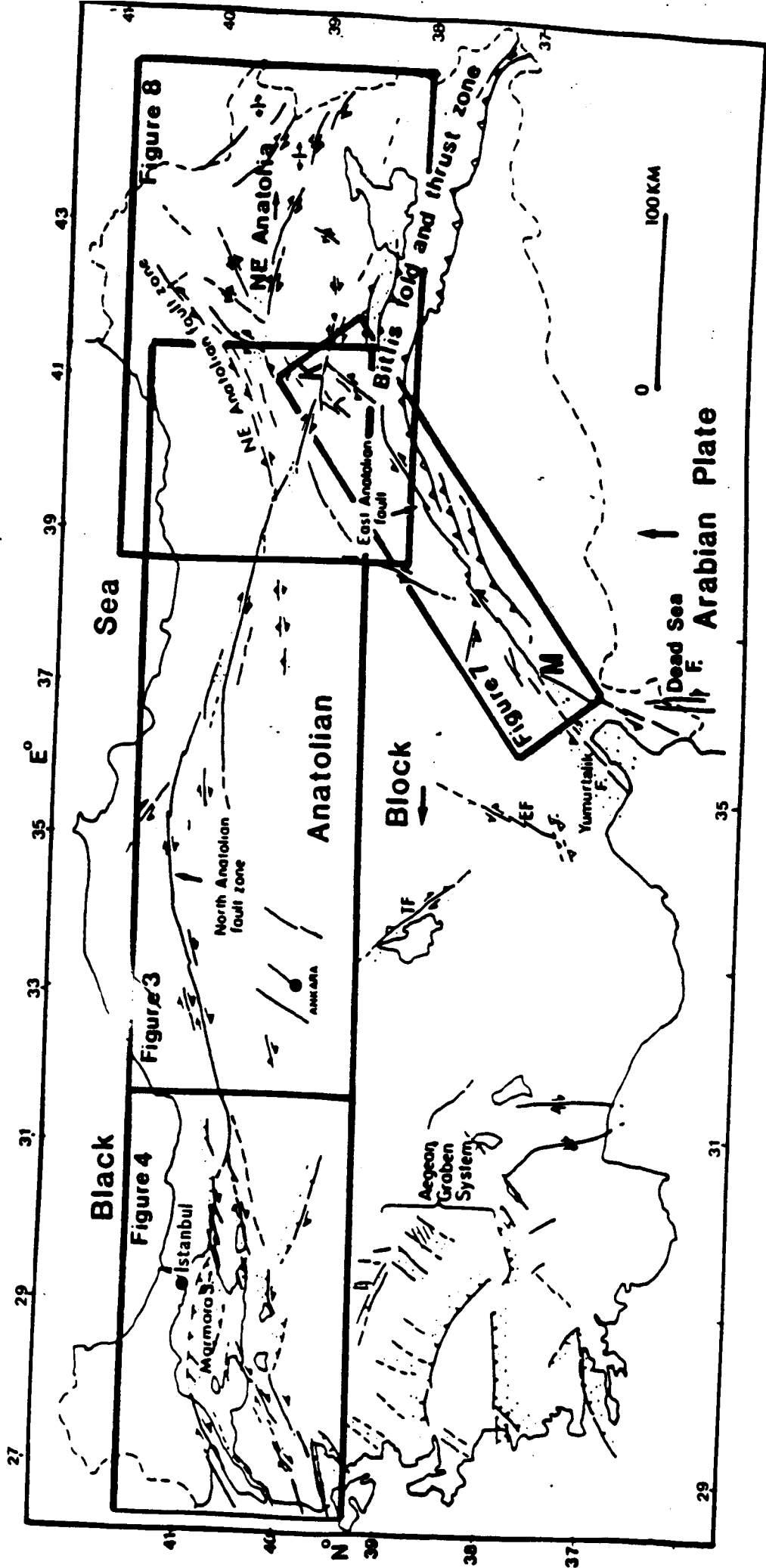
B-BENDS:



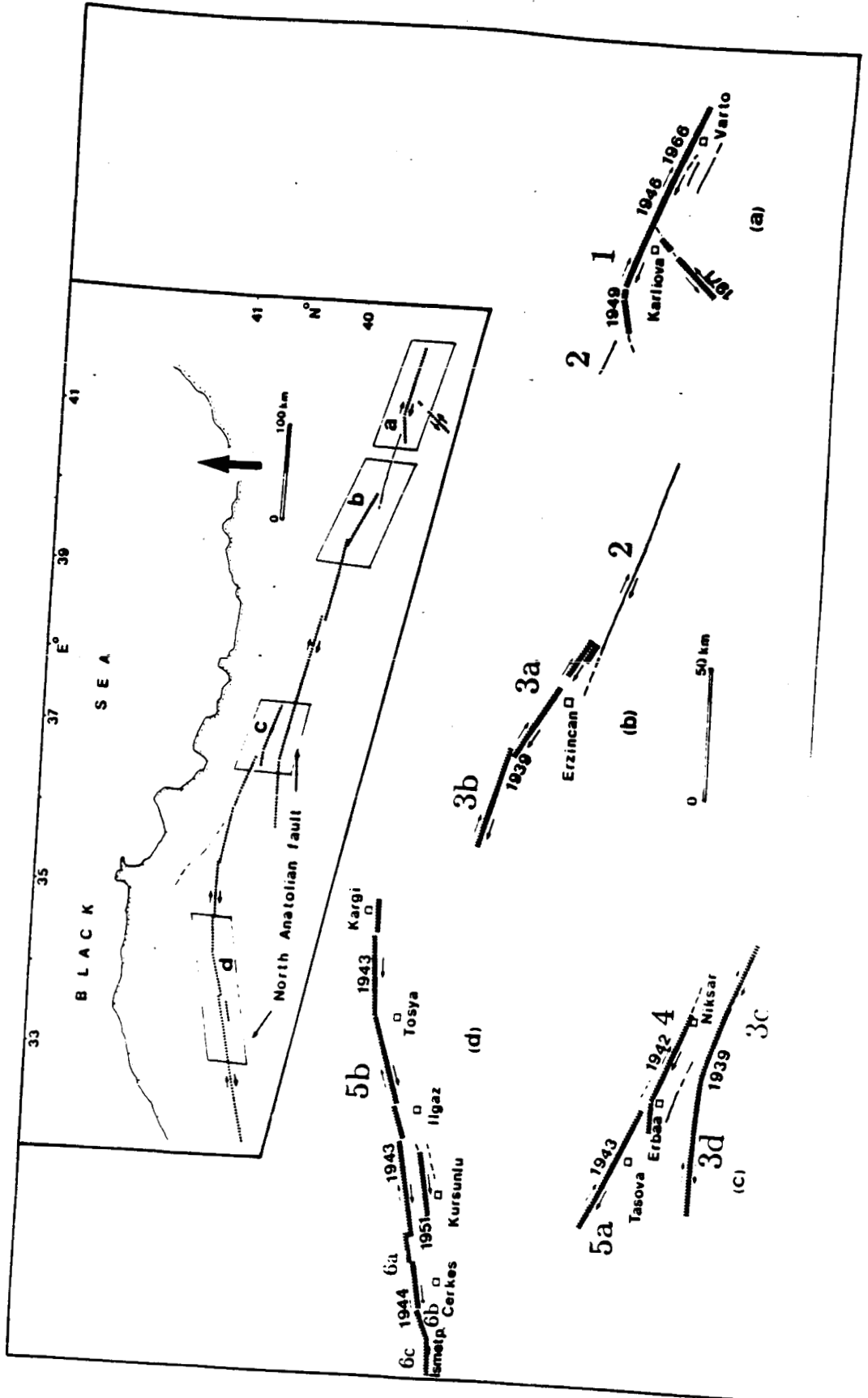
C-CROSS-SECTIONAL VIEWS:



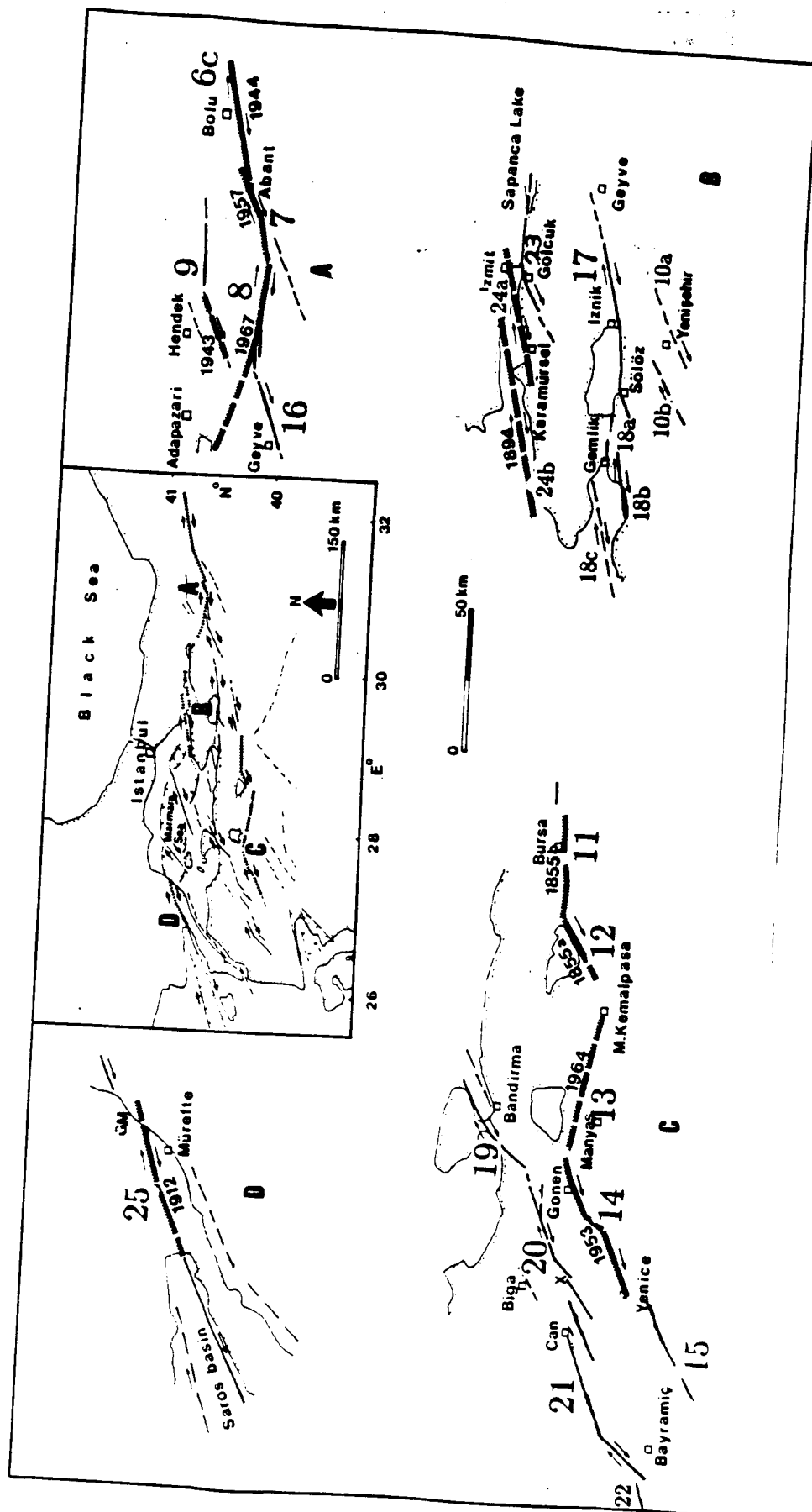
ORIGINAL PAGE IS
OF POOR QUALITY



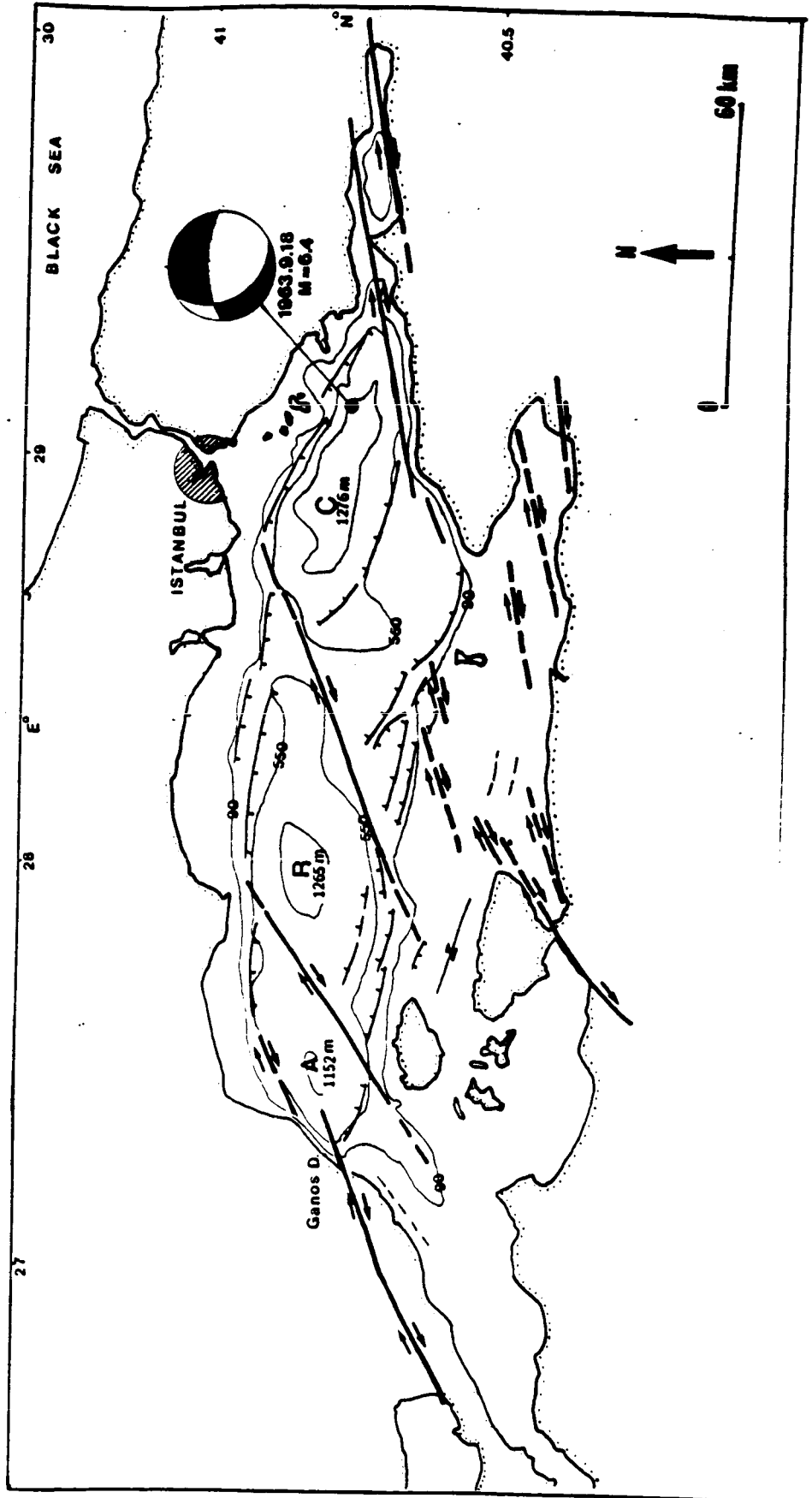
ORIGINAL PAGE IS
OF POOR QUALITY

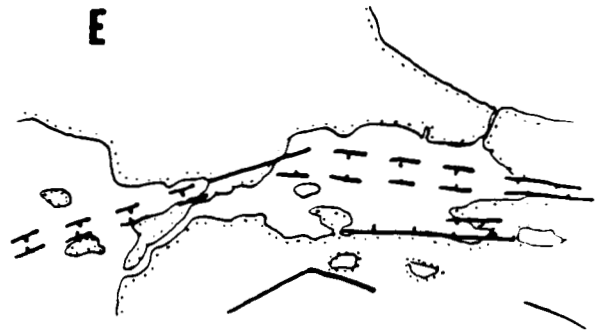
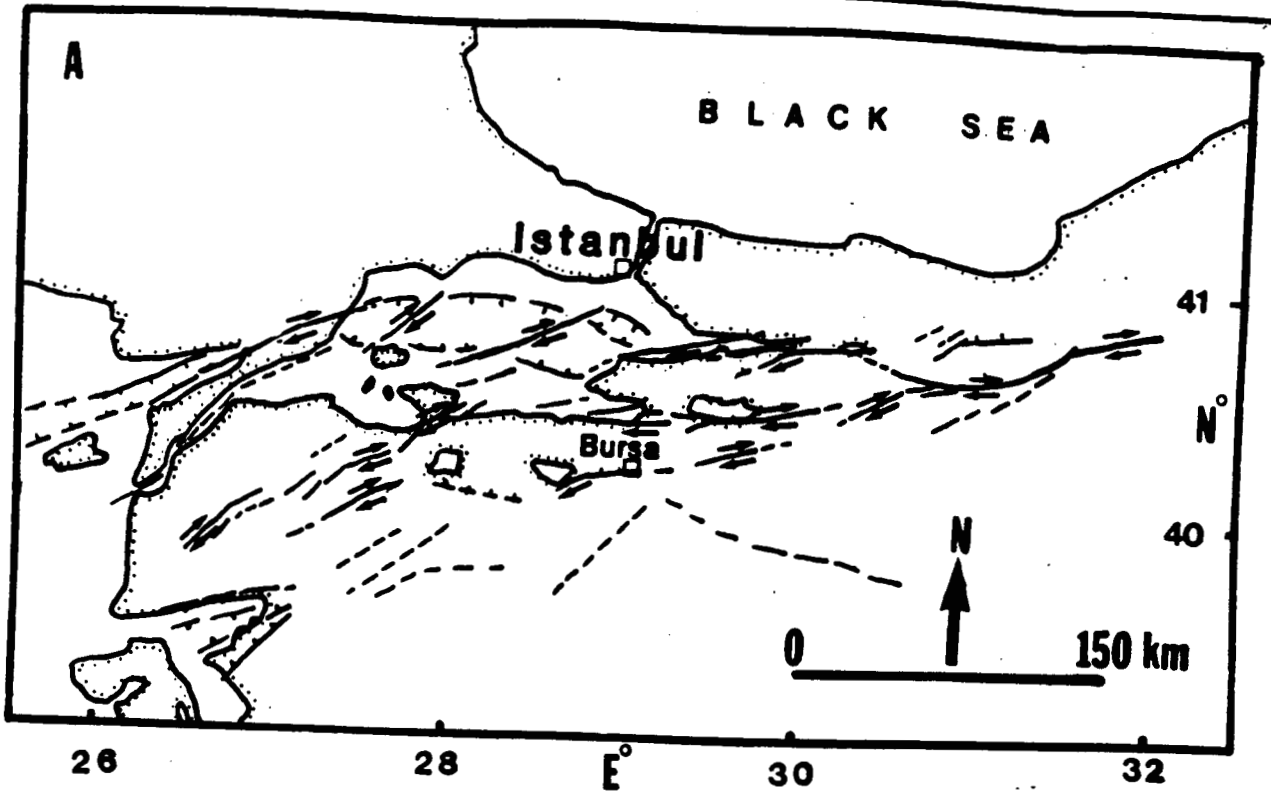


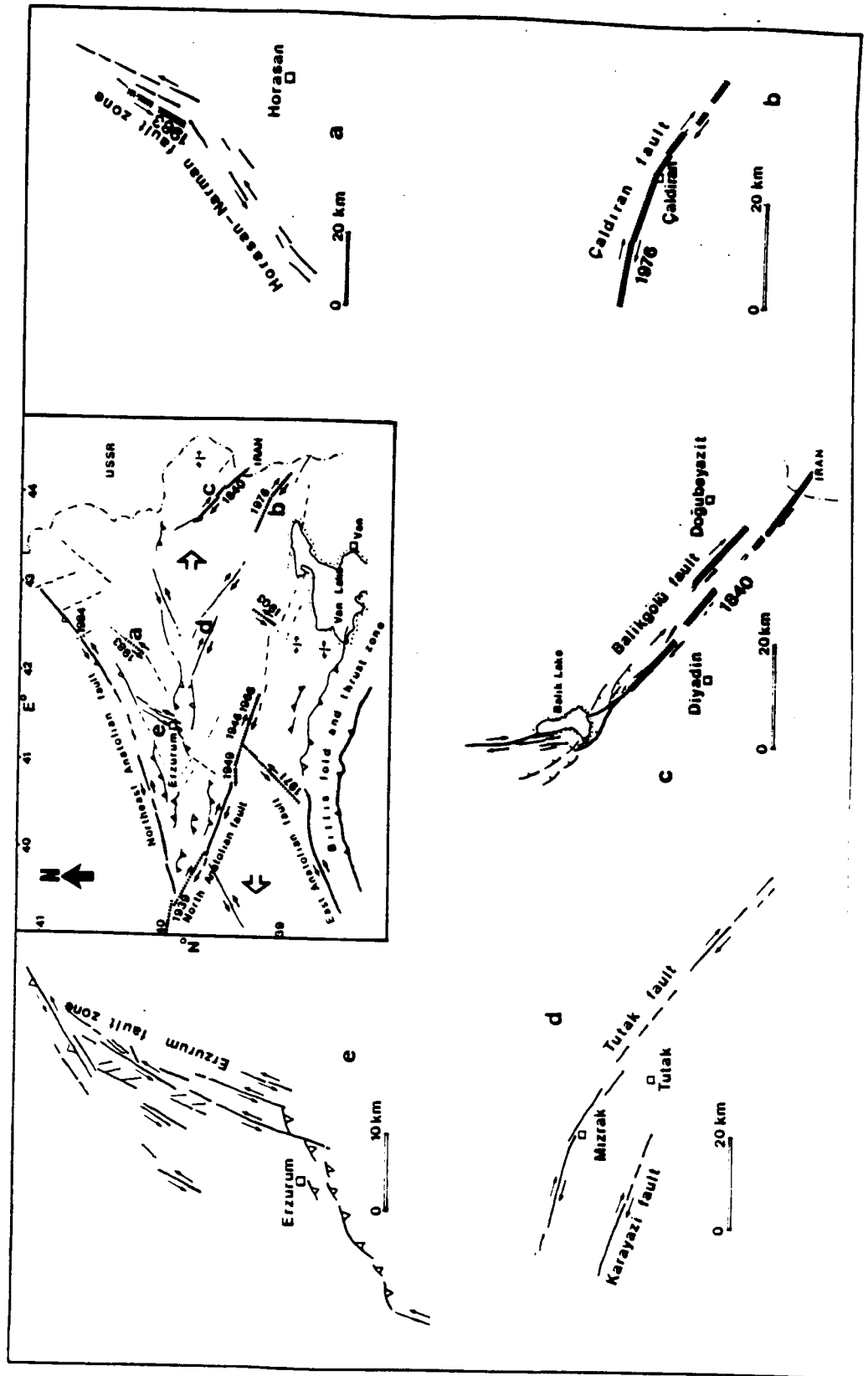
ORIGINAL PAGE IS
OF POOR QUALITY



ORIGINAL PAGE IS
OF POOR QUALITY



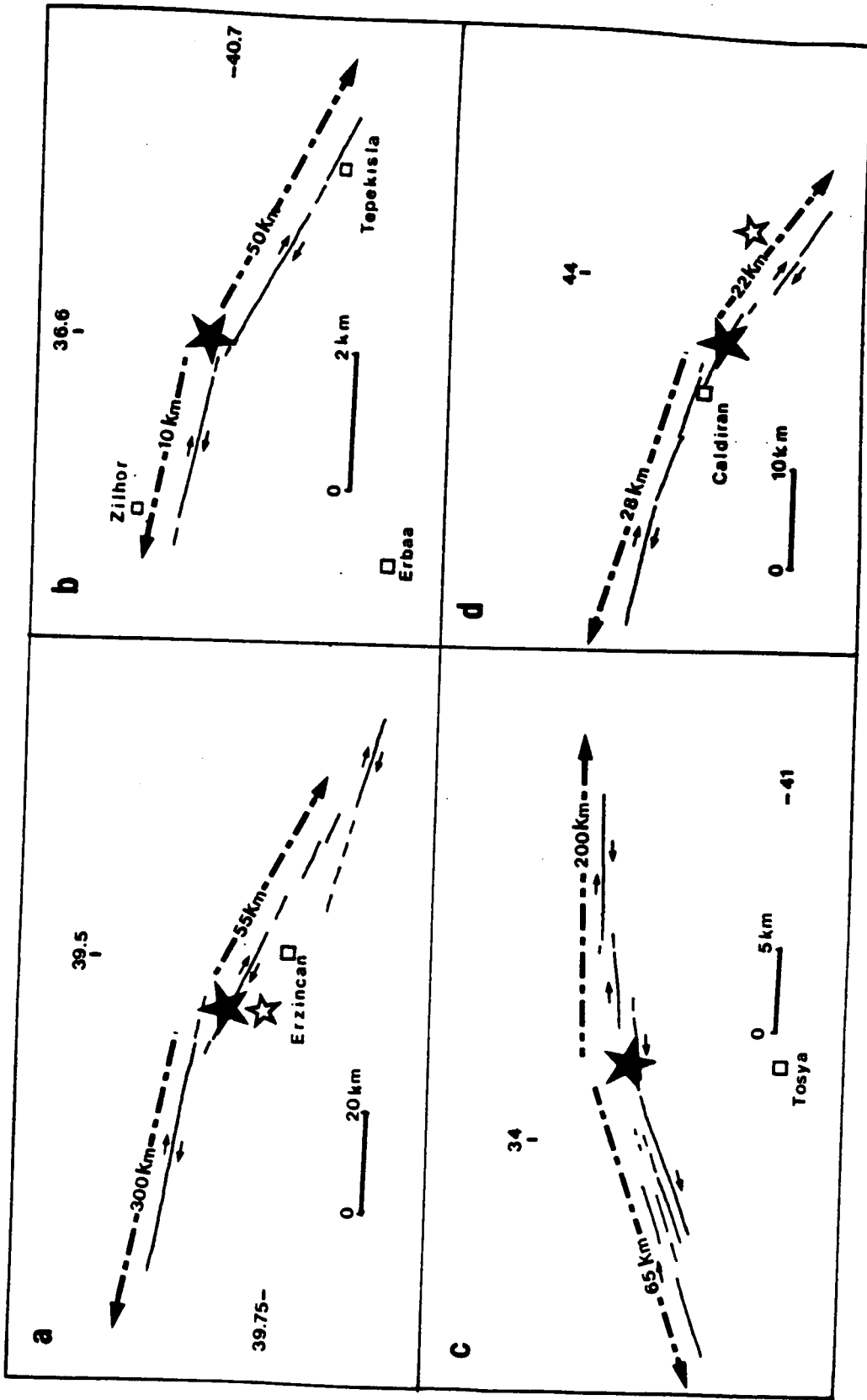




ORIGINAL PAGE IS OF POOR QUALITY

6

Schematic Geometric Fault Patterns		Unruptured Segments	
Single Bend	Ruptured Segments		
	1976 ET-Çaldıran 1855° NAF Seg. 11-12 1983° ET-Horasan-Narman *only 1 side of bend; 1855-2 events	NAF Seg. 21 NAF Seg. 9° ET-Erzurum *ruptured left of bend in 1943	$\alpha = 17-19^\circ$ $\alpha = 26^\circ$ $\alpha = 16^\circ$ $\alpha = 22^\circ$ $\alpha = 17^\circ$ $\alpha = 35^\circ$
	Bend/Stepover Combinations: (a)	1939 NAF Seg. 3c, 3d, 4° 1942 NAF Seg. 4, 5a° *stepover caused segmentation	NAF Seg. 23, 24a $\alpha = 20^\circ, d = 4-5 \text{ km}$
(b)	1949 NAF Seg. 1 ruptured right of stepover only	NAF Seg. 19 EAF Seg. 3 $\alpha = 10^\circ, d = 4 \text{ km}$ $\alpha = 17^\circ, d = 2 \text{ km}$	$\alpha = 16^\circ, d = 5 \text{ km}$
(c)	NAF Seg. 17 $\alpha = 20^\circ$		
(d)	1944 NAF Seg. 6a, 6b, 6c 1967 NAF Seg. 7, 8° 1953 NAF Seg. 14 *two ruptures (1957, 1967) - see text	ET-Erzurum EAF Seg. 7b EAF Seg. 6, 7 $\alpha 1 = \alpha 2 = 35^\circ, L = 17 \text{ km}$ $\alpha = 18^\circ, L = 1 \text{ km}$ $\alpha = 17^\circ, L = 60 \text{ km}$	$\alpha = 15^\circ, L = 10 \text{ km}$ $\alpha 1 = 10^\circ, \alpha 2 = 20^\circ, L = 6 \text{ km}$ $\alpha = 17^\circ, L = 10 \text{ km}$
(e)	1912 NAF Seg. 25 1939 NAF Seg. 3a, 3b, 3c 1943 NAF Seg. 5a, 5b	NAF Seg. 16 NAF Seg. 20 NAF Seg. 18 $\alpha = 17^\circ, d = 2.5 \text{ km}, L = 35 \text{ km}$ $\alpha = 19^\circ, d = 3.5 \text{ km}, L = 18 \text{ km}$ $\alpha = 13^\circ, d = 7 \text{ km}, L = 20 \text{ km}$	$\alpha = 14^\circ, L = 30 \text{ km}, d = 8 \text{ km}$ $\alpha = 20^\circ, L = 100 \text{ km}, d = 4 \text{ km}$ $\alpha = 15^\circ, L = 65 \text{ km}, d = 2 \text{ km}$
(f)	ET-Tutak-Karayazi $\alpha = 19^\circ, d = 16 \text{ km}, L = 20 \text{ km}$		
(g)	1840 ET-Balikgözü only section to right of bend $\alpha = 35^\circ, d 1 = d 2 = 4 \text{ km}$ $L 1 = 12 \text{ km}, L 2 = 35 \text{ km}$		
(h)	1939 Seg. 2, 3a only to left of stepover $\alpha = 16^\circ, d = 6 \text{ km}$	EAF Seg. 4, 5, 6 $\alpha = 9^\circ, d = 7.5 \text{ km}$	
(i)	1971 EAF Seg. 1, 2a, 2b, 2c only to right of double bend $\alpha 1 = 19^\circ, \alpha 2 = 30^\circ$ $L = 25 \text{ km}, d = 15 \text{ km}$	NAF Seg. 2, 3b to right of stepover $\alpha = 15^\circ, d = 5 \text{ km}$	$\alpha 1 = 19^\circ, \alpha 2 = 30^\circ$ $L = 25 \text{ km}, d = 15 \text{ km}$



APPENDIX II

THE SEGMENTATION, SEISMICITY AND EARTHQUAKE POTENTIAL OF
THE EASTERN PART OF THE NORTH ANATOLIAN FAULT ZONE

A. Barka

M.N. Toksöz

K. Kadinsky-Cade

L. Gülen

Earth Resources Laboratory
Massachusetts Institute of Technology
42 Carleton Street
Cambridge, MA 02142

April, 1987

ABSTRACT

Historical and instrumental earthquakes of the North Anatolian fault zone in the vicinity of the Erzincan basin have been examined in relation to fault segmentation. Results of this study suggest that each segment may have its own characteristic earthquakes. The epicenter of the 1939 great Erzincan earthquake ($M=8$) occurred near a 20° restraining bend located about 50 km from the eastern end of the 360 km long segment that ruptured during that earthquake. This segment was terminated at each end by releasing stepovers. Aftershocks mostly occurred in the releasing stepover/releasing bend area located at the eastern end of this segment. Historical records suggest that the 1939 event is characteristic of great earthquakes that occur approximately every 300 years on this segment. Recurrence times of large earthquakes (I = VIII - IX) is about 100 to 150 years in the Erzincan region. The segment to the east of the Erzincan segment is identified as a potential seismic gap. It is approximately 100 km long, and extends from the Erzincan releasing stepover to a restraining stepover-bend combination near Yedisu. This segment last ruptured in 1784. It is the only segment of the 900 km long main section of the North Anatolian fault that did not experience a large earthquake during the well-known 1939-1967 sequence of $M_s = 7-8$ earthquakes that ruptured the fault zone between Varto and the western end of the Mudurnu valley.

INTRODUCTION

It has recently been acknowledged that fault geometry plays a critical role in the earthquake rupture process (e.g., Segall and Pollard, 1980; Bakun *et al.*, 1980; Lindh and Boore, 1981; King and Nabelek, 1985; Sibson, 1986; Schwartz and Coppersmith 1986; Barka and Kadinsky-Cade, 1987). The term "fault geometry" includes stepovers, bends, and their many combinations. Each geometric pattern appears to have a characteristic dynamic rupture mechanism. Through fault geometry one can define fault segments, each having its own characteristic earthquakes.

In this paper we identify an approximately 100 km long fault segment in the eastern part of the North Anatolian fault zone which has not ruptured in the last 200 years. This segment is defined by geometric discontinuities. Through the analysis of geometric discontinuities along this and neighboring segments we examine the effect of fault geometry on the location of large earthquake epicenters, foreshocks, aftershocks and interpreted sites of strain accumulation.

The largest known earthquake to have occurred on the North Anatolian fault (NAF) is the 1939 Erzincan earthquake ($M_s = 8.0$). This earthquake caused great damage and killed 32,700 people. It ruptured a section of the NAF that extends from the Erzincan basin to the Amasya province, with surface breaks covering a distance of 360 km. The right-lateral displacement reached 3.7 m in places (Pamir and Ketin, 1941; Ketin, 1948, 1969; Ambraseys, 1970). Both historically and during modern times, the Erzincan area has been one of the most active seismic regions in Turkey (Sieberg, 1932; Ergin *et al.*, 1967; Soysal *et al.*, 1981; Tables 1 and 2).

Figure 1 shows major tectonic elements of Turkey in an area where the northward motion of the Arabian plate causes active convergence. As a result, the Anatolian block escapes westward and the northeast Anatolian block eastward (Ketin, 1948, McKenzie 1972; Kasapoglu and Toksöz, 1983; Gülen, 1984; Dewey *et al.*, 1986). The Anatolian block is bounded by the right-lateral North Anatolian fault to the north, and by its conjugate, the East Anatolian fault, to the south. These two fault zones intersect at the Karliova Triple junction. (Ketin, 1966; Allen, 1969; McKenzie, 1972; Dewey, 1976; Tchalenko, 1977; Sengör, 1979; Toksöz *et al.*, 1979, Jackson & MacKenzie, 1984; Sengör *et al.*, 1986; Dewey *et al.*, 1986). The eastern part of the Anatolian block is divided into two smaller blocks (A_1 and A_2 Figure 2) by the left-lateral strike-slip Ovacik fault. This fault intersects the NAF zone at the southeast end of the Erzincan basin. The eastward escape of the NE Anatolian block is complicated by the extensive internal deformation and by the existence of a number of sub-blocks. A dominant tectonic feature in this region is the NAF, which forms a boundary between the two blocks escaping in opposite directions. The NAF intersects the Northeastern Anatolian fault (NEAF, forming the northern boundary of the NE Anatolian block) northwest of Erzincan (Figures 1 and 2). Figure 2 shows major blocks and boundary faults between the Erzincan and Karliova triple junctions.

Between 1939 and 1967 most of the North Anatolian Fault west of Erzincan ruptured through a westward migrating series of major earthquakes, as shown in Figure 1. Earthquakes along the NAF east of Erzincan followed a more complicated pattern, as can be seen in Figure 2.

Fault Segments

Based on the geometric discontinuities of the main fault traces and extent of ruptures of large earthquakes we have identified the fault segments. The

North Anatolian fault zone consists of several segments as shown in Figure 2 (Barka and Kadinsky-Cade, 1987; Barka and Gülen, 1987).

Segment 1: This segment extends from Karliova to the Yedisu restraining stepover, where it bends around to the southwest, changing direction by 16° in a convergent sense. Segment 1 has a clear physiographic expression, particularly along the Elmali Valley (Allen, 1969). During the last 50 years this segment has ruptured in two separate earthquake sequences. The first sequence includes the 1946 Varto and 1949 Elmali earthquakes ($M=6.0$ and $M=7.0$ respectively), and the second includes the 1966 $M=7.0$ Varto earthquake and its aftershocks. ($M=5.3-6.2$; see also Table 2).

Segment 2: This segment strikes $N 70^\circ W$ and is approximately 100 km long. Segment 2 extends from the Yedisu plain in the east to the Erzincan alluvial plain (western end). The physiographic fault expression is very clear where the fault runs along the Euphrates valley and through the village of Caykomu. The physiographic expression disappears, however, as soon as the segment enters the Erzincan alluvial plain, although the segment may continue further west under the plain. The 1784 earthquake, which last ruptured this entire segment, created surface breaks along a 90 km distance, and caused 1m of vertical displacement (Ambraseys, 1975). The 1967 $M=6$ Pülümür earthquake was also located along this segment. Surface breaks for the 1967 event were, however, only 4 km long; this earthquake was accompanied by 20 cm of right-lateral surface displacement (Ambraseys, 1975).

Segment 3: This segment is defined by the extent of surface rupture produced by the 1939 Great Erzincan earthquake. Segment (3) is divided into 4 subsegments. Subsegment 3a is 60 km long, and has a strong physiographic expression in its western half. It is separated from segment (2) by a 4-5 km wide

releasing stepover which forms the Erzincan basin. This basin is characterized by short en-echelon strike-slip faults and contemporaneous volcanics. Subsegment 3a is separated from 3b by a 20° restraining bend. Subsegment 3b is about 100 km long, and extends from this bend, situated about 10 km NW of the Erzincan basin, to Susehri - the location of another pull-apart basin (Hempton and Dunn, 1983). Subsegment 3c extends from Susehri to the Niksar basin through the Kelikit valley. It is 110 km long and relatively straight. Southwest of the Niksar basin a 15° restraining bend separates subsegment 3c from 3d. Subsegment 3d is 90 km long, and ends south of Amasya where the 1939 earthquake rupture stopped.

The epicenter of the 1939 Great Erzincan earthquake was located near the 20° restraining bend separating subsegments 3a and 3b. Many of the 1939 earthquake aftershocks caused damage in the Erzincan and Niksar pull-apart basins (Ergin *et al.*, 1967; Tabban, 1980; see also Riad and Meyer, 1983). A fault plane solution for a moderate size earthquake ($M_b = 4.8$, 11/18/1983) near the city of Erzincan is characterized by ENE-WSW extension (International Seismological Centre Bulletin solution), in agreement with our interpreted pull-apart character of the Erzincan basin.

Northeast Anatolian Fault - This fault zone consists of several segments with a combined length of approximately 350 km. The southwesternmost segment (Segment A) is located to the north of the Erzincan region (Figure 2). Approximately 70 km long, it strikes NE-SW. Although very little is known about this fault segment, it is assumed to have an oblique movement, consisting mostly of left-lateral slip with a subordinate thrust component. (Tatar, 1978). The study of earthquake records (Soysal *et al.*, 1981; Sipahioglu, 1983; Riad and Meyers, 1985) indicates that it might be less active than the segments of the North Anatolian Fault zone. Apart from the 1939 Tercan earthquake ($M=5.9$) and

several aftershocks of the 1939 great Erzincan earthquake, the only known historical event associated with this segment is the 1254 I=IX earthquake. This event caused surface breaks to occur over a 50 km length on segment A (Ambraseys, 1975).

Ovacik fault - This is another left-lateral fault. It is located near Ovacik, and extends up to the southeast end of the Erzincan basin. This fault is about 120 km long and trends NE-SW. Near Ovacik, where the fault cuts Quaternary alluvial fans, physiographic expressions are very clear (Arpat and Saroglu, 1975). The Ovacik fault has also been participating in the opening of the Erzincan basin. The only earthquake might have occurred on the Ovacik segment is the 01/28/1960 M=5.9 event (macroseismic location; Ergin *et al.*, 1987). There are no historical events that can be specifically associated with this segment.

It should be noted that the area between segments 2 and 4, including the Ovacik fault and segment A of the NEAF zone, is located within the serpentinite-rich ophiolites and ophiolitic melange associated with the Anatolid/Taurid-Pontid suture zone.

Seismicity

Historical Earthquake Records

The history of damaging earthquakes in the Erzincan region was recognized and well documented even before the great earthquake of 1939 (Ali Kemal, 1932). Sieberg (1932) listed some of the Erzincan earthquakes and stated that between 1045 and 1784, at least 17 catastrophic earthquakes had occurred in the Erzincan region. In Table 1 we have tabulated the significant earthquakes affecting the Erzincan region since 1000 A.D., based on sources referenced in the table.

Figure 3a is an intensity-time plot of known earthquakes which have affected the Erzincan region. From this figure, earthquakes can be categorized according to three sizes: (a) small and moderate, with Modified Mercalli intensity $I \leq VIII$, (b) large earthquakes with $VIII \leq I \leq IX$ and (c) great earthquakes for which $I \geq X$. According to Figure 3a, at least 3 great earthquakes have occurred during the last 1000 years, including the one in 1939. Ambraseys (1970) reported that the 1045 earthquake produced a surface break of a length comparable to the one which occurred in 1939; and that the 1458 earthquake caused the death of about 32,000 people, comparable to the casualties of the 1939 earthquake. The 1668 earthquake is controversial. With the exception of Ambraseys (1975), most of the existing references describe it as an earthquake of intensity about VIII-IX. Ambraseys (1975) reports that the 1668 earthquake produced a 380 km surface break and that the lateral displacement was as much as 4 m, which is again comparable to that of 1939. At least 10 large earthquakes ($VIII \leq I \leq IX$) have occurred in the Erzincan region since 1000 A.D., causing considerable damage and large numbers of casualties.

Figure 3b shows the number of earthquakes that occurred between 1000 and 1900 in the Erzincan region, versus intensity. The dashed line is drawn only through the $I \geq VIII$ points, because the historical record may be incomplete for smaller events. According to this plot, the recurrence interval for the great earthquakes in category (c) (intensity X or greater) is about 400-450 years if the 1668 event is excluded. With the 1668 earthquake, the recurrence interval becomes about 300 years. These recurrence intervals, combined with the amount of displacement created during the great earthquakes (3-4m), give a slip-rate of approximately 1 cm/yr. This is comparable to the creep rate observed at Ismetpasa, on the central part of the NAF, from geodetic measurements (Eren *et al.*, 1984) and creepmeter data (Toksöz, 1984, USGS

report). Note that the 1 cm/year slip rate estimated here for the NAF zone near Erzinan does not include a possible additional creep component. This slip-rate is at least two times higher than that obtained from geological (Plio-Quaternary) results along the NAF (0.4-0.5 cm/yr, Seymen, 1975. Barka and Hancock, 1984). This reveals that the motion may be progressively accelerating or episodic. Note also that segments 1-3 form a boundary between opposite-moving blocks (the Anatolian and Northeast Anatolian blocks). Thus a higher slip rate is expected in this area than along the main section of the NAF to the west. From Figure 3b the recurrence interval for large earthquakes ($VIII \leq I \leq IX$) is approximately 100-150 years.

Instrumental Earthquake Records

Figure 4 shows the distribution of epicenters for earthquakes with $M_s > 4.9$, that have occurred between Erzinan and Varto since 1900. These events are listed in Table 2. The following points should be made concerning the listed earthquakes:

- a) There is a quiescent period between 1900 and 1930 in the Erzinan region.
- b) Although Pamir and Ketin (1941) did not have any field observation (Ketin 1987, pers. communication), they showed ESE-WNW trending isoseismals covering the area between Tercan and Baskoy for the epicenter of the 1939/11/21 Tercan earthquake that may have been on the NEAF zone. This is not only suggested by some catalogs, but also by the amount of damage that occurred in and near Karakulak (e.g., 130 buildings collapsed), and in some other destroyed villages which are all situated next to the fault zone (Pamir and Ketin, 1941; Ergin *et al.*, 1967; Tabban, 1980).
- c) The December 27, 1939 Erzinan earthquake ($M=8$) is one of the largest

earthquakes to have occurred in this area. We will summarize known information concerning foreshocks, main shock, aftershocks, and surface breaks in the Erzincan region. Pamir and Ketin (1941) reported that two foreshocks were felt within the week preceding the main shock in the Erzincan region. The epicenter of the main shock was within the Erzincan region in the range $39.7^{\circ} - 39.8^{\circ}\text{N}$, $39.4^{\circ} - 39.5^{\circ}\text{E}$ (e.g. Tillotson, 1940; Pamir and Ketin, 1941; Ergin *et al.*, 1967; Karnik, 1969; Dewey, 1976). The main surface breaks were associated with segment 3. Within the basin some discontinuous extension cracks striking WNW-ESE were also observed, and in the salt playa east of Erzincan the fissures were 80-100 cm wide (Pamir and Ketin, 1941). The villages along the northern margin of the Erzincan basin were completely destroyed by either the main shock or the aftershocks. The eastern end of the surface breaks coincided with the eastern end of the Erzincan basin (Pamir and Ketin, 1941; Ketin 1969). Numerous aftershocks occurred in the Erzincan region as well as in many other places (e.g. Nature, 1940 a, b, c): According to Nature (1940c), on February 3, 1940, two villages were destroyed in the Erzincan region (close to the NEAF zone, segment A) by a shock which also killed 45 people and injured many more. Pamir and Ketin (1941) also state that between February 3 and 20, 1940, many earthquakes were felt in the region. However, available earthquake catalogs do not contain many of these earthquake records. Aftershocks 11, 14, 15, 17, and 18 (listed in Table 2) were felt strongly in the Erzincan region and caused some damage in the villages. In particular, aftershock 15 caused 40 buildings to collapse, and aftershock 18 was responsible for 15 deaths and 100 injuries (Tabban, 1980). Most of the aftershocks were located in or near the Erzincan basin.

d) Although some catalogs indicate that the August 17, 1949 earthquake ($M=6.7-7$) was close to the eastern end of segment 2, this earthquake was on the

easternmost segment of the NAF zone, called the *Kartiova-Elmalı* segment (Lahn, 1952) (Segment 1 in Figure 2).

e) According to some catalogues, the epicenter of the 1960/01/28 ($M=5.9$) earthquake might have occurred near the northeastern part of the Ovacik fault (see Figure 5 and Table 2) (Ergin *et al.*, 1967; Tabban, 1980).

f) The relocated epicenter of the 1967/07/26 $M=5.6-6.2$ earthquake (Dewey, 1976) was located on the eastern half of segment 2, although the macroseismic epicenter was in Pülümür.

Discussion and Conclusions

It is possible to make a correlation between the pattern of seismic activity and the geometry and distribution of active fault segments in the Erzincan region. Both historical data and the 1939 earthquake have shown that great earthquakes in this region can be associated with segments 3 a, b, c, d. The epicenter of the 1939 earthquake occurred near the 20° restraining bend between subsegments 3s and 3b of the NAF. (Barka and Hancock, 1982; Barka and Kadinsky-Cade, 1987). Furthermore, observations of compressional deformation and uplifting within the young deposits along subsegments 3a and 3b can be interpreted as surface expressions of high strain accumulation in the area, which eventually results in the occurrence of very large earthquakes. Since the recurrence interval for great earthquakes is about 300-400 years, the last earthquake having occurred in 1939, at present the probability of an earthquake of comparable magnitude is small.

In the Erzincan region, many of the small to moderate aftershocks (category a in Figure 3a) can be related to the releasing stepover area in the

eastern half of the Erzincan basin, between segments 2 - 3a and the Ovacik fault (Barka and Gülen, 1987). Moreover the fault plane solution of the 1983/11/18 earthquake ($M_4.8$), located near the city of Erzincan, shows normal faulting (Figure 5); this clearly supports the idea of a tensile stress regime produced by the pull-apart extension in the Erzincan basin. Some of the small to moderate earthquakes in the area may also be associated with the Ovacik fault, with segment A of the NEAF zone, or with internal block deformation, as in the case of the Kigi-Karliova area in block A_1 (Figure 4). There have been no large earthquakes (category b) for at least 200 years in the vicinity of Erzincan, excluding the segment 1 and Varto earthquakes (1946, 1949, 1966). The last large earthquake occurred in 1784 and was located on segment 2, according to Ambraseys (1975) (Figure 6a), who also reported 90 km surface faulting along a 115° trend. Although the damage and casualties were less severe than in 1939 (Sieberg 1932), the 1784 earthquake was extremely destructive for the Erzincan region, killing 5,000-15,000 people (see Table 1). The recurrence interval for category b events is about 100-150 years, and earthquakes most likely correspond to segment 2, the Ovacik fault or segment A of the NEAF zone. Of these, segment 2 has the highest potential for generating large earthquakes in the near future, because (a) segments 1-3a of the NAF zone form a boundary between the eastward-moving NE Anatolian block and the main westward-moving Anatolian block, so that the rate of movement is naturally expected to be higher than along other parts of the NAF zone; and (b) during the 20th century segment 2 is the only segment along the NAF zone which has not experienced a large earthquake between Varto and the western end of the Mudurnü valley (900 km) (see also Ambraseys and Zatopek 1969). Note that segment 1 has already broken twice in the last 40 years (Figure 6c,d). The largest event which has occurred on segment 2 during the instrumental period (since 1900) is the 1967 Pülümür earthquake ($M_s = 5.6 - 6.2$), (Figure 6d). Ambraseys (1975) has reported that

this earthquake produced a short rupture, 4 km long, with 20 cm maximum dextral slip, at the eastern half of segment 2. However, if we consider the approximately 100 km length of segment 2, the 1967 event is not large enough to fill the gap (Figure 7). Therefore segment 2 appears to have the highest potential for a large earthquake in the Erzincan region in the near future. The segment 2 gap, which is separate from the gap mentioned by Toksöz *et al.*, (1979; see Figure 7), was first mentioned by Ambraseys and Zatopek (1969).

Only a few poorly located earthquakes (e.g., 1960, M=5.9) can be associated with the Ovacik fault since 1900. Although the rate of movement is somewhat smaller along this fault than on the NAF zone (Barka and Gülen, 1987), the Ovacik fault segment is another candidate for future large earthquakes. Segment A of the NEAF zone is similar to the Ovacik fault. The 1939/11/21 Tercan earthquake and 1940/02/03 (#12 in Table 2) aftershock of the great 1939/12/26 earthquake might have occurred on segment A. From the historical earthquake records, we are only aware of the 1254 large earthquake, which created 50 km of surface faulting along segment A, trending 60° with 5 m (?) maximum vertical displacement (Ambraseys, 1975).

The unruptured fault segments, including segment 2, the Ovacik fault, and Segment A, occur within the serpentinite-rich ophiolitic complexes in the vicinity of Erzincan. Thus creep is an expected phenomenon which probably takes up some of the motion along the fault segments. Nevertheless this does not exclude the potential for future large earthquakes.

In conclusion, defining segmentation of the fault zones through geometric discontinuities and combining resulting segments with existing earthquake data can provide information about seismic gaps and earthquake rupture processes. A possible explanation for the high concentration of seismic activity in the

Erzincan region is the fact that many different fault segments begin, terminate or intersect within that region. The geometric arrangement of fault discontinuities (restraining bends, triple junctions and releasing stepovers) and the rock type (e.g., serpentinite) contribute to the relative ease or difficulty of movement along fault segments in the region. These factors are responsible for the division of earthquakes into categories a, b or c. Our interpretation of fault geometry and earthquake data in the Erzincan region suggests that a large earthquake similar to the 1784 event is expected to occur soon. This earthquake could cause considerable damage in Erzincan and surrounding areas. Further detailed studies are required in order to better characterize this seismic hazard.

REFERENCES

ORIGINAL PAGE IS
OF POOR QUALITY

- Ali, K. Erzincan Earthquakes, Erzincan province year-book, 110-115, 1932.
- Allen, C.R., Active faulting in northern Turkey: Contr. No. 1577. Div. Geol. Sci., Calif. Inst. Tech., 32 p., 1969.
- Alsan, E., Tezucan, L. and Bath, M. *An earthquake catalogue for Turkey for the interval 1913-1970*. Kandilli Observatory Seismology Dept. Report No. 7-75. 166 pp., 1975.
- Ambraseys, N.N. Some characteristic features of the North Anatolian fault zone. *Tectonophysics* 9, 143-165, 1970.
- Ambraseys, N.N. Studies in historical seismicity and tectonics, in: *Geodynamics of Today*, The Royal Soc. London, 7-16, 1975.
- Ambraseys, N.N. and Jackson, J.A. Earthquake hazard and vulnerability in the northeastern Mediterranean: the Corinth earthquake sequence of February-March 1991. *Disasters*, 5, 355-368, 1991.
- Ambraseys, N.N. and Finkel, C.F. 1987. The Anatolian earthquake of 17 August 1668. Proceedings of the Symposium on Historical Seismograms & Earthquakes. Ed. W.H.K. Lee, 400-407, 1987.
- Arpat E., and Saroglu, F. Some recent tectonic events in Turkey. *Türk Jeol Kur Bul.* 18, 91-101, 1975.
- Arpat, E. The 1976 Caldiran earthquake: *Yeryuvarı ve İnsan* 2, 29-41, 1977.
- Bakun, W.H., Stewart, R.M., Bufe, C.G. and Marks, S.J. Implication of seismicity for failure of a section of San Andreas Fault. *Bull. Seism. Soc. Am.* 70, 185-202, 1980.

- Barka, A.A. Some Neotectonic features of the Erzincan basin. Earthquake Symposium, Atatürk University, special publication, Erzurum (Turkish with English Abst.) pp. 115-125, 1984.
- Barka, A. and Hancock, P.L. Neotectonic deformation patterns in the convex-northwards arc of the North Anatolian fault, in *The Geological Evolution of the Eastern Mediterranean* (edited by Dixon, J.G. and Robertson, A.H.F.), Special publication Geol. Soc. London, 763-773, 1984.
- Barka, A.A. and Hancock, P.L. Relationship between fault geometry and some earthquake epicenters within the North Anatolian fault zone, *Progress in Earthquake Prediction*, edited by A.M. Isikara and A. Vogel, Friedr. Vieweg and John, F.R.G., 2, pp. 137-142, 1982.
- Barka, A.A. and Kadinsky-Cade, K., Strike-slip fault geometry and earthquake activity in Turkey, *Tectonics*, 1987
- Barka, A.A. and Gülen, L. Tectonic escape origin and complex evolution of the Erzincan pull-apart basin, Eastern Turkey, *Geol. Soc. Amer. Bull.* 1987
- Can, R. Seismo-tectonics of the North-Anatolian fault zone. M. Phil. Thesis University of London, 255 pp., 1974
- Dewey, J.W. Seismicity of Northern Anatolia, *Bull. Seism. Soc. Am.* 66, 843-868, 1976.
- Eren, D., Akkas, N. and Erdik, M. Finite element modelling of Eastern Mediterranean regime. Unpublished report Middle East Technical University Ankara, Turkey, 1984

- Ergin, K. Güclü, U. and Uz, Z. A catalogue of earthquakes for Turkey and surrounding area. *Ist. Tek. Uni. Mad. Fak. yay.* 24.189 pp., 1967.
- Erzincan Yilligi. Erzincan earthquakes. Year-book of the Erzincan province, 225 pp., 1967.
- Gülen, L. Sr. Nd. Tb isotope trace elements, Geochemistry of calcaline and alkaline volcanics, Eastern Turkey. Ph.D. Thesis, Massachusetts Institute of Technology. 232 pp., 1984.
- Jackson, J. and McKenzie, D. Active tectonics of the Alpine-Himalayan Belt between western Turkey and Pakistan. *Geophys. Journ. R. Ast. Soc.* 77, 185-265, 1984.
- Karnik, V. *Seismicity of the European area*. D. Reidel Pub. Com., Dordreet, Holland, Part I, 365 pp., 1969.
- Karnik, V. *Seismicity of the European area*. D. Reidel Pub. Com., Dordreet, Holland, Part II, 218 pp., 1971.
- Kasapoglu, E. and Toksöz, M.N. Tectonic consequences of the collision of the Arabian and Eurasian plates: finite element models, *Tectonophysics*, 100, 71-96., 1983.
- Ketin, I. Über die tektonisch-mechanischen Folgerungen aus den grossen anatolischen Erdbeben des letzten Desenniums. *Geol. Rdsch.*, 36, 77-83, 1948.
- Ketin, I. Über die nordanatolische horizontalverschiebung, *Bull. Min. Res. Explor Inst. Turkey*, 72, 1-28 pp., 1969.
- King, G. and Nabelek, J. Role of fault bends in the initiation and termination of

- earthquake rupture. *Science*, 228, pp. 984-987, 1985.
- Lahn, E. Seismic activity in Turkey from 1947-1949, *Bull. Seism. Soc. Amer.*, 42, pp. 111-114, 1952.
- Lindh, A.G., and Boore, D.M. Control of rupture by fault geometry during the 1988 Parkfield earthquake, *Bull. Seism. Soc. Am.*, 71, pp. 95-118, 1981.
- McKenzie, D. Active tectonics of the Mediterranean Region. *Geophys. J. R. Astr. Soc.*, 30, 109-185, 1972.
- Nature*, The earthquake in Turkey, 145, 62, 1940a.
- Nature*, The earthquake in Turkey, 145, 98, 1940b.
- Nature*, Aftershocks of the earthquake in Turkey, 145, 259, 1940c.
- Nature*, 1940d. Earthquakes in Turkey, 145, 346.
- Pamir, N. and Ketin, I. Das Erdbeben in der Türkei vom 27 und 28 Dezember, 1939. *Geol. Rundsch.* 31, 77-78, 1940.
- Pamir, H.N. and Ketin, I. Das Anatolische Erdbeben Ende 1939, *Geol. Rundsch.*, 32, 278-287, 1941.
- Parajes, E., Akyol, I. H. and Altinli, E. Le tremblement de terre d'Erzincan du 17 Decembre 1939. *Revue Fac Sci Univ Istanbul*, XVI, 177-222, 1941.
- Pinar, N. and Lahn, E. Earthquake catalogue of Turkey. Bayin Bakan. Yapi Imar Isle. Reis yayin. 6. 36. Ankara, 1952.
- Riad, S. and Meyers, H. Earthquake catalog for the Middle East countries 1900-1983. World Data Center A. Report, SE-40. 133, 1985.

Salomon-Calvi, W. Die Fortsetzung der Tonaelinie in Kleinasien. *Yük. Zira. Enst. Calis*, 9, pp. 11-13, 1936.

Study of earthquakes in Turkey, MTA. Enst. Yay. Sei B. No:5, L-121, 1940.

Schwartz, D.P., and Coppersmith, K.J. Seismic hazards: New trends in analysis using geologic data, in *Active tectonics*, National Acad. Press, Washington, D.C., pp. 215-230, 1986.

Segall, P. and Pollard, D.D. Mechanics of discontinuous faults, *J. Geophys. Res.*, 85, pp. 4337-4350, 1980.

Sengor, A.M.L. and Kidd, W.S.F. Post-collisional tectonics of the Turkish-Iranian Plateau and a comparison with Tibet, *Tectonophysics*, 55, pp. 361-376, 1979.

Sengor, A.M.C., Görür, N. and Saroglu, F. Strike-slip faulting and related basin formation in zones of tectonic escape: Turkey as a case study. I: Biddke, K.T. and Christie-Blick, N. (eds.). *Strike-slip faulting and Basin Formation*, Society of Econ. Paleont. Min., Sp. Pub. pp. 227-264, 1985.

Seymen, I. Tectonic aspects of the North Anatolian fault zone within the Kelkit valley. Ph.D. Thesis, Ist. Tek. Uni. 152 pp., 1975.

Sibson, R.H. Earthquakes and lineament infrastructure, *Phil Trans R. Soc London*, 317, pp. 63-79, 1986.

Sieberg, A. Untersuchungen über Erdbeben und Bruchscholenbau im oestlichen Mittelmeergebiet. *Denk d. Mediz. Natu. Ges. zu Jena*, Bd. 18, pp. 159-273, Jena, 1932.

- Sipahioglu, S. Seismo-tectonic features of the North Anatolian fault zone, Ph. D. Thesis, Ist. Univ. Fen Fak. Jeofizik Böl., 169 pp., 1982.
- Sipahioglu, S. An evaluation of earthquake activity of the Horasan-Narman region before the 30 October 1983 earthquake. *Yeryuvarı ve İnsan* 8, 3. pp. 12-15, 1983.
- Soysal, H., Sipahioglu, S., Kolcak, D. and Altinok, Y. Historical earthquake catalogue of Turkey and its vicinity. Turkish Scienc. Res. Found. TBAG 341, 122 pp., 1981.
- Tabban, A. Geology and earthquake activity of the cities, T.C. İmar. İskan Bakanligi. Aft. İleri Genel. Mu. Ankara, 343 pp., 1980.
- Tatar, Y. Tectonic investigations on the North Anatolian fault zone between Erzincan and Refahiye, *Publ. Inst. Earth. Sci., Hacettepe Univ.* 4, 201-138, 1978.
- Tillotson, E. The Earthquake in Turkey, *Nature*, 145, pp. 13-15, 1940.
- Toksöz, M.N., Shakal, A.F. and Michael, S.J. Space-time migration of earthquakes along the North Anatolian fault zone and seismic gaps, *Pageoph.*, 117, pp. 1258-1269, 1979.
- Toksöz, M.N. Seismicity and earthquake prediction studies in Turkey. Unpublished USGS proposal, 1984.

FIGURE CAPTIONS

- Figure 1.** Tectonic map of Turkey showing the surface rupture along the North Anatolian and other faults due to major earthquakes since 1900. The Anatolian and NE Anatolian blocks are wedged out to the west and east respectively by the convergence of Arabia and Eurasia as shown in the inset map (lower left). The rectangle in the figure delineates the area of study and is enlarged in Figure 2. (Compiled from Arpat & Saroglu 1972; Arpat 1976; Barka 1984; Sengör et al., 1986).
- Figure 2.** Simplified geometry of major blocks and their boundary fault zones between Erzincan and Karliova. Thick and dashed zones and dates indicate ruptured fault segments and dates of related earthquakes, respectively. Dotted area is the Erzincan basin. A_1 and A_2 are sub-blocks within the Anatolian block.
- Figure 3.** (a) Earthquake activity histogram of the Erzincan region. I, Intensity, T, time. Numbers above the dots are the number of casualties resulting from each particular event. a, b, c are the categories of earthquakes, S-2, S-3, S-4 and S-A are the fault segments. For explanation and references see the text and Tables 1 and 2 respectively. (b) \log (number of earthquakes) versus intensity, 1000 - 1900, in the Erzincan region. The dashed line is drawn through the $I \geq VIII$ data points ($\log N = -0.271 I + 2.98$).
- Figure 4.** Distribution of earthquake epicenters ($M > 4.9$) in the easternmost part of the NAF zone between Erzincan and Karliova for the interval 1900-1983. A = instrumental data only, B = macroseismic information only, C = best of instrumental or macroseismic information, D = instrumental and macroseismic data agree. Details are given in Table 2.
- Figure 5.** Fault plane solutions between Erzincan and Karliova (McKenzie, 1972). Note that a) the 1983/11/19 earthquake, $M_s = 4.8$, has a normal fault solution which agrees with the opening of the Erzincan basin and b) solutions east of the Karliova junction have a clear thrust component.
- Figure 6.** Sequence of events which produced surface faulting in the Erzincan-Karliova region in the last 200 years. For explanation see text.
- Figure 7.** Space-time distribution of surface ruptures of 20th century earthquakes, indicating a clear seismic gap between 39.8 and $40.8^\circ E$, where segment 2 lies. The area to the east of 41.8° has been identified already as another seismic gap (Toksöz et al., 1979).

Table 1. List of historical earthquakes
in the Erzincan Region.

Number	Date	Intensity (I)	Number of casualties
(1)	1045	X-XI	
(2)	1161	VI	
(3)	1165	VII	
(4)	1168	VI	
(5)	1168	VIII	
(6)	1170	VIII-IX	12,000
(7)	1236	VI	
(8)	1251	VIII	
(9)	1254-55	VIII	
(10)	1268	IX	16,000
(11)	1287	VIII	15,000
(12)	1289	VIII	
(13)	1308	VI	
(14)	1356	V	
(15)	1366	VI	
(16)	1374	VII	
(17)	1422	VIII	
(18)	1433	VI	
(19)	1458	X	
(20)	1543	VII	32,000
(21)	1578	VIII	
(22)	1605	?	1,500-15,000
(23)	1667-8	VIII-X	Half of the town was destroyed
(24)	1784	VIII-IX	
(25)	1887	VI	5,000-15,000

* Documented from: Sieberg 1932, A. Kema 1932, Solomon-Calv. 1936-1940, Parejas *et al.*, 1941, Pinar and Lahn 1952, Ergin *et al.* 1967, Ambraseys 1970, 1975, Karuk 1972, Can 1974, Jewey 1976, Soysal *et al.*, 1981, 1982, Siparoglu 1982, 1983

ORIGINAL PAGE IS
OF POOR QUALITY

ORIGINAL PAGE IS
OF POOR QUALITY

Table 2. List of instrumental earthquakes with $M_s > 4.9$, for the 1900-1983 interval in the eastern part of the NAF zone.

Number	Dates	Epicenter		M	Reference
		Lat. N	Long. E		
(1)	1907/04/06	*39.30	40.40	4.9	3,2
		Damage at Kigi			2
(2)	1909/--/--	*39.3	40.3	5	4
		Kigi			2
(3)	1909/05/03	*39.	40	5.3	4
		(Tercan?)			2
(4)	1930/04/09	*39.6	39.3	5.	3
(5)	1930/12/10	39.8	39.1	5.6	1
		39.5	39.4	5.4	4
		*39.7	39.2	5.6	3
		Slight damage at Kernak and Erzincan			2
(6)	1934/11/12	39.2	40.5	5.9	1
		*39.	41.	5.8	4
(7)	1935/05/11	*39.3	40.6	6.1	4
(8)	1935/10/13	*39.4	40.2	5.1	1
		39.3	40.5	4.8	4
		39.4	40.5	5.	3
(9)	1939/11/21	*40.	39.7	5.9	1
		39.7	40.4	4.7	(?)4
		39.8	39.7	5.9	3
		43 deaths at Erzincan, heavy damage at Karakulak			2
(10)	1939/12/26	*39.8	39.4	8	1
		39.7	39.5	8	4
		39.8	39.5	7.9	3
(11)	1939/12/29	*39.7	39.7	5	4
(12)	1940/02/03	40.1	39.9	?	5
		45 deaths, Besin and Pulur destroyed			
(13)	1940/02/04	*39.7	39.5	5	3

Number	Dates	Epicenter		M	Reference
		Lat. N	Long. E		
(14)	1940/04/22	39.5	40.	5.2	1
		*39.7	39.7	5.	4
		39.6	39.9	4.9	3
		at Erzincan			
(15)	1940/05/29 40 buidings collapsed in the villages, vicinity of Erzincan	*39.7	39.7	5.	4
					2
(16)	1940/09/11	*39.9	38.8	5.	4
(17)	1941/11/08	*39.7	39.7	5.3	4
		39.7	39.7	5.	3
		at Erzincan			2
(18)	1941/11/12	39.9	39.4	5.9	1
		*39.7	39.7	5.7	4
		39.7	39.4	5.9	3
		15 deaths, 100 injured at Erzincan			2
(19)	1946/5/31	*39.3	41.1	5.9	1
		40.	41.5	6	4
		39.3	41.2	5.7	3
		839 deaths at Varto and Usturkiran			2
(20)	1946/12/13	*slight damage at Pulumur		5.2	2
(21)	1949/8/17	39.	40.5	6.7	1
		39.4	40.9	6.5	4
		39.6	40.6	7.	3
		*39.4	40.8		6
		300 deaths at Karliova			2
(22)	1949/8/17	39.6	40.4	5.2	1
		*39.5	40.6	5.	4
		40.1	40.6	5.3	3
(23)	1949/8/17	*39.6	40.8	5.2	3
(24)	1949/11. 01	*39.3	40.3	4.9	3
		slight damage at Kigi			2
(25)	1950 02. 04	*39.3	41.	4.9	3
(26)	1950 08. 27	*39.4	41.	4.9	3
		two deaths at Varto			2
(27)	1953. 12. 15	39.7	41.2	5.5	1
		39.1	41.4	5.3	4

ORIGINAL PAGE IS
OF POOR QUALITY

Number	Dates	Lat. N	Epicenter Long. E	M	Reference
(28)	1954/03/28	*39.1	41.	5.2	4
(29)	1954/10/24	*40.	40.	5.8	4
(30)	1957/07/07	39.2	40.2	5.5	1
		*39.2	40.3	5.3	4
		39.4	40.5	5.1	3
		7 injured at Kigi			2
(31)	1959/01/14	*39.5	40.4	5.1	3
(32)	1959/09/10	39.7	41.4	5.8	1
		39.6	41.7	5.1	4
		*damage at Varto			2
		(39.3	41.4)		
(33)	1959/10/25	*39.2	41.5	5.	1
		39.3	41.6	4.8	4
(34)	1959/12/25	*39.1(?)	41.6(?)	6.2(?)	4
(35)	1960/01/28	40.1	38.6	5.	1
		*39.5	39.5	5.9	4
		felt at Kemah and Erzincan			2
(36)	1960/06/09	39.9	39.5	5.	1
		*39.5	39.5	4.8	4
(37)	1964/09/4	39.	40.2	5	1
		*39.8	40.3,40.2	4.6	4
		felt at Cayirli			2
(38)	1964/11/16	39.4	40.3	5.1	1
		*39.8	39.9	4.8	4
		39.5	40.3	4.9	3
		felt at Erzincan			2
(39)	1965/08/31	*39.4	40.7	5	
		39.3	40.8	4.8	4
		39.4	40.8	5.6	3
		25 deaths, 40 injured at Karliova			2
(40)	1966/03/07	*39.2	41.5	5.3	1
		39.1	41.6	6	4
		39.2	41.6	5.6	3
		4 deaths at Varto			2

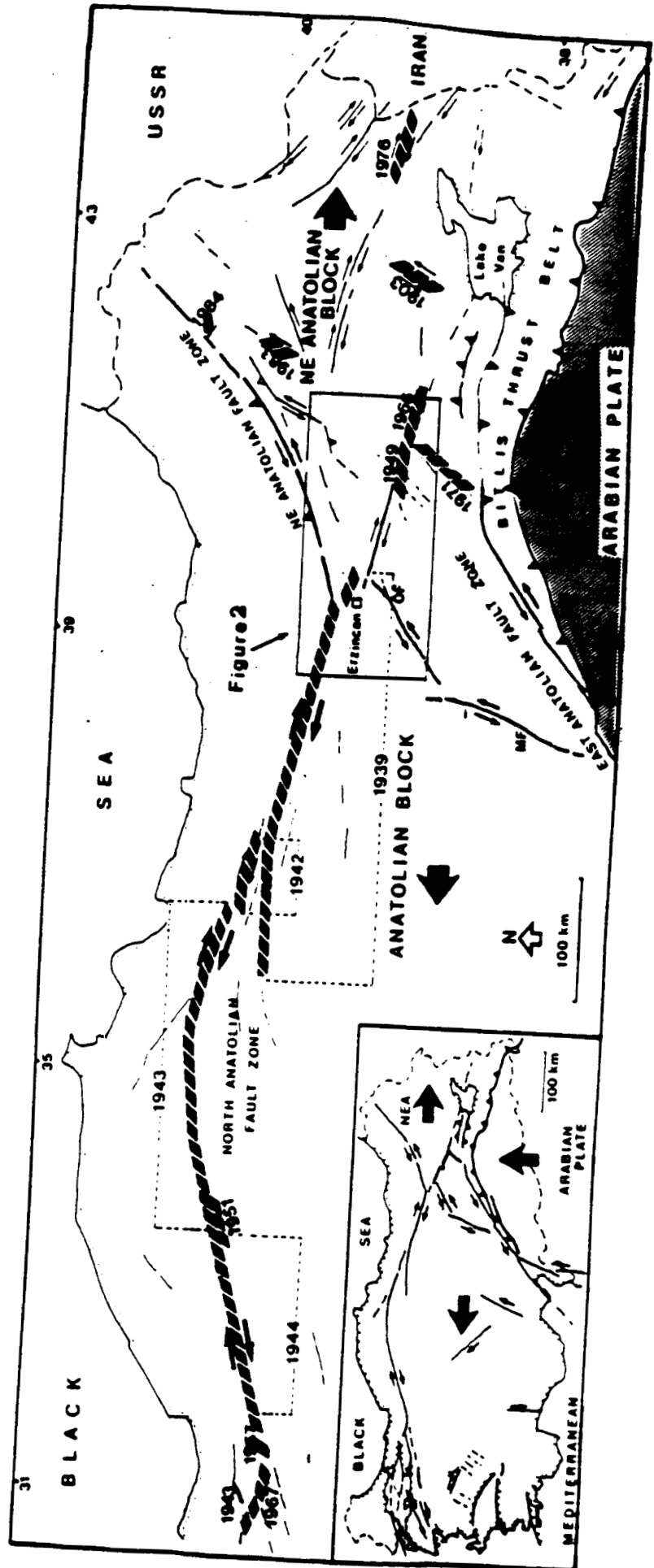
Number	Dates	Epicenter		M	Reference	
		Lat. N	Long. E			
(41)	1966/08/19	*39.2	41.5	6.8	1	
		39.2	41.6	7.1	4	
		39.2	41.6	6.9	3	
		2394 deaths at Varto and its vicinity				2
(42)	1966/08/19	*39.3	41.2	5	1	
		39.4	41.3	5.3	3	
(43)	1966/08/14	*39.3	41.1	5	1	
		39.	41.8	5.1	3	
(44)	1966/08/20	*39.4	40.9	5.3	1	
		39.4	40.9	5.3	1	
		39.4	40.9	5.1	4	
		39.4	41	6.2	3	
Damage at Karliova					2	
(45)	1966/08/20	39.1	39.8	5.5	1	
		*39.1	40.7	5.4	4	
		39.2	40.7	6.1	3	
(46)	1967/01/30	*39.4	41.5	5	3	
(47)	1967/07/26	*39.5	40.3	5.6	1	
		39.5	40.4	6.2	4	
		39.5	40.3	6.2	3	
		97 deaths at Pulumur				2
		39.5	40.4	5.6	7	
4km surface faulting						
118 azimuth, 20 cm right-lateral displacement					7	
(48)	1968/09/24	*39.2	40.3	5.1	1	
		39.2	40.1	5.1	4	
		39.2	40.3	5.1	3	
2 deaths, 87 injured at Kigi						
6 km length of surface faulting						
150 azimuth, 25 cm vertical displacement					2,7	
(49)	1968/09/25	*39.3	40.2	5.1	1	
		39.2	40.2	4.8	4	
(50)	1969/09/10	*39.3	41.4	5.2	1	
		39.2	41.4	5	4	
		39.3	41.4	5.2	3	
(51)	1970/09/03	3 injured at Kemahy			2	

Number	Dates	Epicenter		M	Reference
		Lat. N	Long. E		
(52)	1971/05/22	*39.1	40.6	5.4	3

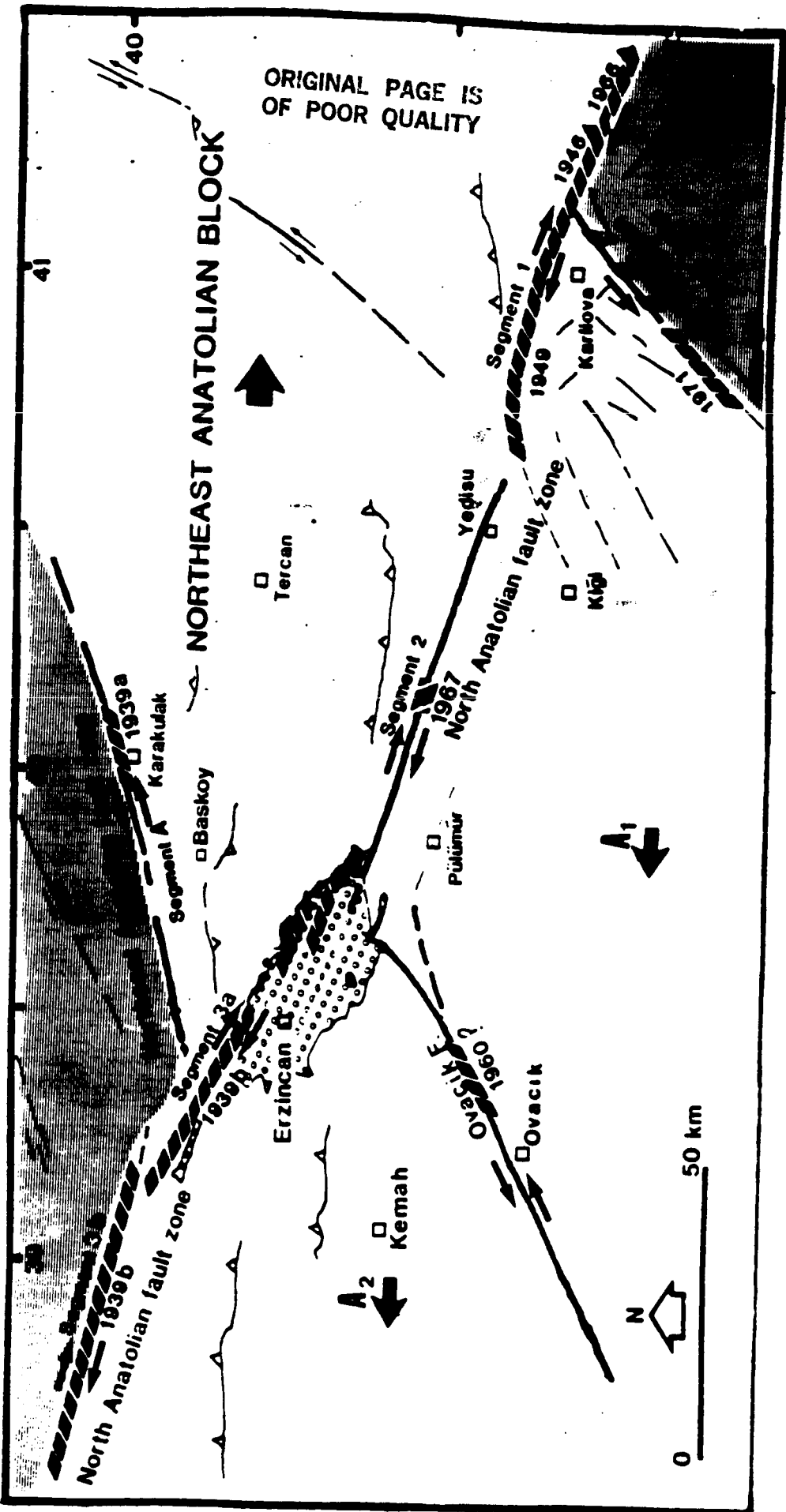
* Indicates preferred epicenter location which is shown in Figure 4.

- 1) Dewey, 1976
- 2) Tabban, 1980
- 3) Soysal et al., 1981; Sipahioglu, 1983
- 4) Riad and Meyers, 1985
- 5) Nature, 1940c
- 6) Lahn, 1952
- 7) Ambraseys, 1975

ORIGINAL PAGE IS
OF POOR QUALITY



ORIGINAL PAGE IS OF POOR QUALITY



NORTHEAST ANATOLIAN BLOCK

North Anatolian fault zone
1939b

Segment 1
1849

Segment 2
1967

Segment 3a
1939b

Segment A
1939a

North Anatolian fault zone
1960?

Ovacik

Kemah

Püümür

Yedigöller

Tercan

Kış

Karlıova

Baskoy

Karakulak

Erzincan

Ovacik

Kemah

Püümür

Yedigöller

Tercan

Kış

Karlıova

Baskoy

Karakulak

Erzincan

Ovacik

Kemah

Püümür

Yedigöller

Tercan

Kış

Karlıova

Baskoy

Karakulak

Erzincan

Ovacik

Kemah

Püümür

Yedigöller

Tercan

Kış

Karlıova

Baskoy

Karakulak

Erzincan

Ovacik

Kemah

Püümür

Yedigöller

Tercan

Kış

Karlıova

Baskoy

Karakulak

Erzincan

Ovacik

Kemah

Püümür

Yedigöller

Tercan

Kış

Karlıova

Baskoy

Karakulak

Erzincan

Ovacik

Kemah

Püümür

Yedigöller

Tercan

Kış

Karlıova

Baskoy

Karakulak

Erzincan

Ovacik

Kemah

Püümür

Yedigöller

Tercan

Kış

Karlıova

Baskoy

Karakulak

Erzincan

Ovacik

Kemah

Püümür

Yedigöller

Tercan

Kış

Karlıova

Baskoy

Karakulak

Erzincan

Ovacik

Kemah

Püümür

Yedigöller

Tercan

Kış

Karlıova

Baskoy

Karakulak

Erzincan

Ovacik

Kemah

Püümür

Yedigöller

Tercan

Kış

Karlıova

Baskoy

Karakulak

Erzincan

Ovacik

Kemah

Püümür

Yedigöller

Tercan

Kış

Karlıova

Baskoy

Karakulak

Erzincan

Ovacik

Kemah

Püümür

Yedigöller

Tercan

Kış

Karlıova

Baskoy

Karakulak

Erzincan

Ovacik

Kemah

Püümür

Yedigöller

Tercan

Kış

Karlıova

Baskoy

Karakulak

Erzincan

Ovacik

Kemah

Püümür

Yedigöller

Tercan

Kış

Karlıova

Baskoy

Karakulak

Erzincan

Ovacik

Kemah

Püümür

Yedigöller

Tercan

Kış

Karlıova

Baskoy

Karakulak

Erzincan

Ovacik

Kemah

Püümür

Yedigöller

Tercan

Kış

Karlıova

Baskoy

Karakulak

Erzincan

Ovacik

Kemah

Püümür

Yedigöller

Tercan

Kış

Karlıova

Baskoy

Karakulak

Erzincan

Ovacik

Kemah

Püümür

Yedigöller

Tercan

Kış

Karlıova

Baskoy

Karakulak

Erzincan

Ovacik

Kemah

Püümür

Yedigöller

Tercan

Kış

Karlıova

Baskoy

Karakulak

Erzincan

Ovacik

Kemah

Püümür

Yedigöller

Tercan

Kış

Karlıova

Baskoy

Karakulak

Erzincan

Ovacik

Kemah

Püümür

Yedigöller

Tercan

Kış

Karlıova

Baskoy

Karakulak

Erzincan

Ovacik

Kemah

Püümür

Yedigöller

Tercan

Kış

Karlıova

Baskoy

Karakulak

Erzincan

Ovacik

Kemah

Püümür

Yedigöller

Tercan

Kış

Karlıova

Baskoy

Karakulak

Erzincan

Ovacik

Kemah

Püümür

Yedigöller

Tercan

Kış

Karlıova

Baskoy

Karakulak

Erzincan

Ovacik

Kemah

Püümür

Yedigöller

Tercan

Kış

Karlıova

Baskoy

Karakulak

Erzincan

Ovacik

Kemah

Püümür

Yedigöller

Tercan

Kış

Karlıova

Baskoy

Karakulak

Erzincan

Ovacik

Kemah

Püümür

Yedigöller

Tercan

Kış

Karlıova

Baskoy

Karakulak

Erzincan

Ovacik

Kemah

Püümür

Yedigöller

Tercan

Kış

Karlıova

Baskoy

Karakulak

Erzincan

Ovacik

Kemah

Püümür

Yedigöller

Tercan

Kış

Karlıova

Baskoy

Karakulak

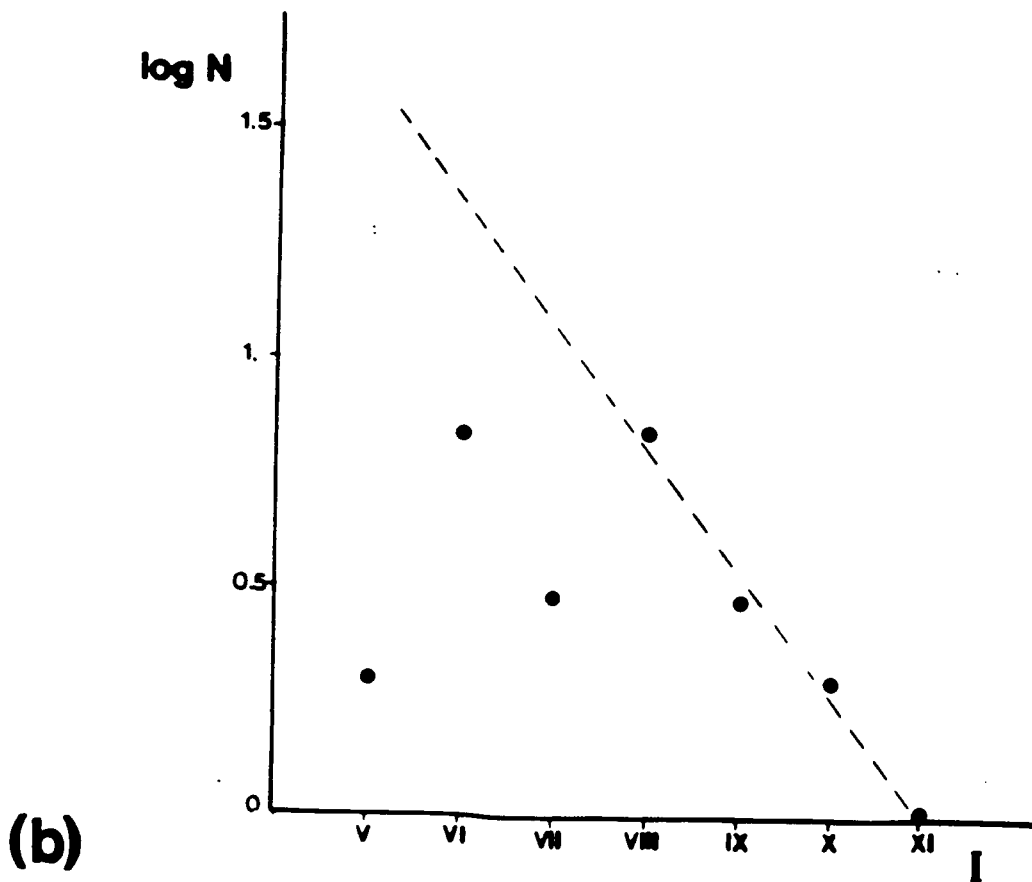
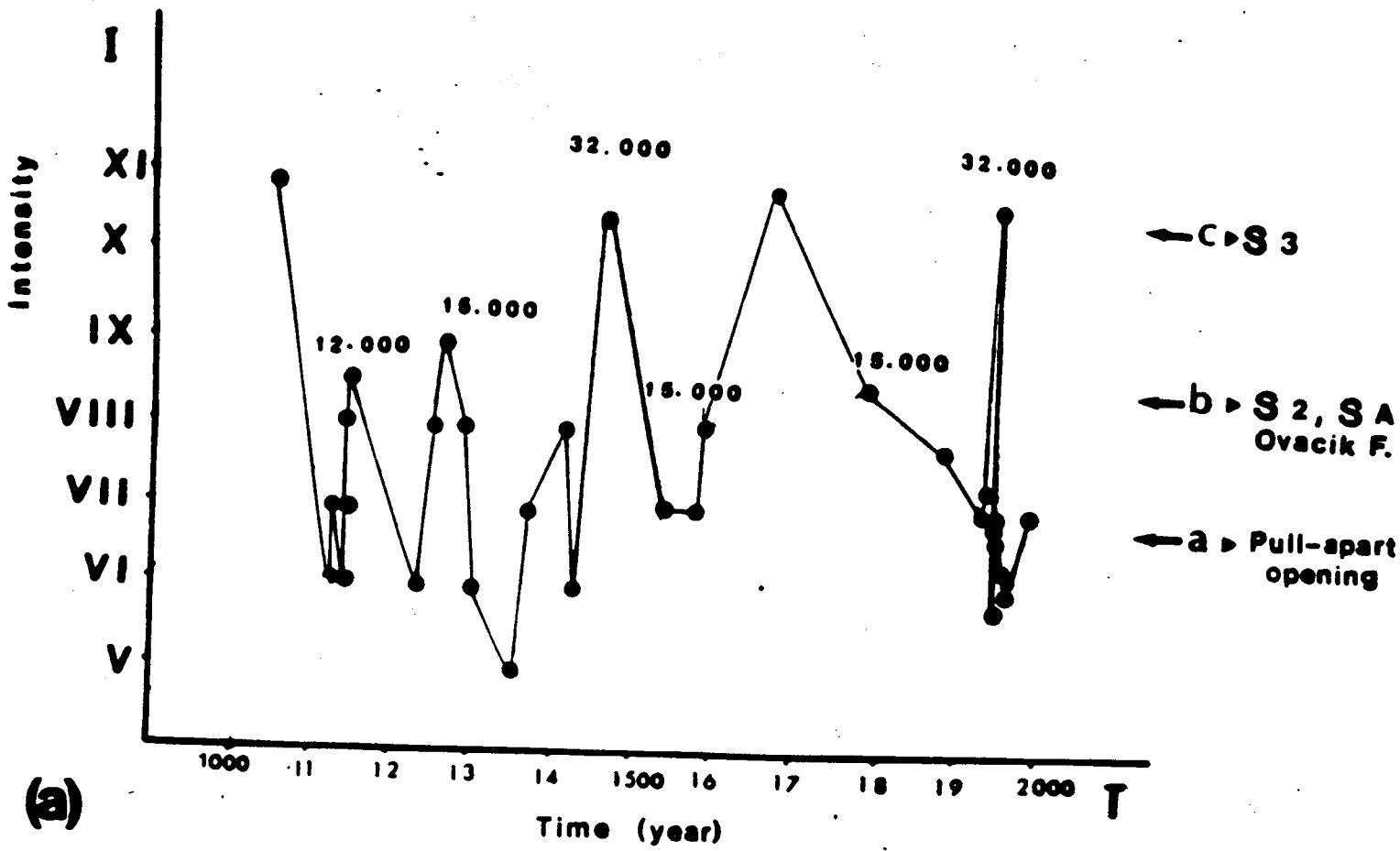
Erzincan

Ovacik

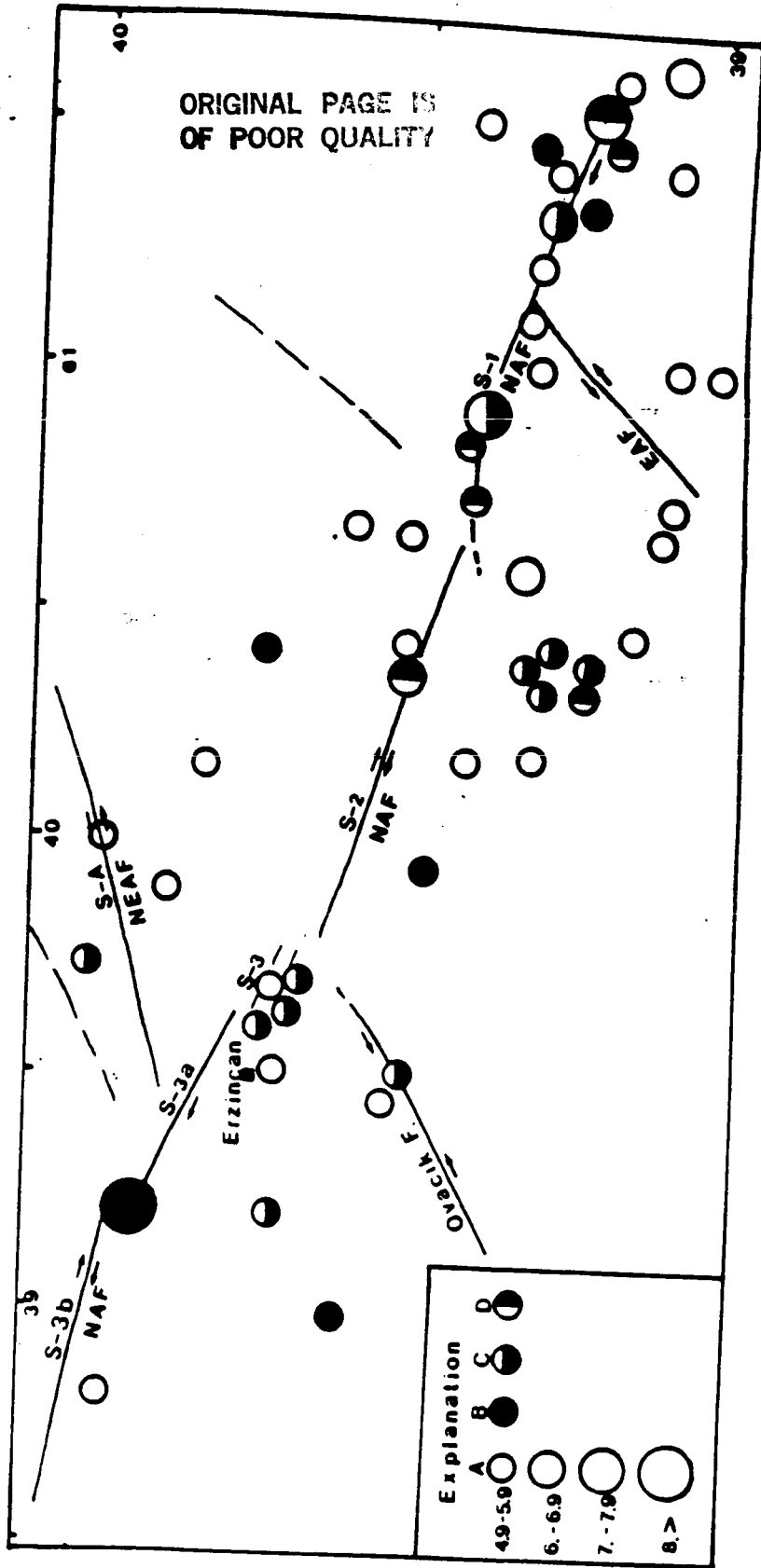
Kemah

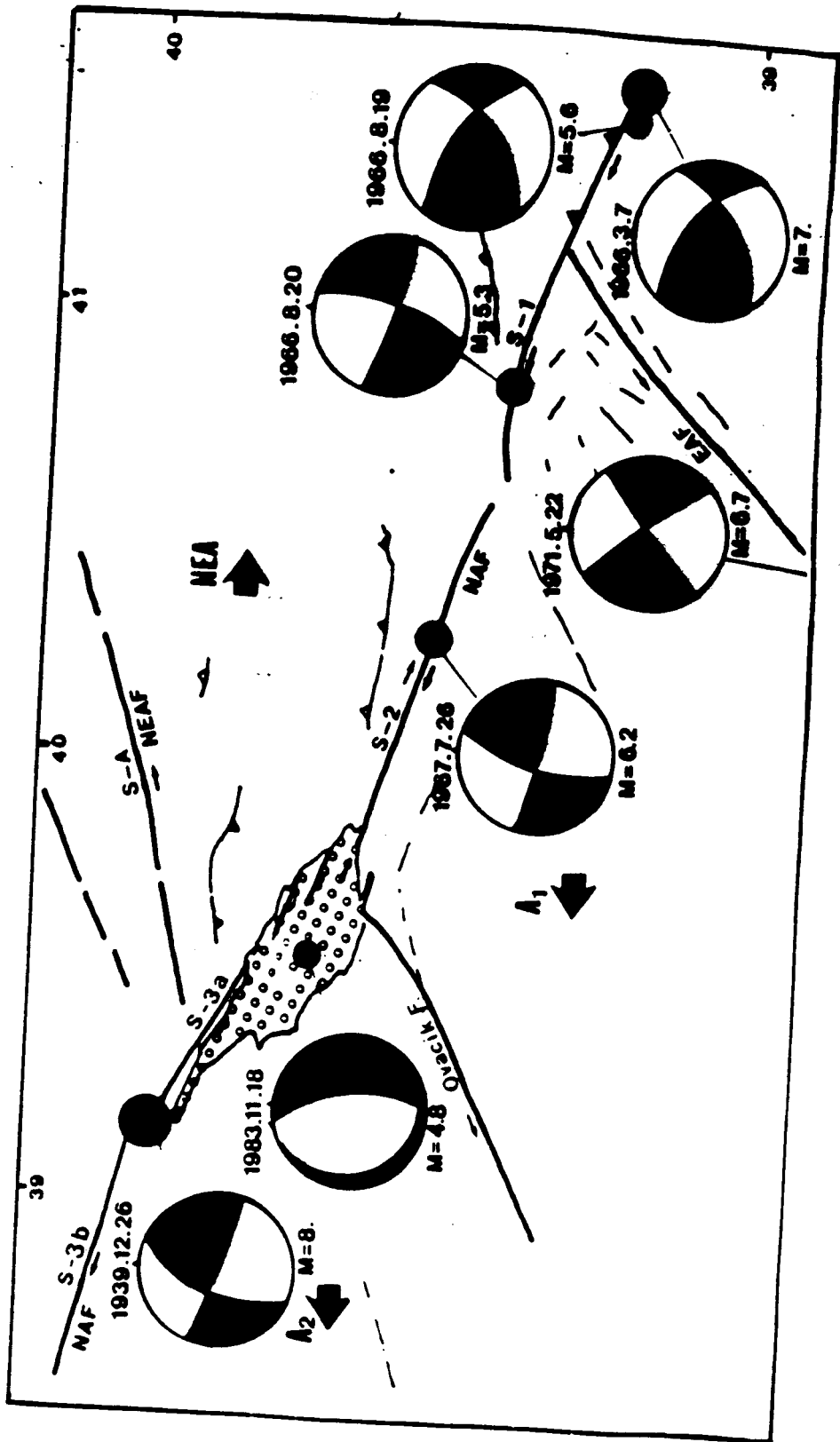
Püümür

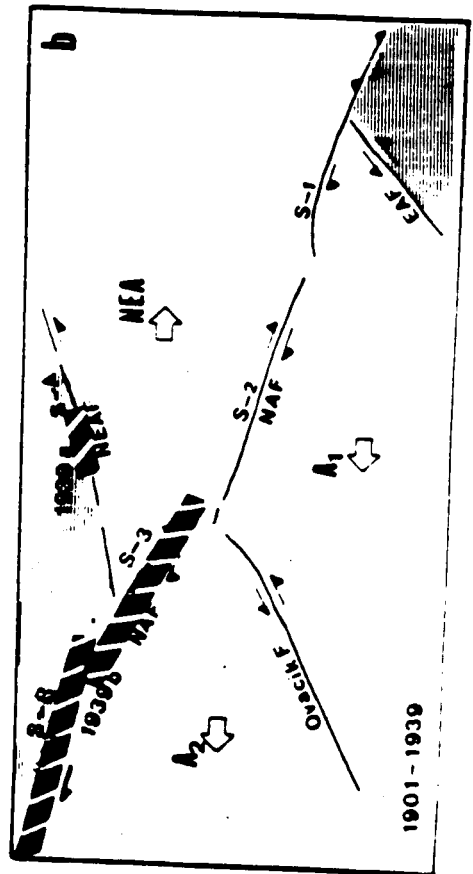
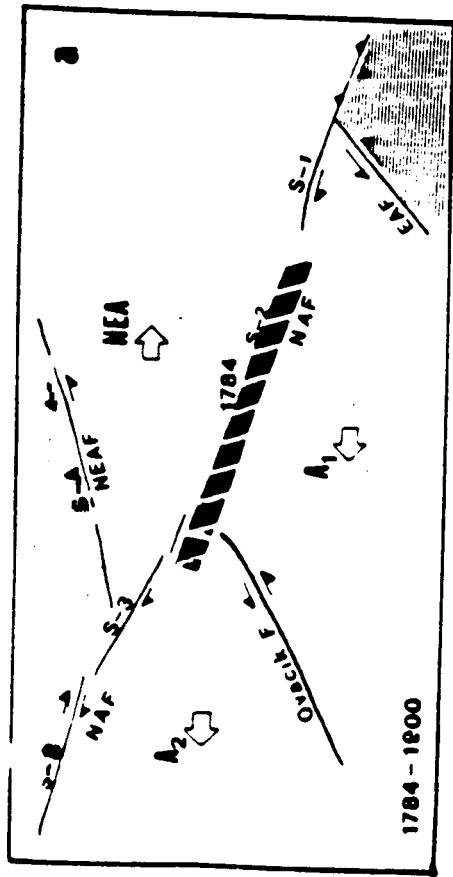
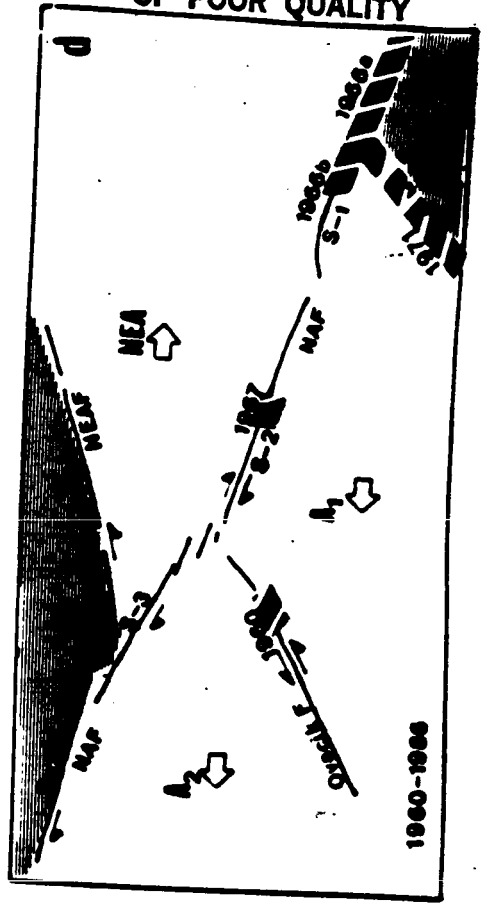
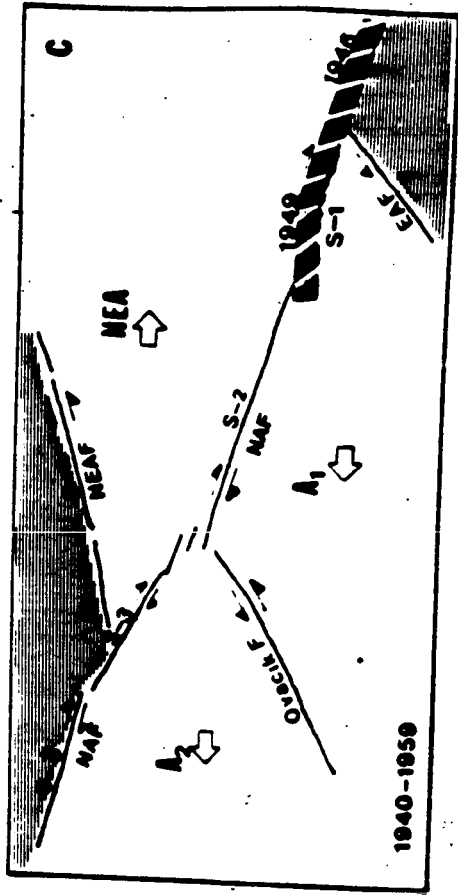
Yedigöller

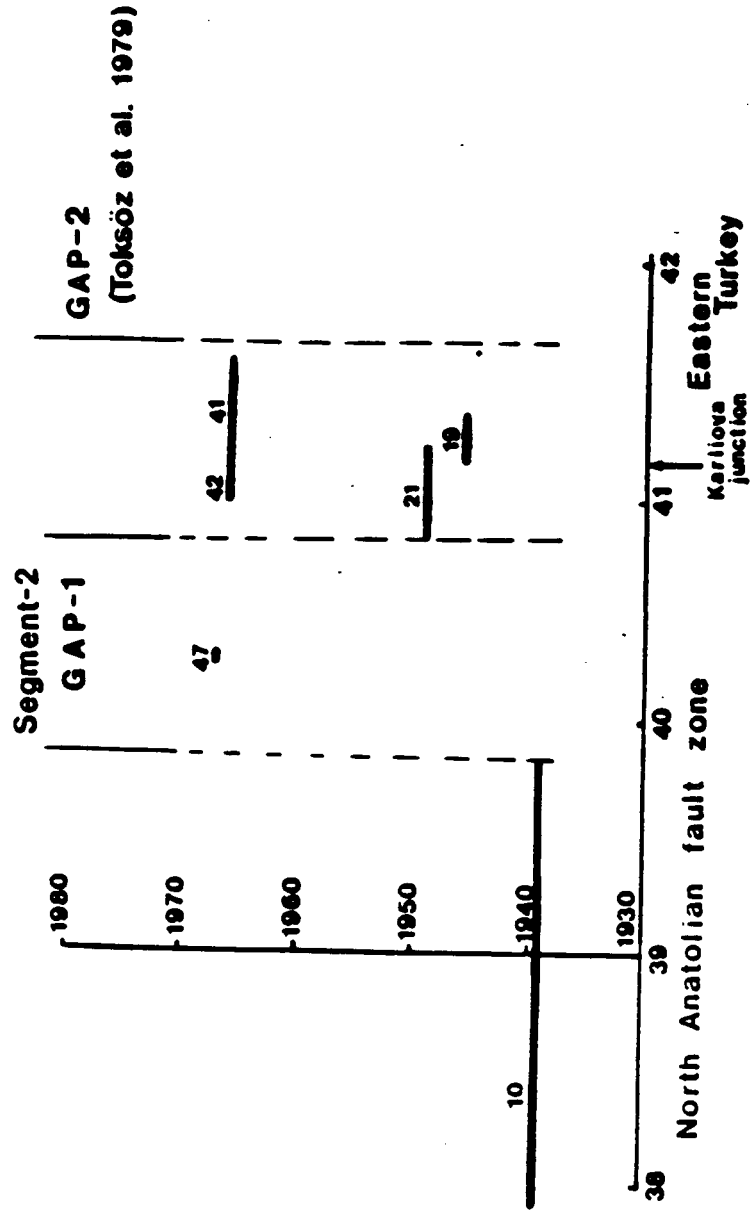


ORIGINAL PAGE IS
OF POOR QUALITY









APPENDIX III

**TECTONIC ESCAPE ORIGIN AND COMPLEX EVOLUTION
OF THE ERZINCAN PULL-APART BASIN, EASTERN TURKEY.**

AYKUT BARKA

AND

LEVENT GÜLEN

**Earth Resources Laboratory
Department of Earth, Atmospheric and Planetary Sciences,
Massachusetts Institute of Technology,
Cambridge, Massachusetts 02139, U.S.A.**

September, 1986

**Submitted to
Geological Society of America Bulletin**

C-2

ABSTRACT:

A new tectonic model is presented for the pull-apart opening of the Erzincan basin in an effort to explain the relationship between continental block kinematics and basin formation. Our field studies indicated that the Erzincan pull-apart basin is not a typical rhombic pull-apart basin, but it has a rather complex, two-stage pull-apart opening mechanism. This complexity is created by the nature of the tectonic escape of crustal blocks, following the continental collision of the Arabian and Eurasian plates along the Bitlis Suture Zone in eastern Turkey.

The first stage of westward pull-apart opening occurs between two divergent segments of the North Anatolian Fault Zone, along which westward tectonic escape of the Anatolian block is taking place, creating the northern part of the Erzincan Basin.

The second stage of translational-rotational basin opening is initiated as a result of fragmentation of the Anatolian Block and one of the segments of the North Anatolian Fault Zone by the formation of the obliquely oriented, left-lateral strike-slip Ovacik Fault. The present day basin geometry indicates 9 ± 1 km. left-lateral offset and approximately 10° clockwise block rotation along the Ovacik Fault.

This complex, two-stage, divergent and translational-rotational, pull-apart basin opening mechanism quite satisfactorily accounts for the geometry of the Erzincan Basin and is well supported by the available geological evidence.

INTRODUCTION:

Although the "Pull-apart basin" concept was first introduced in 1966 (Burchfiel and Stewart), it has received the attention of structural geologists since 1974 with the papers of Crowell(1974a, b) on basins in southern California. Within the last decade a large body of knowledge have been acquired through detailed geological and geophysical studies and a significant progress had been made in understanding the mechanism of different types of pull-apart basin formation and evolution in strike-slip settings. A collection of papers and their references, that are contained in two books (Ballance and Reading, 1980; Biddle and Christie-Blick, 1985), which are devoted to strike-slip basin formation and sedimentation, provide an excellent review on pull-apart basins.

The purpose of this paper is to discuss the origin and evolution of the Erzincan pull-apart basin (hereafter referred to as the EPAB) emphasizing the important role of continental block kinematics in the basin formation, and present a new, complex pull-apart mechanism for basins in continental collision areas where tectonic escape prevails.

The EPAB is situated on the North Anatolian Fault Zone (NAFZ) and its long axis strikes in NW-SE direction being parallel to the general trend of the fault zone (Figure-1). The EPAB is approximately 50 km. long and widens towards SE reaching 15 km. width. Two other left-lateral faults, the Northeast Anatolian fault and the Ovacik fault obliquely intersect the NAF zone at the NW and SE of the basin, respectively (Figure-1).

The EPAB has recently attracted considerable attention in the literature. However, as shown in Figure-2a and b, it has been described as a typical rhombic pull-apart basin

bounded by two parallel master faults belonging to the segments of the NAFZ in all the previous studies (Şengör, 1979; Aydın and Nur, 1982; Hempton and Dunne, 1984; Şengör et al., 1985). Our detailed field studies have indicated that the EPAB is not a typical rhombic pull-apart basin, but it has a rather complex pull-apart mechanism and basin evolution due to the critical role of the obliquely oriented (non-master), Ovacik fault (Figure-3).

In the proceeding sections we will present the details of stratigraphy and structure of the EPAB based on our field observations and discuss the pull-apart mechanism and basin evolution within a regional tectonic framework.

GEOLOGICAL SETTING AND STRATIGRAPHY:

In this region, there were two branches of Neo-Tethys before Eocene (Stöcklin, 1974; Şengör and Yilmaz, 1981). The northern branch used to separate the Pontides from the Anatolide/Tauride platform and closed in Eocene forming the Pontide-Anatolide/Tauride suture zone (PATSZ). Further south, the continental collision of the Anatolide/Tauride platform with the Arabian plate took place in mid-late Miocene (Hall, 1976; Perincek, 1980; Şengör and Yilmaz, 1981). This closure eliminated the southern branch of the Neo-Tethys forming the Bitlis Suture zone (BSZ). The continental collision along the BSZ caused further deformation and modified the northern PATSZ along which, E-W trending narrow compressional basins occurred. These basins are bounded by mostly E-W trending thrusts and their internal deformation delineates E-W trending folds. As a result of the continued convergence following the continental collision along the BSZ, the formation of the North Anatolian, East Anatolian, and Northeast Anatolian fault zones, which make up the boundaries of major continental blocks such as Anatolian and Northeast Anatolian blocks (Figure-1), tectonically overprinted some of the existing basins and created new ones.

to the tectonic escape of continental blocks away from the maximum compression zone (Ketin, 1948; McKenzie, 1972; Gülen, 1984; Şengör et al., 1985).

The stratigraphic characteristics of the Neogene-Quaternary sedimentary sequences in eastern Turkey indicate that there are three main stages of deposition being related to the above tectonic evolution of this region.

The first stage is associated with the wide-spread early Miocene transgression (Irritz, 1972; Luttig and Steffens, 1976; Şengör and Kidd, 1979) which deposited sandstone/limestone lithologies passing upwards into shallow marine marls and reefal carbonates (Ketin, 1950; Altinli, 1966; Şengör and Kidd, 1979). This facies unconformably overlies older sedimentary units or ophiolitic melange lithologies of the Pontide-Anatolide/Tauride suture zone, reaching up to 750m. thickness (Ketin, 1950; Nebert, 1961; Altinli, 1966). A marine regression towards late Miocene time, coeval with the continental collision along the BSZ, is indicated by the increasing evaporitic intercalations and appearance of lacustrine and fluvial sediments in the stratigraphic record (Ketin, 1950; Altinli, 1966; Kurtman et al., 1978; Bektaş, 1981).

The second stage of deposition filled approximately E-W trending narrow compressional basins located close proximity to the suture zones. The Muş basin (Kurtman et al., 1978; Şaroğlu and Güner, 1981; Şengör et al., 1985) and Cayirli-Tercan basin (Ketin, 1950; Irritz, 1972) are typical examples of this kind (Figure-1). The Mihar-Ahmediye basin which is situated to the NW of the EPAB, also falls in this category (Figure-3). This stage is characterized by lacustrine and fluvial facies represented by evaporite/sandstone/marl/conglomerate lithologies. The thickness of this unit varies from place to place reaching up to 1750m. (Kurtman, 1972; Tatar, 1978). Nebert (1961)

reported Hipparion fossils from these sediments, indicating late Miocene age, which is also confirmed by Irritz(1972), in the western extension of the Mihar-Ahmediye basin.

The third and final stage of deposition occur either within compressional basins as a continuation of the second stage (e.g. Mus basin, Cayirli-Tercan Basin), or within newly formed basins along strike-slip fault zones (e.g. EPAB, Nksar Basin; see Figure-1). Mostly lacustrine and fluvial deposits of Plio-Quaternary age represent this stage.

In the EPAB, all the exposed basin sediments belong to this third stage of deposition, which is characterized by Plio-Quaternary fluvial facies, that contains playa deposits, coarse clastics and basin margin conglomerates (Figure-3). Conglomerates are composed of clasts of ophiolitic melange and Cretaceous-early Miocene carbonates. Occasional thin tephra and crossbedded thick conglomerate layers are two characteristics of this sequence. Thickness of this fossil-barren conglomerates reach up to 200m. Moreover, sand to boulder size fragments and their ungraded, immature appearance suggest a rapid deposition in a tectonically active environment. Unfortunately, the total thickness of the sediments in the EPAB basin is not known, because of the non-existence of deep wells and seismic data. However, if it is assumed that the basin length versus sediment thickness relationship of Hempton and Dunne(1984) is correct then, one can infer about 2.5 to 3km. sediment thickness for the EPAB as a rough approximation. In the EPAB, alluvial fans are more developed along the northern margin. They are steep and composed of recent debris flows and coarse grained braided stream deposits. Along the southern margin, fan sediments are deposited more gently and contain no recent debris flows. Braided stream flows are also finer grained on the southern fans (Hempton and Dunne, 1984). The central part of the basin is filled mostly by silts, sands, and gravels. The Euphrates river becomes a meandering type as soon as it enters into the basin. A large salt playa abuts the meander plain at one of the lowest basin elevations containing thermal and

soda springs. In contrast to the Euphrates river, Çardakdere and Eysel rivers (Figure-3) preserve their braided character within the basin. Moreover, at least two levels of terraces are developed along these rivers. The upper terrace is about 40-50m. higher than the present river base, while no terraces were observed along the Euphrates river.

About 15 small volcanic cones are aligned along the northern margin, while only one cone occurs close to the southern margin of the basin. They consist of dacites and rhyolites. The age of the volcanism is 3.1-0.25m.y.(Baş,1979; Hempton and Linneman,1984).

STRUCTURAL GEOLOGY

A general N-S compressional tectonic regime dominates the neotectonics of the whole region in eastern Turkey due to the continuing active convergence following the mid-Miocene continental collision along the Bitlis suture zone. For example early-middle Miocene sediments are folded and thrust throughout this region (Pamir and Ketin, 1941; Altinli, 1966; Tatar, 1978), as well as along the northern margin of the Arabian plate (Rigo de Righi and Cortesini,1964; Ketin,1966; Perinçek, 1980; Özkaya,1982). As shown in Figure-3, early-middle Miocene limestone units and the E-W trending Mihar-Ahmediye basin sediments are folded with fold axial traces striking E-W and the basin is bounded by E-W trending thrusts in the north and south. Many other Miocene basins exhibit similar deformational styles in eastern Turkey (Kurtman et al.,1978; Şaroğlu and Güner,1981; Şengör et al.,1985).

The EPAB differs from the above mentioned basins because of its NW-SE trending long axis and its apparent younger age. The basin's NW-SE trend parallels the trend of the NAFZ and this suggests an intimate genetic relationship between the NAFZ and EPAB. In fact, the NAFZ forms the entire northern boundary of the EPAB and serves as a major

te- fault. The NAFZ consists of three major segments in this region (Figure-3). The geometry and the interaction of these segments are extremely important for the understanding the origin and evolution of the EPAB.

SEGMENT-1: This easternmost segment is about 75 km. long and trends 110° N azimuth. The best physiographic fault expressions, such as linear valley and ridges, are developed to the east of the Tanyeri village. The southern block is uplifted about 30 m. relative to the northern one along this segment.

SEGMENT-2: This segment forms the northern boundary of the EPAB. It has approximately 55 km. length and trends 125° N azimuth. The southeastern end of this segment consists of a number of small en echelon faults. Fault traces and related shear zone deformation are best developed near Bahik village. As shown in Figure-4, the fault plane steeply dips to the south and the southern block is uplifted. The analysis of structures indicate a dominant right-lateral strike slip and a subordinate thrust components along the Segment-2. Furthermore, along the northwestern half flower type of thrusting (Harding et al., 1985) are also common. The 15° difference between the Segment-1 and 2 trends, along with an approximately 4 km. releasing stepover between them indicate that these two segments functioned as divergent master faults at the initial opening stages of the EPAB.

SEGMENT-3: This segment starts around Ahmediye village and extends westward about 320 km. striking 105° N azimuth (Figure.3). Within the area of interest, it shows clear geomorphologic fault expressions in the vicinity of the Mihar village. The 1939 Great Erzincan earthquake ($M=8.0$) activated not only this segment, but also Segment-2, producing 4 m. right-lateral and 1 m. vertical displacements with the uplifted southern block (Pamir and Ketin, 1941; Ketin, 1969). The 20° difference between the trends of the

Segment-2 and 3 forms a restraining bend to the NW of the EPAB where the epicenter of the 1939 Erzincan earthquake is located (Figure.5c).

OVACIK FAULT: The Ovacik fault is also another important structural element which contributed to the evolution of the EPAB (Figure.3). It is a left-lateral strike-slip fault and is mapped in detail by Arpat and Şaroğlu (1975). The Ovacik fault is obliquely positioned relative to the NAFZ and starts from the southeastern end of the EPAB, extends about 120km. towards SW with 80° N azimuth. It cuts the Quaternary glacial moraines of the Ovacik basin (located to the south of the study area, see Figure-1) where the fault plane steeply dips SE indicating dominant left-lateral strike-slip and subordinate thrust components with the uplifted southern block.

The mechanical interpretation of the above mentioned segments of the NAFZ is shown in Figure.5a. According to this interpretation, Segment-1 and 3 are main displacement shears (D-shear), Segment-2 is a Riedel shear (R-shear), and the southeastern end of the Segment-2 has also a R1-shear (Riedel within Riedel, Tchalenko,1970).

Relative stress directions obtained from analysis of mesoscopic scale fractures measured in the Neogene-Quaternary sediments are shown in Figure-5b. In this analysis, single , conjugate faults and slickenslide lineations were used (Hancock and Barka, 1981; Angelier, 1984; Hancock,1985). Stress orientations that are obtained from the analysis indicate NNW-SSE compression and related ENE-WSW extension which agree with a secondary stress field related to the right-lateral NAFZ.

The fault plane solutions of 1939.12.26 (M=8.0), 1967.7.26 (M=5.6), and 1983.11.18 (M=4.8) earthquakes are given in Figure.5c. These solutions are consistent with the above interpretation of mesoscopic fracture analysis. Note that, the solution obtained from

1983.11.18 earthquake gives an ENE-WSW extension and clearly differs from the others. This can be interpreted as an indication for the active opening of the EPAB and will be further elucidated in the next section.

ORIGIN AND EVOLUTION OF THE ERZINCAN PULL-APART BASIN (EPAB):

Contrary to the northern margin of the EPAB, our detailed field studies and aerial photo interpretations show no evidence that the southern margin of the basin is controlled by an active strike-slip fault which extends southeastward, well outside of the basin limits (see Figure-2), as suggested by Şengör(1979), Aydın and Nur(1982), and Hempton and Dunne(1984). Although the southern boundary of the basin is quite linear, in fact bounded by a fault, this fault is abruptly terminated by the Ovacik Fault (Figure-3). As a result, the southern basin boundary fault does not form an echelon master fault pair with the northern one (Segment-2 of the NAFZ) to open the EPAB as a "typical rhombic pull-apart basin". Furthermore, the basin margin and alluvial fan slopes in the north are at least twice as steep than the ones along the southern boundary, suggesting that, these basin bounding faults have different characters.

It seems that, the pull-apart opening of the EPAB first occurred between the Segment-1 and 2 of the NAF zone (Figure-5). In fact, this area has the lowest elevation within the EPAB and is occupied by the alluvial plain of the Euphrates river and a salt playa. Since, there is a 15° angle and 4km. releasing stepover between these segments, they can function as divergent master faults (see Mann et al., 1983 for detailed discussion on divergent master faults). This configuration can open only a westward widening pull-apart basin (the basin area labeled with M in Figure-5a). However, even this arrangement is not satisfactory to explain the present-day basin geometry, which exhibits southeastward widening, where the pull-apart stepping is narrow. We suggest:

that, even though it is not a "master fault", the left-lateral strike-slip Ovacik fault (Figure-3 and 5) is responsible for the opening of the basin area labeled with N in Figure-5a. Thus, modification of the original basin geometry by the critical contribution of the Ovacik fault does not only explain the complex pull-apart opening of the EPAB by solving the above geometric problem satisfactorily, but also negates the need to search for or infer a major strike-slip master fault which would extend well to the east of the Ovacik fault. Based on the above discussion and presented evidence, we suggest the following model for the origin and evolution of the EPAB.

The continental collision along the Bitlis Suture zone in mid-late Miocene time caused the break up of the Anatolide/Tauride platform into a number of continental blocks (e.g. Anatolian block, Northeast Anatolian block) by the formation of major strike-slip faults such as the North Anatolian, East Anatolian, and Northeast Anatolian fault zones (Figure-1). Under the N-S compression, the Anatolian and Northeast Anatolian blocks tectonically escape from the zone of maximum compression westward and eastward, respectively. The eastern part of the NAFZ functions as a common strike-slip boundary between those blocks. According to our interpretation, the two segments of the NAFZ (Segment-1 and 3) initially had roughly 20 km. wide releasing stepover with a separation of 60 km. in the Erzincan area (Figure-6a). The aspect ratio of the original stepover ($20/60=0.33$) corresponds to approximately 20° angle, which allows formation of a R-shear in between, rather than 20 km. wide pull-apart opening (Figure-6a). Being consistent with en echelon structures of a strike-slip fault zone which evolves under simple shear (Tchalenko and Ambraseys, 1970; Wilcox et al., 1973; Harding, 1974; Barlett et al., 1982; Hancock, 1985), newly formed Segment-2 (R-shear) makes 15° angle with Segment-1, leaving 4 km. stepover (Figure-6b). This small, secondary stepover and the 15° divergence angle causes the initial westward pull-apart opening of the EPAB due to the right-lateral displacement along the NAFZ, caused by the westward escaping Anatolian block.

(Figure-6c). The beginning of the volcanic activity within the EPAB is probably related to this stage, because about 15 small volcanic cones are aligned along the southeastern part of the Segment-2 (Figure-3 and 6c). If this assumption is true, then the timing of this stage can be estimated as roughly 3.1 m.y. before present, based on the oldest ages obtained from the volcanics.

After some amount of initial opening (M1 area after ca. 25 km. right-lateral displacement), eastern part of the Anatolian block, as well as the Segment-1 of the NAFZ, were further divided into two; A1, A2 blocks and S-1a, S-1b segments, respectively (Figure-6d), by the formation of the left-lateral strike-slip Ovacik fault. This break up of the Anatolian block is probably confined only to the upper 10-15km, brittle zone of the continental crust, but at present we do not have any direct evidence to substantiate it. The fragmentation of the Anatolian block into A1 and A2 blocks was probably required because of the locking effect of the restraining bend, where the Segment-2 and 3 of the NAFZ intersect, against the westward motion of the Anatolian Block. The presence of unexpected positive flower structures along the northwestern half of the Segment-2 and Segment-3, indeed suggest such a locking effect, indicating intense compression around the restraining bend region (Figure-3 and 6d). Also the occurrence of great earthquakes (M =8) in this region provide another supporting evidence. Having this new block configuration, the segments of the NAFZ and the Ovacik Fault can accomplish the westward tectonic escape of the A2 block under continuing N-S compression.

Now, the tectonic escape is also accompanied by a clockwise rotation of the A2 block relative to A1 along the Ovacik Fault. This clockwise rotation is caused by the restraining intersection along the NAFZ, in comparison to the straight, freely moving Ovacik Fault. While great earthquakes produce intermittent right-lateral displacements along the NAFZ by unlocking the restraining bend, the built up of shear strain during locked

ORIGINAL PAGE IS
OF POOR QUALITY

periods cause clockwise rotation of the A2 block relative to A1. The block rotation kinematics may be further clarified with the following row-boat analogy (However, this should not be taken literally, because we think that continental blocks act like semi-rigid bodies during deformation.). Consider a row-boat cruising westward, the rows are in towed position. If only the northern side row is inserted into the water, then the row-boat rotates clockwise, pivoting around the row-water interface point, while still sliding westward. In this example, the row-boat represents the A2 block, the northern row, that is inserted into the water, acts like the restraining bend increasing drag forces along the northern side. Having this block kinematics in mind, we suggest that, the southern basin boundary of the EPAB (S-1a, Figure-6d) was the former westward continuation of the Segment-1. As a result of the formation of the left-lateral Ovacik Fault, Segment-1 was broken into two pieces (S-1a and S-1b) and the S-1a has been escaping westward and rotating clockwise since then. This mechanism implies that the S-1a functions as a clockwise rotating break away zone for the second stage opening of the basin area labeled with N in Figure-6d. The fault plane solution of the 1983.11.18 earthquake ($M=4.8$, see Figure-5c), which gives WSW-ENE extension, provides a compelling evidence for the above interpretation. Thus, the complex two-stage, divergent and translational-rotational, pull-apart opening model for the EPAB quite satisfactorily explains the basin geometry and is well supported by the available geological evidence.

Moreover, we estimate about 9 ± 1 km. left-lateral displacement along the Ovacik Fault, based on the present-day geometry of the EPAB. This offset, in turn, gives approximately 10° clockwise rotation for the A2 block relative to A1, if the restraining bend, where Segment-2 and 3 of the NAFZ intersect, is assumed to be the pole of rotation (Figure-6d).

While this complex opening is in progress in the southeastern half of the basin, the northwestern tip is uplifting as evidenced by the occurrence of hanging river terraces along Esesi and Çardakdere rivers and by the vertical block movements observed along the faults (Figure-3 and 6d). These features may be explained by compressional and drag forces exerted to the NW part of the Segment-2 and Segment-3, by the westward escaping, clockwise rotating A2 block, which pivots around the restraining bend while being slightly tilted southeastwards. However, an important distinction needs to be made here. The southeastward tilting of the A2 block could produce the above uplift features, if indeed the vertical block movements observed along the faults (indicated by pluses and minuses in Figure-6d) are associated with the tilting. However, apparent vertical block movements could also be produced, partly by aseismic, viscoelastic deformation of crustal blocks along fault zones (Nur and Mavko, 1974; Thatcher et al., 1980; Reillinger, 1986). Alternatively, the clockwise rotating break away zone could be responsible for the uplifting of only the northwestern part of the EPAB. If the restraining bend region is assumed to be the pole of rotation, then the extension rate, the subsidence rate, and presumably the width of the crustal slivers, that are sliced off from the break away zone, will gradually increase from NW towards SE of the basin. The vertical rotation of these gravitationally unstable crustal slivers (thinner, lighter NW tip, as opposed to thicker, heavier SE end) would produce relative uplifting for the northwestern part of the EPAB. Although, this second mechanism is quite likely to operate, at present, we can not prefer decisively one of the above two models with the available data. Of course, a combination of the two would be a third possibility.

We can go one more step further and speculate that the extreme southeastern tip of the basin will eventually be closed with development of folding and thrusting (Figure-6c) because of the intensifying compressional strain as a result of the A1 block's northward penetration, which is facilitated by the left-lateral strike-slip displacement along the

ORIGINAL PAGE IS
OF POOR QUALITY

Ovacik fault. In fact, early stages of this deformation has already started to take place within a wedge shaped area defined by the Ovacik fault and Segment-1 of the NAFZ, as evidenced by E-W trending recent thrusting and active folding (Figure-3 and 6d).

Our above model is based on only field geology data. Future paleomagnetic and geodetic studies to test and quantify continental block rotations and tilting, radiometric age determinations on fault segments to better constrain the timing of the evolutionary stages, and deep drilling-seismic profiling to reveal the details of structure will be of great value towards testing our proposed model and an improved understanding of complex pull-apart basin formation and evolution.

Finally, we believe that this work emphasises the utmost importance of meticulous field studies, along with a regional tectonic approach, for the study of pull-apart basins in particular, and of a detailed knowledge of the fine scale continental/crustal block structure and its continuously changing nature for the study of continental tectonics in general.

ACKNOWLEDGEMENTS:

The field work studies were supported by the ITIT joint project (#8212) between Mineral Research and Exploration Institute of Turkey and Geological Survey of Japan. One of us (A.A.B.) thanks to Dr. Hirokazu Kato of GSJ for his continuous encouragement. We gratefully acknowledge M.N. Toksöz for his support and B.C. Burchfiel for his constructive criticism.

REFERENCES:

- Altinil, E., 1966, Geology of Eastern and Southeastern Anatolia, Bull. Miner. Res. Explor. Inst., Turkey, v.66, p.37-75.
- Angelier, J., 1984, Tectonic analysis of fault data sets., J. Geophys. Res., v.89, p.5835-5848.
- Arpat, E. and Şaroğlu, F., 1975, Some recent tectonic events in Turkey., Bull. Geol. Soc. Turkey., v.18, p.91-101 (in Turkish).
- Aydin, A. and Nur, A., 1982, Evolution of pull-apart basins and their scale independence., Tectonics, v.1, p.91-106.
- Ballance, P. F. and Reading, H. G., 1980, (eds.), Sedimentation in oblique-slip mobile zones: Int. Assoc. Sediment. Spec. Publ. 4, Blackwell Scientific Publications, 265p.
- Barka, A. A., 1984, Some neotectonic features of the Erzincan basin., Earthq. Symp. Spec. Publ. Ataturk Univ., Erzurum, Turkey., p.115-125 (in Turkish).
- Barlett, W. L., Friedman, M., and Logan, J. M., 1981, Experimental folding and faulting of rocks under confining pressure: Part IX: wrench faults in limestone layers., Tectonophysics, v.79, p.255-277.
- Baş, H., 1979, Petrologische und geochemische Untersuchungen an subrezenten Vulkaniten der nordanatolischen Störungzone (Abschnitt Erzincan-Niksar), Türkei, Diss., Univ. Hamburg, 116p.
- Bektaş, O., 1981, Geological characteristics of the North Anatolian Fault Zone and local ophiolitic problems of the Erzincan-Tanyeri region., PhD. Thesis, Univ. Trabzon, Turkey, 196p.(in Turkish).
- Biddle, K. T. and Christie-Blick, N., 1985, eds., Strike-slip faulting and basin formation., Spec. Publ. 37., Soc. Econ. Paleont. Miner., 386p.
- Burchfiel, B. C. and Stewart, J. H., 1966, Pull-apart origin of Death Valley, California., Bull. Geol. Soc. Am., v., p.9-442.
- Crowell, J. C., 1974a, Sedimentation along the San Andreas Fault, California., In: Dott, R.H.; Jr. and Shaver, R.H.(eds.) Modern and ancient geosynclinal sedimentation., Soc. Econ. Paleont. Min. Spec. Publ. 19, p.292-303.
- Crowell, J. C., 1974b, Origin of late Cenozoic basins in southern California., Soc. Econ. Paleont. Min. Spec. Publ. 22, p.190-204.
- Dewey, J.F., Hempton, M.R., Kidd, W.S.F., Şaroğlu, F. and Şengör, A.M.C., 1986, Shortening of continental lithosphere: the neotectonics of eastern Anatolia-a young collision zone., In: Coward, M.P. and Ries, A.C.(eds.) Collision Tectonics., Geol. Soc. Spec. Publ. 19, London., p.36.

- Gülen, L., 1984, Sr, Nd, Pb isotope and trace element geochemistry of calc-alkaline and alkaline volcanics, eastern Turkey., PhD. Thesis, Massachusetts Institute of Technology, 232p.
- Hall, R., 1976, Ophiolite emplacement and the evolution of the Taurus Suture Zone, southeastern Turkey., *Bull. Geol. Soc. Am.*, v.87, p.1078-1088.
- Hancock, P.L., 1985, Brittle microtectonics: Principles and practice., *J. Struc. Geol.*, v.7, p.437-457.
- Hancock, P.L. and Berka, A.A., 1981, Opposed shear senses inferred from neotectonic mesofracture systems in the North Anatolian Fault Zone., *J. Struc. Geol.*, v.3, p.383-392.
- Harding, T.P., 1974, Petroleum traps associated with wrench faults., *Bull. Am. Assoc. Petrol. Geol.*, v.60, p.365-378.
- Harding, T.P., 1985, Seismic characteristics and identification of negative flower structures, positive flower structures and positive structural inversion., *Bull. Am. Assoc. Petrol. Geol.*, v.69, p.582-600.
- Hempton, M.R. and Dunne, L.A., 1984, Sedimentation in pull-apart basins: Active examples in eastern Turkey., *J. Geol.*, v.92, p.513-530.
- Hempton, M.R. and Linneman, S.R., 1984, Volcanism in the Erzincan pull-apart basin: Age, composition and tectonic significance., *Abstr., EOS*, v.65, p.84.
- International Seismological Centre Bulletin, 1983.
- Irritz, W., 1972, Lithostratigraphie und tektonische Entwicklung des Neogenes in Nordostanatolien., *Beih. Geol. Jb.*, 120p.
- Ketin, I., 1948, Über die tektonisch-mechanischen Folgerungen aus den grossen anatolischen Erdbeben des letzten Dezenniums., *Geol. Rdsch.*, v.36, p.77-83.
- Ketin, I., 1950, Geological report of 46/4 and 47/3 quadrangles (1/100,000 scale), Erzincan-Askale region, *Miner. Res. Explor. Inst. Report No. 1863*, Ankara, Turkey (in Turkish).
- Ketin, I., 1969, Über die nordanatolische horizontalverschiebung., *Bull. Min. Res. Explor. Inst., Turkey*, v.72, p.1-28.
- Kurtman, F., Akkuş, M.F., and Gedik, A., 1978, The geology and oil potential of the Muş-Van region. In: Degens, E.T. and Kurtman, F. (eds.) *The geology of Lake Van*. *Min. Res. Explor. Inst., Turkey, Publ.* v.169, p.124-133.
- Kurtman, F. and Akkuş, M.F., 1971, Intermountain basins in eastern Anatolia and their oil possibilities., *Bull. Min. Explor. Inst., Turkey*, v.77, p.1-9.
- Luttig, G. and Steffens, P., 1976, Explanatory notes for the paleogeographic atlas of Turkey from the Oligocene to the Pleistocene., *Bundesanstalt für Geowissenschaften und Rohstoffe, Hannover*, 64p.

- Mann, P., Hempton, M.R., Bradley, D.C., and Burke, K., 1983, Development of pull-apart basins., *J. Geol.*, v.91, p.529-554.
- McKenzie, D., 1972, Active tectonics of the Mediterranean region., *Geophys. J. R. astr. Soc.*, v.30, p.109-185.
- Nebert, K., 1981, Geological structure of the region between source areas of Kelkit and Red rivers., *Bull. Miner. Res. Explor. Inst. Turkey.*, v.57, p.1-49 (in Turkish).
- Nur, A. and Mavko, G., 1974, Postseismic viscoelastic rebound., *Science*, v.183, p.204-206.
- Özkaya, I., 1981, Origin and tectonic setting of some melange units in Turkey., *J. Geol.*, v.90, p.269-278.
- Pamir, H.N. and Ketin, I., 1941, Das anatolische Erdbeben Ende 1939., *Geol. Rdsch.*, v.32, p.279-287.
- Perinçek, D., 1980, Sedimentation on the Arabian shelf under the control of tectonic activity in Tauride belt., *Proc. Fifth Petrol. Congr. Turkey, Ankara*, p.77-93.
- Reilinger, R., 1986, Evidence for postseismic viscoelastic relaxation following the 1959 M=7.5 Hebgen Lake, Montana, Earthquake., *J. Geophys. Res.*, v.91, p.9488-9494.
- Rigo de Righi, M. and Cortesini, A., 1964, Gravity tectonics in foothills structure belt of southeast Turkey., *Bull. Am. Assoc. Petrol. Geol.*, v.48, p.1911-1937.
- Şaroğlu, F. and Güner, Y., 1981, Factors effecting geomorphological evolution of eastern Turkey: relationships among geomorphology, tectonics, and volcanism., *Bull. Geo. Soc. Turkey.*, v.24, p.39-50 (in Turkish).
- Şengör, A.M.C., 1979, The North Anatolian transform fault: its age, offset and tectonic significance., *J. Geol. Soc. London.*, v.136, p.269-282.
- Şengör, A.M.C. and Kidd, W.S.F., 1979, Post-collisional tectonics of the Turkish-Iranian Plateau and a comparison with Tibet., *Tectonophysics*, v., p.1-376.
- Şengör, A.M.C. and Yılmaz, Y., 1981, Tethyan evolution of Turkey: a plate tectonic approach., *Tectonophysics*, v.75, p.181-241.
- Şengör, A.M.C., Görür, N., and Şaroğlu, F., 1985, Strike-slip faulting and related basin formation in zones of tectonic escape: Turkey as a case study., In: Biddle, K.T. and Christie-Bilck, N. (eds.) *Strike-slip faulting and basin formation.*, Soc. Econ. Paleont. Min. Spec. Publ. 37, p.227-264.
- Stöcklin, J., 1974, Possible ancient continental margins in Iran. In: Burk, C.A. and Drake C.L. (eds.) *The geology of continental margins*, Springer-Verlag, New York p.873-887.
- Tatar, Y., 1978, Tectonic investigations on the North Anatolian Fault Zone between Erzincan and Refahiye., *Yerbilimleri*, v.4, p.201-236 (in Turkish).
- Tchalenko, J.S., 1970, Similarities between shear zones of different magnitudes., *Bull. Geol. Soc. Am.*, v.81, p.1625-1640.

ORIGINAL PAGE IS
OF POOR QUALITY

Tchalenko, J.S. and Ambraseys, N.N., 1970, Structural analysis of the Das-e-Bayaz (Iran) earthquake fractures., Bull. Geol. Soc. Am., v.81, p.41-60.

Thatcher, W., Matsuda, T., Kato, T., and Rundle, J.B., 1980, Lithospheric loading by the 1896 Riku-u Earthquake, northern Japan: implications for plate flexure and asthenospheric rheology., J. Geophys. Res., v.85, p.6429-6435.

Wilcox, R.E., Harding, T.P., and Seely, D.R., 1973, Basic wrench tectonics., Bull. Am. Assoc. Petrol Geol., v.57, p.74-96.

FIGURE CAPTIONS:

Figure-1: Major tectonic elements of eastern Turkey, where the post-collisional N-S convergence between the Arabian Plate and Pontides cause the escape of continental blocks westward and eastward as indicated by large arrows. The study area is enclosed by dashed lines. Major faults are highlighted with thick lines. Other active faults, that have been mapped, are also shown. Abbreviations are: Erz, City of Erzincan; EF, Ecemiş Fault; MF, Malatya Fault; CTB, Çayirli-Tercan Basin; MB, Muş Basin; NB, Niksar Basin; OB, Ovacik Basin.

Figure-2: Two previous pull-apart mechanism interpretations for the Erzincan Basin. a- From Aydin and Nur (1982) depicting the EPAP as a typical rhombic pull-apart basin bounded by the en echelon NAFZ segments. Q, Quaternary; T, Tertiary; pM&M, Paleozoic and Mesozoic basement; HS, hot spring; VC, volcanic cone; F, fault. b- Hempton and Dunne's (1984) interpretation of the EPAB, which is quite similar to Aydin and Nur's (1982) above interpretation.

Figure-3: Geological map of the Erzincan pull-apart basin and its vicinity. A generalized stratigraphic column is given as an inset. t1 and t2 denote two levels of terraces that are mapped along the Çardakdere and Esesi rivers. Note the lack of terraces along the Euphrates river and its meandering nature.

Figure-4: A sketch of a natural trench on the Segment-2 of the NAFZ, where surface breaks of 1939 Erzincan earthquake passed through (looking in the SE direction), showing shear zone related deformation features such as fault planes, folds, and extension fissures. The stereonet (lower hemisphere projection) illustrates the geometrical orientation

ORIGINAL PAGE IS
OF POOR QUALITY

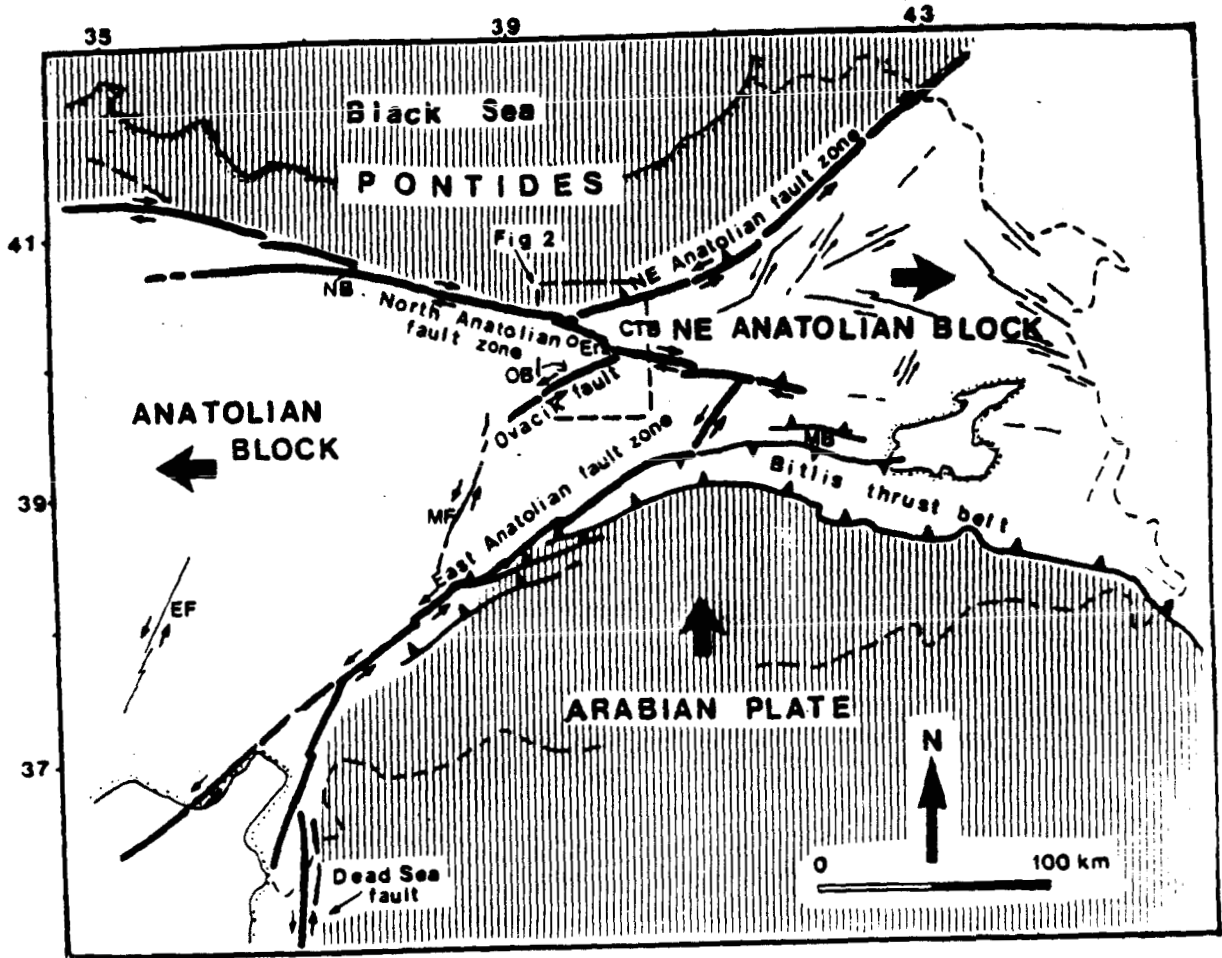
of these structures and their stress directions. A man figure depicting one of us (A.A.B., 1.68m. tall) is shown for scale.

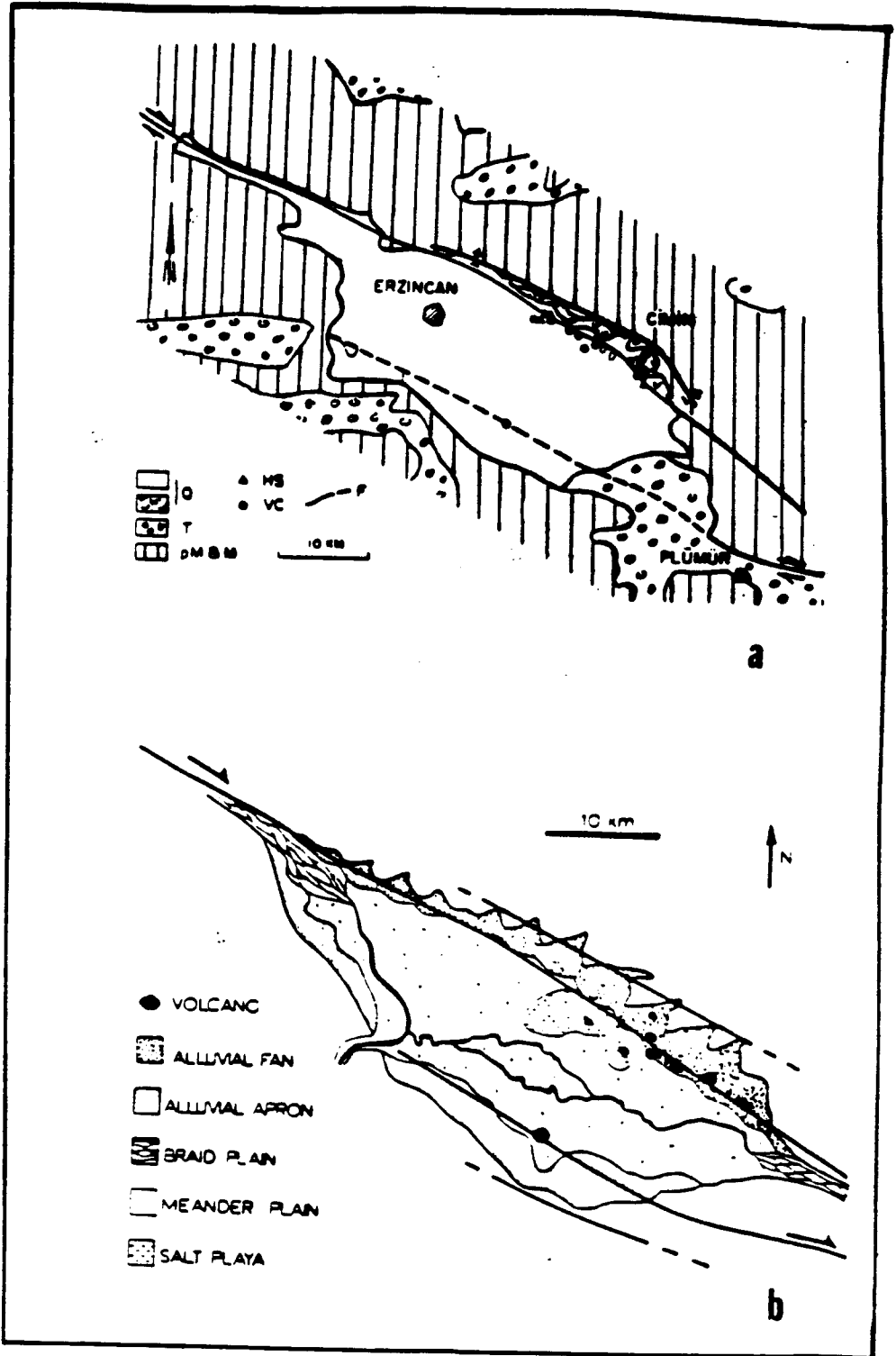
Figure.5: Interpretation of tectonic structures in the EPAB. a- A mechanical interpretation of the fault segments (S-1,2,3) of the NAFZ. D, main displacement shear; R, Riedel; R1, Riedel within the Riedel. b- Map showing analysis of mesoscopic scale faults measured within the Neogene-Quaternary sediments, showing NNW-SSE compression and ENE-WSW extension along the NAFZ (large arrows). Streonets are equal-area, lower hemisphere projection of reverse (planes with teeth), normal, and strike-slip (indicated by small arrows) faults. c- Fault plane solutions clearly indicating the active opening of the EPAB. Solutions of 1939.12.26 and 1967.7.26 are from McKenzie (1972) and 1983.11.18 is from International Seismological Centre Bulletin (1983). Magnitudes of the earthquakes are also given on the figure.

Figure-6: Tectonic evolution stages of the EPAB. a- Inferred initial geometry of the S1 and S3 segments of the NAFZ, with 60km. separation (YY') and 20km. wide releasing stepover. b- Formation of a R-Shear (S-2), which fills the gap (stepover) between S-1 and S-3, creates a secondary, roughly 4km. wide releasing stepover, that makes 15 divergence angle with the Segment-1. c- Initial pull-apart opening (ca. 25km. right lateral displacement) of the EPAB (basin area labelled with M1) between non-parallel master (divergent) faults (S-1 and S-2) due to the tectonic escape of the Anatolian and Northeast Anatolian blocks westward and eastward, respectively. Volcanic activity also starts at the eastern part of the basin during this stage. d-The formation of the left-lateral strike-slip Ovacik Fault divides eastern part of the Anatolian Block and the Segment-1 of the NAFZ into two; A1,A2 and S-1a, S-1b segments, respectively. At present, S-1a forms the southern basin boundary and the geometry of the basin indicates 9 ± 1 km left-lateral strike-slip offset for the Ovacik Fault, suggesting clockwise rotation of the

A2 block relative to A1. The southern basin area labeled with N represents the area that has opened due to the translational-rotational motion of the A2 block. Pluses (+) and minuses (-) denote the observed relative vertical movements along the faults (see text for further explanations).

ORIGINAL PAGE IS
OF POOR QUALITY

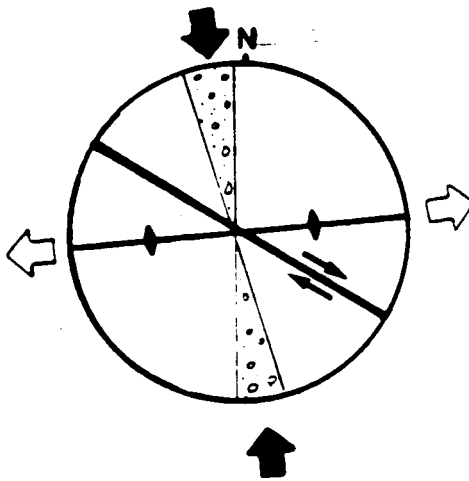
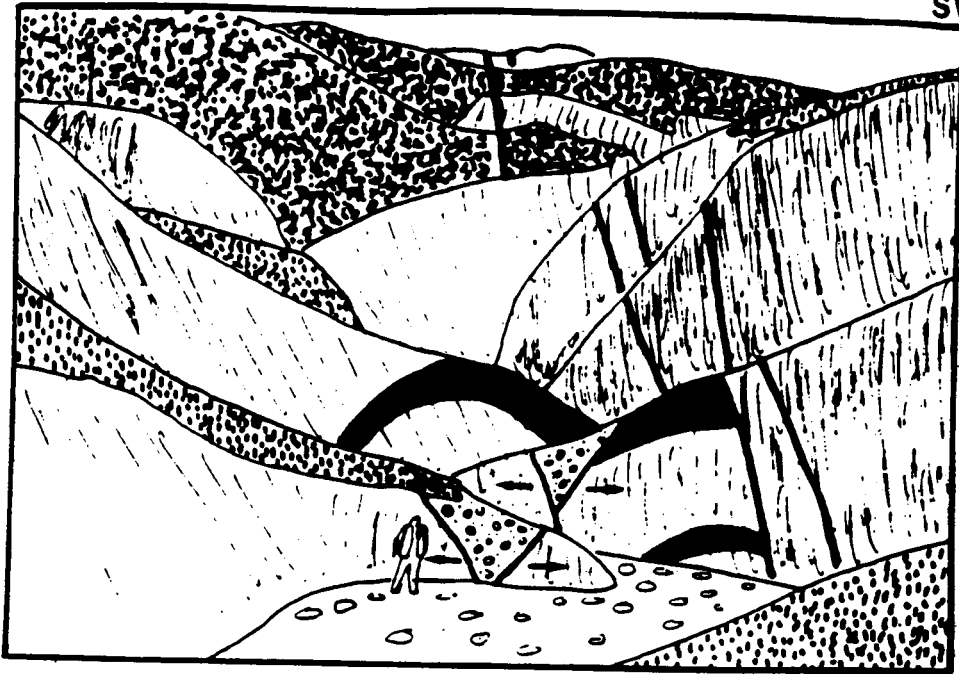




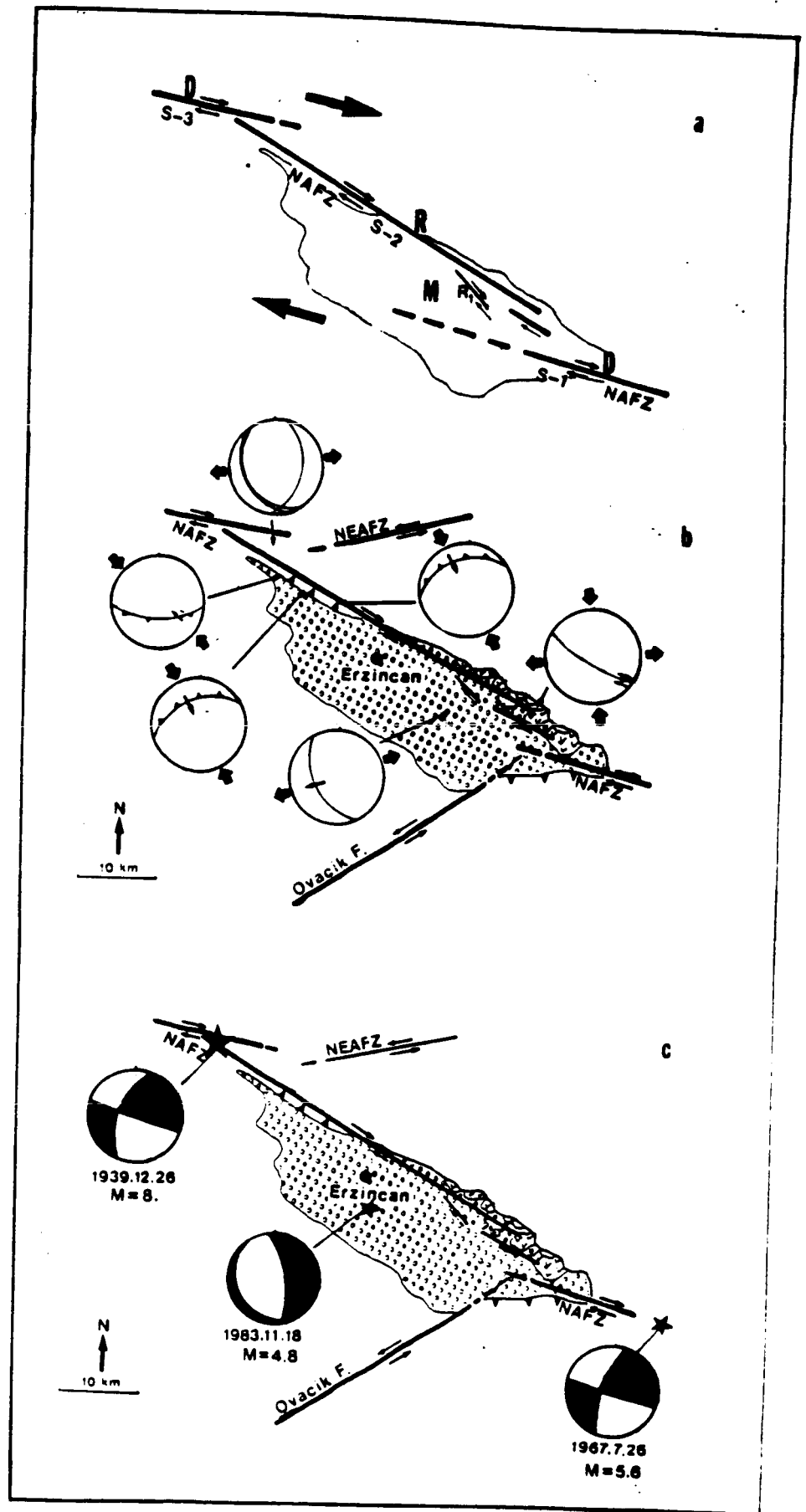
ORIGINAL PAGE IS
OF POOR QUALITY

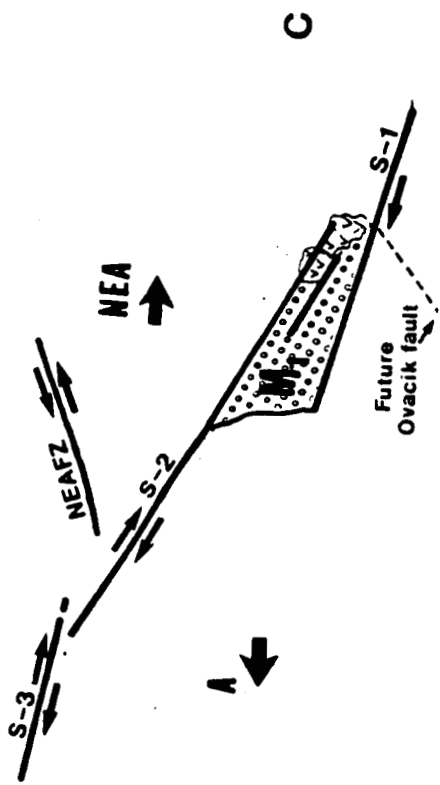
NE

SW

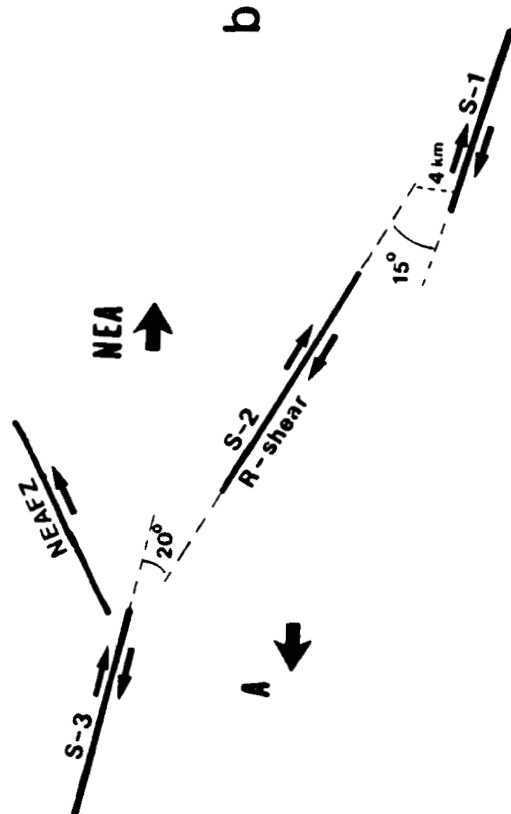
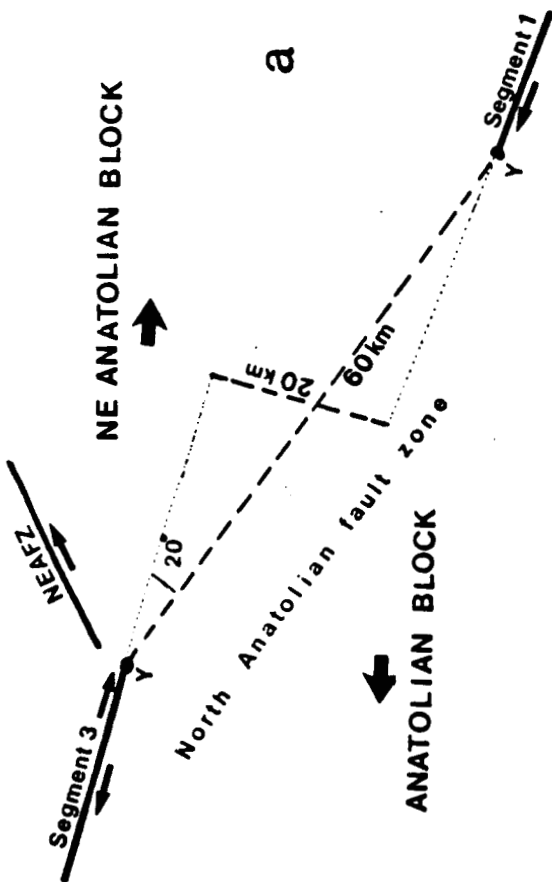
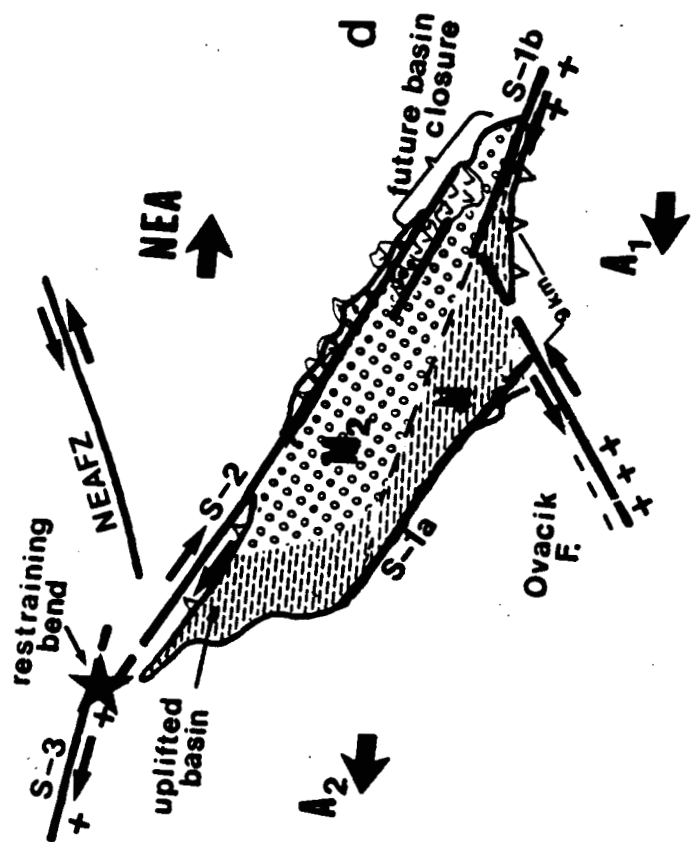


ORIGINAL PAGE IS
OF POOR QUALITY





ORIGINAL PAGE IS OF POOR QUALITY



APPENDIX IV

GLOBAL POSITIONING SYSTEM MEASUREMENTS OF
FAULTING AND REGIONAL DEFORMATION IN TURKEY

M. Nafi Toksoz and Robert E. Reilinger

Earth Resources Laboratory
Department of Earth, Atmospheric, and Planetary Sciences
Massachusetts Institute of Technology
Cambridge, MA 02139

GLOBAL POSITIONING SYSTEM MEASUREMENTS OF FAULTING AND REGIONAL
DEFORMATION IN TURKEY

INTRODUCTION

This is a proposal to use the Global Positioning System (GPS) to investigate relative plate motions, intraplate deformation and fault activity in Turkey. The proposed experiment will consist of repeated determination of selected baselines at approximately two year intervals. We anticipate a joint effort involving our collaborating institutions in Turkey (Middle East Technical University, Earthquake Research Institute, Defense Mapping Agency), WEGENER (Working Group of European Geo-scientists for the Establishment of Networks for Earthquake Research), and the United States (NASA Geodynamics Project, Massachusetts Institute of Technology (MIT), University of Colorado at Boulder). Funding for the United States university participation in this project is being provided by the U.S. National Science Foundation (NSF).

The three primary objectives of this experiment are:

- (1) To monitor strain accumulation and release along the major fault systems in Turkey with special emphasis on the North Anatolian fault (NAF) and East Anatolian fault (EAF).
- (2) To measure directly internal deformations of the Anatolian plate wedged between the Arabian, African, and Eurasian plates. These measurements include: a) Westward "escape" of the Anatolian plate; b) Eastward "escape" of the Northeast Anatolian block; c) North-south compression in Eastern Anatolia; and d) North-south extension in Western Anatolia.
- (3) To determine present-day relative movements of the African, Arabian, Anatolian, and Eurasian plates. This objective is an extension of the NASA/WEGENER Geodynamics Project to measure relative plate movements

in the Eastern Mediterranean with Satellite Laser Ranging (SLR) observations.

We anticipate that this research will enhance our understanding of the deformations induced by collision of continental plates, and the physical processes responsible for the generation of seismic activity in this region, thereby providing an improved basis for earthquake hazard assessment.

PROPOSAL

The details of this proposed measurement campaign were formulated on the basis of discussions with members of the Turkish scientific community who have been working directly with our group at MIT. We have also maintained close coordination with WEGENER with which we will pool our instruments in order to provide sufficient coverage to meet our mutual objectives. We emphasize that all aspects of the proposal are open to discussion and can be revised by mutual agreement.

Instrumentation

All GPS observations will be made with TI 4100 dual frequency receivers. We anticipate that a total of 12 instruments can be assembled for this project. The source of these instruments is truly international and includes agencies in the U.S. and Europe who have agreed to combine their resources in a common project. Our group will be directly responsible for 3 instruments to be obtained from the University NAVSTAR Consortium (UNAVCO) of which MIT is a founding member.

Logistics

MIT will be responsible for transporting the 3 UNAVCO instruments together with 3 trained operators to Ankara. Expenses for instrument transport to and from Turkey as well as all field expenses for these operators will be provided by

MIT through a grant from NSF. We propose that our cooperating Turkish institutions provide 3 additional operators (i.e., one per instrument) as well as a vehicle and driver for each instrument for transport within Turkey. The Turkish operators will be trained in the field if they do not have previous experience with the TI 4100.

Whenever possible existing monumentation will be used. New monuments will be set by the appropriate geodetic agency within Turkey.

Field Operations

Three of the 12 GPS instruments will maintain continuous observations at fiducial sites separated by distances of a few thousand kilometers (e.g., Greenwich, England; Matera, Italy; Dyarbakir, Turkey) in order to provide control on the satellite orbits (a fiducial site is a site with a previously determined well established position, for example from SLR measurements). Three additional SLR sites near the local GPS observations will be observed during each measurement round. This leaves 6 instruments to occupy the mobile GPS sites. Most of the mobile GPS stations will be observed for 3 days with substantial overlap between consecutive observing sessions. We propose a two phase observation scenario consisting of measurements in Western Turkey during the first phase and measurements the following year in Eastern Turkey. These two networks will be tied through overlapping observations at local fiducial points. The proposed sequence of observations for the provisionally selected stations shown on the accompanying map is given below.

A joint reconnaissance will be performed by our Turkish collaborators and one member of our group familiar with GPS field operations.

It can be assumed that repeat measurements will initially be made at two year intervals.

Point Selection

The accompanying map shows provisionally selected GPS sites and existing SLR sites in Turkey. Not shown are the sites near the fault-crossing geodetic networks (i.e., Taskesti, Gerede, and Ismetpasa) along the North Anatolian fault which are being proposed separately by WEGENER. Points were selected for accessibility, to maintain geometric network strength and to most effectively address the important tectonic problems in the region. This includes monitoring the nature of deformation along the NAF and EAF, crustal extension in Western Turkey and ongoing continental collision and associated "escape" of the Anatolian blocks in Eastern Turkey. The network in Eastern Turkey includes two triple junctions: Karliova at the intersection of the NAF and EAF; and Maras at the intersection of the EAF and the Levant transform (i.e., Dead Sea fault zone).

Schedule

The following general schedule is proposed:

- reconnaissance in Western Turkey in the autumn of 1987
- monumentation completed in Western Turkey in the spring of 1988
- first phase of observations in Western Turkey
in September 1988
- reconnaissance in Eastern Turkey immediately following
the first observation period
- monumentation completed in Eastern Turkey in the spring
of 1989
- observations in Eastern Turkey in the autumn of 1989

A possible schedule of observations at the mobile GPS stations shown in the accompanying map is as follows:

Phase I Western Turkey (September 1988) -

day 1: observe sites 1, 2, 3, 4, 5, 6

day 2: move sites 1, 2; observe sites 3, 4, 5, 6

day 3: observe sites 3, 4, 5, 6, 7, 8

day 4: move sites 3, 4, 5, 6; observe sites 7, 8

day 5: observe sites 7, 8, 9, 10, 11, 12

day 6: move sites 7, 8; observe sites 9, 10, 11, 12

day 7: observe sites 9, 10, 11, 12, 13, 14

day 8: move sites 9, 10, 11, 12; observe sites 13, 14

day 9: observe sites 13, 14, 15, 16, 17, 18

day 10: move sites 13, 14; observe sites 15, 16, 17, 18

day 11: observe sites 15, 16, 17, 18, 19, 20

day 12: move sites 15, 16, 17, 18; observe sites 19, 20

day 13: observe sites 19, 20, 21, 22, 23, 24

day 14: move sites 19, 20; observe sites 21, 22, 23, 24

day 15: observe sites 21, 22, 23, 24, 1, 2

Phase II Eastern Turkey (September 1989) -

day 1: observe sites 1, 2, 3, 4, 5, 6

day 2: observe sites 1, 2, 3, 4, 5, 6

day 3: move sites 1, 2; observe sites 3, 4, 5, 6

day 4: observe sites 3, 4, 5, 6, 7, 8

day 5: move sites 3, 4, 5, 6; observe sites 7, 8

day 6: observe sites 7, 8, 9, 10, 11, 12

day 7: move sites 7, 8; observe sites 9, 10, 11, 12

day 8: observe sites 9, 10, 11, 12, 13, 14

day 9: move sites 9, 10, 11, 12; observe sites 13, 14

day 10: observe sites 13, 14, 15, 16, 17, 18

day 11: move sites 13, 14; observe sites 15, 16, 17, 18

day 12: observe sites 15, 16, 17, 18, 19, 20

day 13: move sites 15, 16, 17, 18; observe sites 19, 20

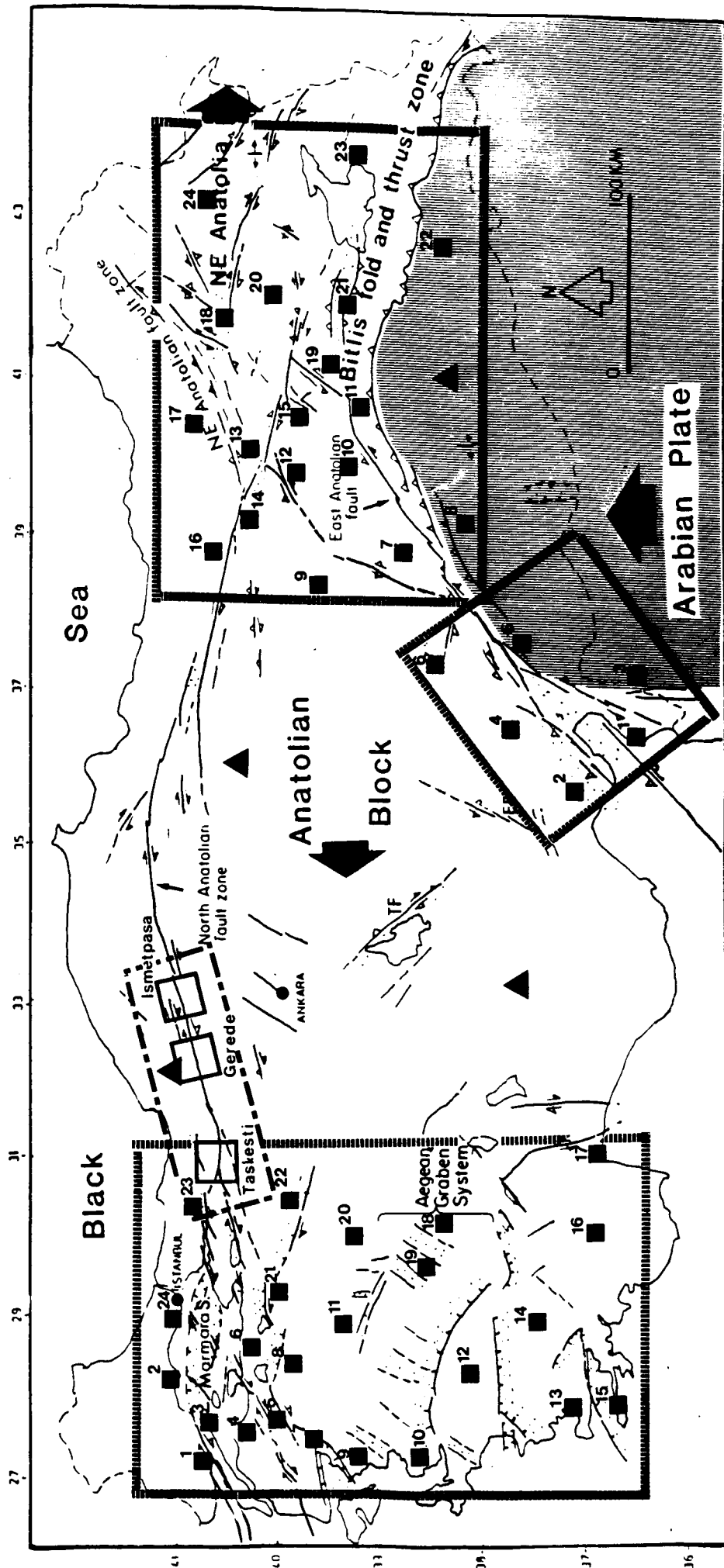
day 14: observe sites 19, 20, 21, 22, 23, 24

day 15: observe sites 19, 20, 21, 22, 23, 24

Data Reduction and Analysis

All participants in the project will have full access to the data collected. Office space, computer time and technical assistance can be provided at MIT for a number of Turkish scientists to participate in data reduction. Agreement between the participants in the project is to be reached on the form and time of publication of the initial results insofar as the conclusions refer to the Turkish geodetic network.

ORIGINAL PAGE IS
OF POOR QUALITY



- ▲ SLR
- Mobile GPS